TARGETING VASCULAR ENDOTHELIAL GLUTAMINASE IN TRIPLE NEGATIVE BREAST CANCER

By

Verra Manka'a Ngwa

Dissertation

Submitted to the Faculty of the

Graduate School of Vanderbilt University

in partial fulfillment of the requirements

for the degree of

DOCTOR OF PHILOSOPHY

in

Cancer Biology

August 12, 2022

Nashville, Tennessee

Approved:

Barbara Fingleton, Ph.D. (Chair)

Julie Rhoades, Ph.D.

Linda Sealy, Ph.D.

Jin Chen, M.D., Ph.D. (Advisor)

DEDICATION

This dissertation is dedicated to all breast cancer patients fighting for their lives and cancer survivors who are winning their battles daily and giving hope to scientists.

In Memoriam:

To my parents, Rose and Mathew Ngwa

ACKNOWLEDGMENT

I would like to express my sincere gratitude and appreciation to the following people, without whom this work would not have been possible.

First and foremost, I am extremely grateful to my mentor, Dr. Jin Chen, for giving me the opportunity to train in her lab as well as her valuable advice, continuous support and guidance throughout my PhD study. Thank you for believing in me and the constant reminders of how good I am especially the high-fives. Being under Jin's mentorship has been an incredible experience and has provided memories and lessons which will stay with me for a lifetime. I would like to thank my committee members both past and present: Drs. Barbara Fingleton, Julie Rhoades, Linda Sealy, and Rebecca Cook for their expertise, scientific guidance, and counsel throughout my training.

I want to thank the present members of the Chen lab: Dr. Deanna Edwards, Yoonha Hwang, Dr. Xiagong Wang, and Breelyn Karno, as well as the past members: Drs. Wenqiang Song, Dana Brantley-Sieders, Shan Wang, Laura Kim, and Eileen Shiuan. I am thankful for the scientific knowledge, critiques, encouragement and most of all their friendship during my graduate training. A special thanks to Dr Deanna Edwards for being an instrumental part of my training. From when I rotated in the lab until my last experiments, Deanna has always listened to my questions and provided me with guidance on how to proceed. I would also like to highlight Dr. Shan Wang for being patient with me as a new-graduate student and for teaching me most of the techniques that were used in this thesis project.

I would also like to thank the Initiative for Maximizing Student Diversity (IMSD) program, specifically the leadership under Drs. Linda Sealy, Roger Chalkley, and Christina Keeton. To Roger and Linda, thank you for sitting and listening to me practice my presentations before my

qualifying exams and providing me with great feedback. It was through the IMSD program that I met my very good friends in graduate school; for that I say thank you!

I would like to thank my previous mentors Drs. Carole Chrestensen and Jonathan McMurry at Kennesaw State University. They both instill in me the love for research. Carole took me into her lab as an undergraduate and taught me the first steps of what research would look like as a career. Jonathan believed in me and allow me to explore my dreams in the lab on a brand-new project. He has been instrumental in my graduate career writing letters of recommendation to every application I did in graduate school and he will always include one of the protein-protein interaction figures from my master's thesis to the letters.

I would like to thank those who supported me financially during my training, specifically Dr. Jin Chen through the T32 Microenvironmental Influences in Cancer Training Program (MICTP) and the National Cancer Institute for the Predoctoral Ruth L. Kirchstein National Research Service Award (F31). Additionally, I want to that the leaders and members of the Program in Cancer Biology for support especially the Cancer Biology Student Association (CBSA).

Last but not the least, I want to thank friends for their love and support throughout my training. I want to thank my friends (Vera Endah, Grace Nebane, Irene Nwatum, Jocelyne Woopong, and Doris Mbua) back home in Cameroon for their constant love and support. For the text messages telling me how strong I am and that they know I could do it. For the Cameroonian community in Nashville, thank you for making life in Nashville not too far away from home.

Finally, I want to thank my family. First to my parents (deceased) for inspiring me especially my mother who passed with breast cancer. To my family back in Cameroon for their constantly encouraging but kept asking me when I will be done with school. To my uncle and his wife Drs.

Mercy (Aunty Mercy) and Emmanuel Chebe thank you for always supporting me throughout my graduate career. Thank you for always encouraging and telling me how far I could go. A special thanks to Aunties Mercy and Perpetual for always praying for me to succeed in graduate school and life as a whole. To my extended family and in-laws, thank you for your constant love and support. I am grateful especially to Dr Gerard Shu Tangyie and his wife Mrs Comfort Anih, for showing me such an amazing love, making sure I was okay after every failed experiment and encouraging me to keep working hard. Truly, it takes a village! Lastly, to my wonderful husband, Adrian, I cannot thank you enough for your unwavering support especially with the children. I could not have done this without you. I love you!

TABLE OF CONTENTS

LIST OF TABLES

LIST OF FIGURES

LIST OF ABBREVIATIONS

2HG	2-hydrocyglutarate
ACK	Ammonium-chloride-potassium
acyl-CoA	Cholesterol acyltransferase
Akt	Protein kinase B
α-KG	Alpha-ketoglutarate
Ang	Angiopoietin
ANOVA	Analysis of variance
ASCT2	Alanine-serine-cysteine transporter 2
ATP	Adenosine triphosphate
AXL	Anexelekto
BCH	System-L inhibitor 2-amino-2-norbornanecarboxylic acid
BPTES	Bis-2-(5-phenylacetamido-1,3,4-thiadiazol-2-yl)ethyl sulfide
CAAs	Cancer-associated adipocytes
CAD	Carbamoyl-phosphate synthetase 2, Aspartate transcarbamoylase, and Dihydroorotase
CAFs	Cancer-associated Fibroblasts
CB-839	Telaglenastat
CCL	C-C chemokine ligand
CD	Cluster of differentiation
CDH5	Cadherin 5
CDK	Cyclin-dependent kinase
CHIP-seq	Chromatin immunoprecipitation sequencing
CoCL2	Cobalt chloride

Cpt	Cisplatin
CPT1a	Carnitine palmitoyltransferase 1a
CRC	Colorectal cancer
Cre	Carbapenem-resistant enterobacteriaceae
CSFR1	Colony stimulating factor 1 receptor
CTLA4	Cytotoxic T-lymphocyte-associated protein 4
CXCL	C-X-C motif chemokine ligand
DAB	3,3′-diaminobenzidine
DAPI	4’,6-diamidino-2-phenylindole
DC101	Anti-VEGF receptor 2 antibody
DCA	Deoxycholic acid
DEG	Differentially expressed genes
DLL4	Delta like canonical notch ligand 4
DON	6-diazo-5-oxo-L-norleucine
DOXO	Doxorubicin HCL
EC	Endothelial cell
DMEM	Dulbecco’s modified eagle’s medium
DNase	Deoxyribonuclease
EGF	Epidermal growth factor
EGFR	Epidermal growth factor receptor
ELISA	Enzyme-linked immunosorbent assay
EPHA2	Ephrin type-a receptor 2
ER	Estrogen receptor
ERK	Extracellular signal-regulated kinase
FACS	Fluorescence-activated cell sorting

FAO	Fatty acid oxidation
FASN	Fatty acid synthase
FBS	Fetal bovine serum
FGF	Fibroblast growth factor
FGFR	Fibroblast growth factor receptor
FITC	Fluorescein isothiocyanate
FLT3	Fms-like tyrosine kinase 3
FMO	Fluorescence minus one
GAC	Glutaminase C
GBM	Glioblastoma multiforme
GDH	Glutamate dehydrogenase
GIST	Gastrointestinal tumor
GLS	Glutaminase
GLS^{ECKO}	Endothelial glutaminase deletion
GLUD	Glutamate dehydrogenase
GLUL	Glutamate-ammonia ligase
GOT	Glutamate–oxaloacetate transaminase
GPNA	Gamma-l-glutamyl-p-nitroanilide
GSEA	Gene set enrichment analysis
GSH	Reduced glutathione
GSK3α/β	Glycogen Synthase Kinase 3 alpha/Beta
GZMB	Granzyme B
HCC	Hepatocellular carcinoma
HER2	Human epidermal growth factor receptor 2
HIF-1α	Hypoxia-inducible factor-1 alpha

HRE	Hypoxia response element
IACUC	Institutional Animal Care and Utilization Committee
ICAM-1	Intercellular adhesion molecule 1
ICI	Immune checkpoint inhibitor
ICIs	Immune checkpoint inhibitors
IDH	Isocitrate dehydrogenase
IF	Immunofluorescence
IFN	Interferon
IHC	Immunohistochemistry
IL	Interleukin
JAK	c-Jun N-terminal kinase
JHU-083	Ethyl 2-(2-Amino-4-methylpentanamido)-DON
KEGG	Kyoto Encyclopedia of Genes and Genomes
KGA	Kidney glutaminase
LAT	Large Amino acid Transporter
LDHA	Lactate dehydrogenase A
Lep	Leptin
LepR	Leptin receptor
LL202	(E)-15,22-Dioxa-4,11-diaza-5(2,5)-thiadiazola-10(3,6)-pyridazina-1,14(1,3)-dibenzenacyclodocosaphan-18-ene-3,12-dione
LLC	Lewis lung carcinoma
LPS	Lipopolysaccharide
Ly6G	Lymphocyte antigen 6 complex, locus G
Ly6C	**L**ymphocyte antigen 6 complex, locus C
M.O.M	Mouse-on-mouse

M1-like	Classically activated macrophages
M2-like	Alternatively activated macrophages
MHC	Major histocompatibility complex
MAPK	Mitogen-activated protein kinase
mCRC	Metastatic colorectal cancer
MDSC	Myeloid-derived suppressor cell
MEK	Mitogen-activated protein kinase kinase
M-MDSC	Mononuclear myeloid-derived suppressor cell
MMTV-Neu	Mouse mammary tumor virus- rat ERBB2
MMTV-PyMT	Mouse mammary tumor virus-polyoma middle tumor-antigen
MPMEC	Mouse pulmonary microvascular endothelial cells
mRNA	Messenger Ribonucleic acid
mTORC1	Mammalian target of rapamycin complex 1
NADPH	Nicotinamide adenine dinucleotide phosphate
NEC	Normal endothelial cells
NES	Normalized enrichment score
NG2	Neural/glial antigen 2
NIH	National Institutes of Health
NK	Natural killer
NOTCH1	Notch receptor 1
NRP-1	Neuropilin receptor-1
NSCLC	Non-small cell lung cancer
OCT	Optimal cutting temperature
OS	Overall survival
OXPHOS	Oxidative phosphorylation

PBS	Phosphate buffered saline
PCR	Polymerase chain reaction
PD1	Programmed death 1
PDGF	Platelet-derived growth factor
PD-L1	Programmed death ligand
PDX	Patient-derived Xenograft
PE	Phycoerythrin
PEDF	Pigment epithelium-derived factor
PerCP	Peridinin chlorophyll protein
PFA	Paraformaldehyde
PFKFB3	6-phosphofructo-2-kinase/fructose-2,6-biphosphatase 3
PI3K	Phosphatidylinositol 3-kinase
PIGF	Placental growth factor
PMN-MDSC	Polymorphonuclear myeloid-derived suppressor cell
PR	Progesterone receptor
qRT-PCR	Quantitative real-time polymerase chain reaction
R5P	Ribose-5-phosphate
RAC	Ras-related C3 botulinum toxin substrate
RAF	Rapidly accelerated fibrosarcoma
RCC	Renal cell cancer
RET	Rearranged during Transfection
Rgs5	Regulator of g protein signaling 5
RIPA	Radioimmunoprecipitation assay
RNAse	Ribonuclease
RNAseq	RNA-sequencing

RPMI	Roswell Park Memorial Institute
RTK	Receptor tyrosine kinase
S6K1	Ribosomal protein S6 kinase beta-1
SDS-PAGE	Sodium dodecyl sulfate polyacrylamide gel electrophoresis
SEM	Standard Error of Mean
shRNA	Short hairpin RNA
SLC1A5	Solute carrier family 1 member 5
SLC7A11	Solute carrier family 7 member 11
SLC7A5	Solute carrier family 7 member 5
SMA	Smooth Muscle Actin
SNAT2	Sodium-dependent neutral amino acid transporter-2
STAT	Signal transducer and activator of transcription
TAp63	Tumor protein p63
TAp73	Tumor protein p73
TAZ	WW domain containing transcription regulator 1
TCA	Tricarboxylic acid
TCR	T cell receptor
TEAD4	TEA domain transcription factor 4
TECs	Tumor endothelial cells
Tek	TEK Receptor tyrosine kinase, or Tie2
TGF-β	Transforming growth factor-beta
T_h	T helper cells
TIE	Angiopoietin receptor
TKI	Tyrosine kinase inhibitor
TME	Tumor microenvironment

TNBC	Triple-negative breast cancer
TNF	Tumor necrosis factor
TP53	Tumor protein 53
Treg	Regulatory T cell
TVN	Tumor vessel normalization
VCAM-1	Vascular cell adhesion molecule 1
VE-Cad	Vascular endothelial cadherin
VEGF-A	Vascular endothelial growth factor
VEGFR2	Vascular endothelial growth factor receptor 2
WT	Wild type
YAP	Yes-associated protein

ORIGINAL PUBLICATIONS

1. **Verra M. Ngwa**, Deanna N. Edwards, Yoonha Hwang,Chi Yan, Ann Richmond, Dana M. Brantley-Sieders, Jin Chen **(In press)**, “Loss of vascular endothelial glutaminase inhibits tumor growth and metastasis, and increases sensitivity to chemotherapy,” Cancer Research Communications

2. Deanna N. Edwards, **Verra M. Ngwa**, Ariel L. Raybuck, Shan Wang, Yoonha Hwang, Laura C. Kim, Sung Hoon Cho, Yeeun Paik, Qingfei Wang, Siyuan Zhang, H. Charles Manning, Jeffrey C. Rathmell, Rebecca S. Cook, Mark R. Boothby, Jin Chen (**2020**), “Selective glutamine metabolism inhibition in tumor cells improves antitumor T lymphocyte activity in triple-negative breast cancer,” Journal of Clinical Investigation

3. **Verra Ngwa**, Deanna Edwards, Mary Philips and Jin Chen (**2019**), “Microenvironmental metabolism regulates anti-tumor immunity,” Cancer Research

4. Deanna N. Edwards, **Verra M. Ngwa**, Shan Wang, Eileen Shiuan, Dana M. Brantley-Sieders, Laura Kim, Albert B. Reynolds and Jin Chen (**2017**), ‘’The receptor tyrosine kinase EphA2 promotes glutamine metabolism in tumors by activating the transcriptional coactivators YAP and TAZ,’’ Science Signaling

CHAPTER I

INTRODUCTION

Overview

Cancer is a major public health burden worldwide and the second leading cause of death in the United States (American Cancer Society). Cancers are characterized by their unique characteristics termed hallmarks, which include sustaining proliferative signals, evading growth suppressors, avoiding immune destruction, enabling replicative immortality, tumor-promoting inflammation, genome instability and mutation, resisting cell death, activating invasion and metastasis, deregulating cellular energetics, and inducing angiogenesis (1,2). These common features provide a frame work for critical areas of research to target and treat cancer.

Deregulation of cellular energetics is one of the key elements of the cancer hallmarks. Cancer cells altered their metabolism to support their high proliferative rates and adapt to the hostile tumor microenvironment (2,3). The Warburg effect, which is the best-known metabolic abnormality in cancer cells, demonstrates an increase in glucose consumption through elevated glycolysis even in the presence of oxygen (aerobic glycolysis) for these rapidly proliferating cells (2,3). In addition to glucose metabolism, some cancer cells have been identified to be addicted to glutamine metabolism. These tumor cells utilize glutaminolysis to support biosynthesis of amino acids, nucleotides, and glutathione (4,5). These molecules are critical to maintain cancer cells biomass and involved in other metabolic pathways that are required for cell survival.

Growing tumors acquire nutrients via diffusion; however, rapidly growing tumors require a vascular system to grow beyond 2 mm^3 in diameter (6). The tumor achieves this through

angiogenesis, the process whereby new blood vessels are formed from pre-existing vessels, by secreting angiogenic factors like VEGF-A and Angiopoietin which promotes the development and stabilization of the tumor vasculature. Unlike normal blood vessels, tumor blood vessels are abnormal and dysfunctional. This abnormality is characterized by tortuous, leaky and chaotic networks of irregular endothelial cells (ECs) lining the tumor vessels. Abnormal tumor vascular network impairs perfusion, obstructs blood flow, and lead to poor leukocyte trafficking and drug delivery (6). Like cancer cells, these angiogenic sprouts are initiated from rapidly proliferating cells that consume glucose, glutamine and other nutrients (7,9,10).

Judah Folkman, almost four decades ago, proposed that tumors depend on a blood vessel network, and inhibiting these blood vessels would cut off blood supply and limit the amount of nutrients and oxygen to the tumors hence choke the tumor to death (6). In the quest for angiogenic inhibitors, Bevacizumab (Avastin), a humanized monoclonal antibody against VEGFA, became the first drug to block blood vessel and was approved in 2004. However, due to resistance and other adverse effects, usage of Avastin and other angiogenesis inhibitors is limited in the clinic. Consequently, other strategies are being investigated to target tumor blood vessels. Indeed, Rakesh Jain proposed that instead of eliminating the abnormal blood vessels, they could be normalized which can lead to improved vessel perfusion and promote drug delivery (11,12). Since the introduction of the concept, all normalization strategies focused on targeting angiogenesis using anti-angiogenic drugs. Peter Carmeliet and his group seized the opportunity to exploit endothelial cell metabolism as a therapeutic target to normalize tumor blood vessels. Proliferative tumor endothelial cells are hyperglycolytic, and inhibiting tumor endothelial cells glycolysis normalized blood vessels, reduced metastasis and promoted drug delivery (13).

Aside from glucose, a growing body of evidence shows that glutamine metabolism provides carbons for biomass production and both carbon and nitrogen for glutathione synthesis that is required for EC proliferation (9,14). Glutamine metabolism also contribute to lipid biosynthesis in ECs through reductive carboxylation. Vascular endothelial-specific deletion of glutaminase *in vivo* suppressed retinal angiogenesis, and negatively affected tricarboxylic acid (TCA) cycle anaplerosis, macromolecule production, and redox homeostasis in ECs (9,14). It remains to be determined whether inhibition of glutamine consumption can normalize tumor blood vessels and enhance antitumor immunity. Herein, we describe the role of vascular endothelial glutaminase (GLS), the enzyme that catabolizes glutamine to glutamate, in breast cancer tumor growth and metastasis and chemotherapy drug delivery. We utilized an inducible transgenic mouse model to delete GLS specifically in the endothelium (GLS^{ECKO}). Our data reveal that GLS loss in endothelium decreases tumor angiogenesis while promoting tumor vessel normalization. GLS^{ECKO} tumors with normalized blood vessels displayed an increase in drug delivery and enhanced anti-tumor effect of chemotherapy. We also report herein, a mechanism which functionally linked endothelial GLS and expression of leptin in tumor cells, a key regulator of metabolic homeostasis. Together, these data demonstrate a crucial role for glutamine metabolism in tumor endothelium, which may be exploited therapeutically to induce vascular normalization and improve drug delivery in solid tumors.

Breast Cancer and Therapeutic Approach

Breast cancer is the most common malignancy in women, and the principal cause of cancer-related death among women in both developed and developing countries (15). According to the American Cancer Society, in 2022, an estimated 287,850 new cases of breast cancer will be diagnosed in women which will lead to an estimated 43,250 deaths. Breast cancer is a heterogeneous disease classified based on four primary molecular subtypes: Luminal A,

Luminal B, Her2-enriched and Triple negative/basal-like (16). These subtypes are described based on their surface protein expression as detailed in Table 1.1. Effective targeted treatment options for ER+/PR+ and HER2+ breast cancers have been developed. ER+ and /or PR+ tumors make up approximately 60% of breast cancer diagnosis and are treated with hormone modulation therapies (e.g tamoxifen and fulvestrant), aromatase inhibitors (e.g. letrozole, exemestane, and anastrozole), and CDK 4/6 inhibitors (eg, palbociclib, ribociclib, abemaciclib) (used in metastasis disease) (17–19). HER2+ tumors represent about 20% of invasive breast cancers and overexpress the HER2 receptor. Treatment of HER2+ tumors involves targeting the HER2 receptor and preventing downstream signaling using monoclonal antibodies (e.g trastuzumab, pertuzumab) (20–22); antibody-drug conjugates (e.g ado-trastuzumab-emtansine, and trastuzumab derutecan); or tyrosine kinase inhibitors (e.g tucatinib, neratinib) (23).

Triple negative breast cancer (TNBC) does not express any of the above receptors hence treatment options are limited with chemotherapy as the main standard of care. In searching for vulnerability in this aggressive subtype, TNBCs are found to be addicted to glutamine metabolism both in pre-clinical and clinical settings (24–26). While breast cancer in general is not very immunogenic, TNBC has been found to be responsive to immune checkpoint inhibitors. Indeed, atezolizumab and pembrolizumab in combination with chemotherapy are well tolerated in TNBC patients with high PD-L1 expression (27), broadening the therapeutic option for TNBC patients. Despite the advances in cancer research in recent years, limited efficacy and drug resistance remains a challenge.

Table 1.1: Molecular subtypes of breast cancer and biomarker expression (summarized from (16)**)**

Molecular subtypes	Identifier	Histological grade	Frequency (%)	Overall 5-year survival
Luminal A	-ER positive and/or PR positive -HER2 negative -Low Ki-67	Low	50-60%	90%
Luminal B	-ER positive and/or PR positive -HER2 negative or positive -High Ki-67	Intermediate/High	10-20%	40%
HER2-enriched	-ER negative and/or PR negative -HER2 positive	High	10-15%	31%
Basal-Like	-ER negative and/or PR negative -HER2 negative	High	10-20%	0
Claudin-low	-ER negative and/or PR negative -HER2 negative	High	12-14%	0

Metabolic Reprograming in Cancer

Altered metabolism is an important hallmark of cancer growth and progression. Metabolic reprogramming provides tumor cells the energy and materials to support their large-scale biosynthesis and rapid proliferation. The concept of altered metabolism started in the 1920s when Otto Warburg observed that tumor cells use glucose to generate lactate despite oxygen-rich environment (aerobic glycolysis) (28,29). Initially, Warburg's theory was based on the fact that neoplastic cells had a dysfunctional mitochondrion. However, studies later revealed that cancer cells were able to use glucose and fatty acids at the same rate as normal cells (30,31). In contrast to normal cells, cancer cells utilize glycolysis to generate glycolytic intermediates for biosynthesis while reducing the production of reactive oxygen species from oxidative phosphorylation (32–34). Advances in metabolic research has made it evident that in addition to glucose, tumor cells also require lipids and amino acids for biomass and proliferation (35). Altered metabolism depends on the dysregulation of several enzymes in the different metabolic pathways, indicating that appropriate intervention against these key enzymes may be leveraged to inhibit tumor growth and metastasis (36). Given the in-depth study in the field of tumor metabolism, I will now focus on reviewing the contributions of glutamine metabolism in supporting cancer growth and progression.

Glutamine Metabolism and Transporters in Cancer

Glutamine is an abundant non-essential amino acid in the human body. It is largely used for energy production (bioenergetics) by replenishing the TCA cycle and feeding in carbon and nitrogen for the synthesis of nucleotides, glutathione (GSH), amino acids and fatty acids (4,37). In the cell, glutaminase (GLS) converts glutamine into glutamate, which acts as a precursor for the antioxidant glutathione. Glutamate is further metabolized to α-ketoglutarate either by

glutamine dehydrogenase (GLUD) or aminotransferases. Through α-ketoglutarate, glutamine enters the TCA cycle as an anaplerotic source of carbons (4,38). In this capacity, glutamine provides nitrogen for biosynthesis of nucleotides, amino acids, and hexosamines, but also serves as a mitochondrial substrate. Glutamine-derived α-ketoglutarate is reduced to citrate by isocitrate dehydrogenase (IDH) enzymes through reductive carboxylation thereby fueling lipid biogenesis. In addition to its role in the reductive carboxylation reaction, IDH mutations generate the oncometabolite, 2-hydroxyglutarate (2HG), which regulates epigenetics by inhibiting demethylase enzymes that are members of the α-ketoglutarate-dependent dioxygenase family (39,40) (Figure 1.1). The accumulation of 2HG in breast cancer is associated with c-MYC activation contributing to an increase in glutamine metabolism through the expression of glutaminase, hence poor prognosis in breast cancer patients (40). Cancer cells can exploit these multiple functions of glutamine to drive tumor growth.

Amino-acid transport systems are essential for the growth of cancer cells, not only because they provide the amino acids required for protein synthesis but also due to their capability of activating signaling pathways involved in cell growth, such as the mammalian target of rapamycin complex 1 (mTORC1). Importantly, glutamine transporters are required to sustain "glutamine addiction" in tumor cells (41,42). Several glutamine transporters exist in mammalian cells, the best studied of which are the alanine-serine-cysteine transporter 2 encoded by *SLC1A5* (ASCT2) gene and the L-type amino acid transporter 1 encoded by the *SLC7A5* (LAT1) gene (43). These two transporters are highly expressed in aggressive forms of breast cancer, including triple-negative and HER2-positive, suggesting that these transporters cooperate to promote tumor growth and progression (44–46). In addition to other neutral amino acids, *SLC1A5* /ASCT2 mediates both the Na^+-coupled influx/efflux of glutamine while *SLC7A5*/LAT1 mediates the efflux of glutamine in exchange of leucine influx into the cells and therefore regulates the activation of mTORC1 (43). Pre-clinical studies showed that ASCT2 is

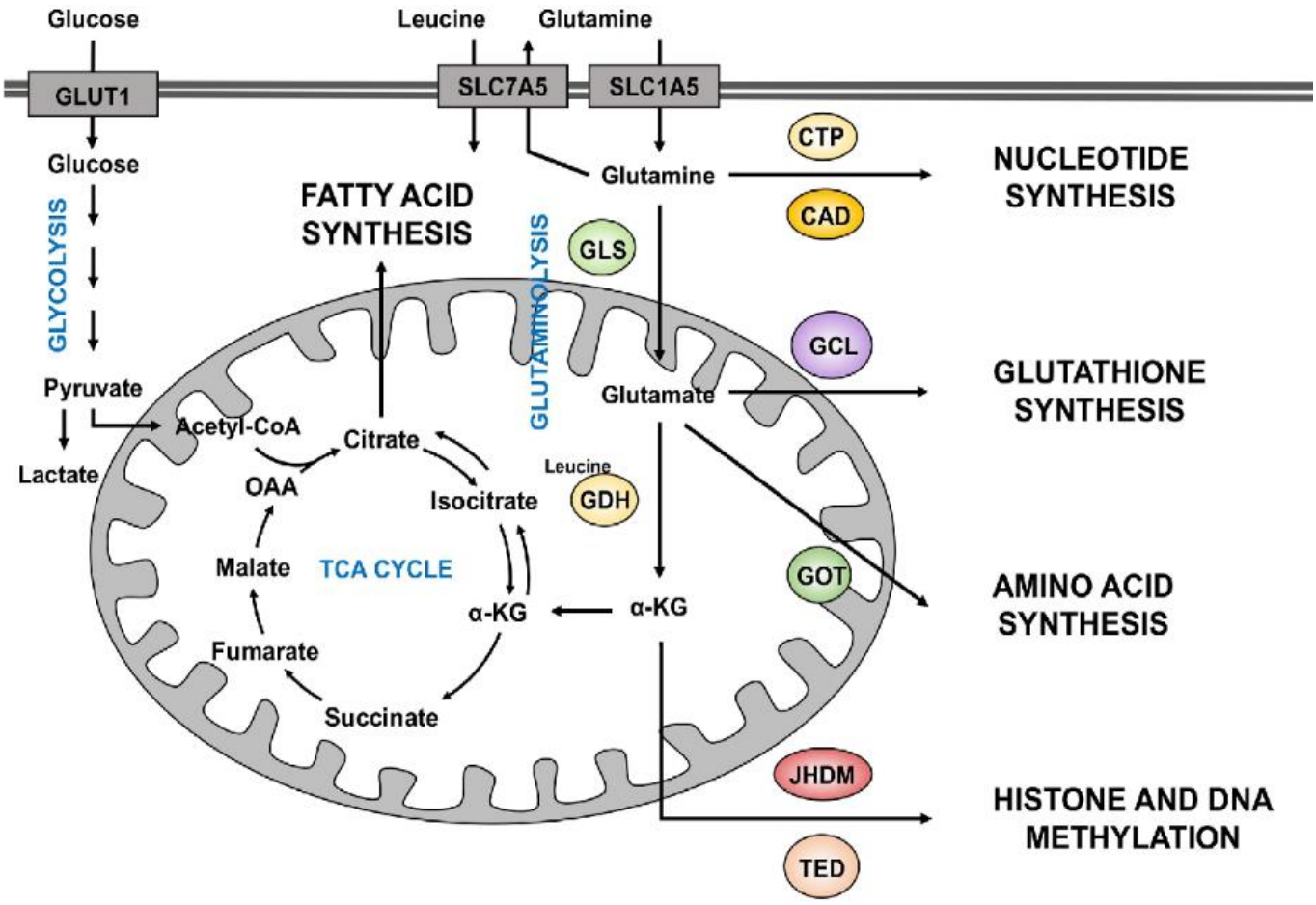

Figure 1.1: Different uses of glutamine metabolism in cancer cells. Glutamine enters the cells through the transporters SLC1A5 or SLC7A5. Once inside the cell, glutamine can contribute to nucleotide biosynthesis directly (through CAD for example) or is converted to glutamate by GLS. It can also be exported outside of the cell in exchange of leucine, a coactivator of GDH. Glutamate can further be converted to α-KG by GDH. Glutamate can also contribute to the synthesis of glutathione through the activity of different enzymes, including GCL. Amino acid synthesis is supported by the aminotransferases (GOT) which converts glutamate to α-KG. Glutamine-derived α-KG enters the TCA cycle to produce energy for the cell or proceed backwards via the reductive carboxylation to provide an alternative source of lipid synthesis. Additionally, α-KG is a co-substrate of dioxygenase enzymes (JHMD and TED) require in the regulation of histone and DNA methylation. **(**Review in Nguyen T and Duran R.V., *Cancer Drug Resist*. 2018**)**

responsible for glutamine-dependent cell growth in basal-like breast cancer and showed that ASCT2 loss is sufficient to significantly reduce basal-like breast cancer cell growth *in vitro* and *in vivo* (47). In another study, the role of *SLC7A5*/LAT1 was investigated in breast cancer growth and progression. The authors showed that applying an *SLC7A5*/LAT1 inhibitor, 2-aminobicyclo-(2,2,1)-heptane-2-carboxylic acid (BCH) or knocking down the transporter in triple-negative and HER2-positive human breast cancers cell lines significantly inhibited cell growth (46). The expression of these transporters have emerged as major pro-tumoral transporters with increased expression levels correlating with poor patient prognosis in different cancer types (48–51) including breast cancer (45,52), suggesting the potential of glutamine transporters as prognostic biomarkers for breast cancer.

Once inside the cell, glutamine is catabolized to glutamate by glutaminase (GLS), which represents the rate-limiting step of glutaminolysis (53). Two isoforms of GLS exist in mammals: the kidney-type glutaminase (GLS1 or GLS) and liver-type glutaminase (GLS2) (54). GLS1 is up-regulated in some human cancers including breast and is associated with a higher disease stage and poor prognosis (24). Additionally, GLS exists as two alternative splice variants, known as glutaminase C (GAC) and kidney glutaminase (KGA). These two isoforms have the same N-terminal and catalytic domains but different C-termini with unknown function. The KGA isoform is expressed in most human tissues except liver, while GAC is only expressed in specific tissues, such as heart and kidneys (24,55), making GAC a more selective target for tumor cells. Oligomerization is both sufficient and necessary for KGA and GAC activation with the formation of tetramers from dimers, enhanced by inorganic phosphate, to encompass full enzymatic activity (56,57). The GAC isoform, the more catalytically active form of GLS, is often overexpressed in human cancers especially in breast cancers and is associated with sensitivity to glutamine withdrawal (58,59). Furthermore, glutamine-dependent breast cancers are less efficient of synthesizing glutamine from glutamate using glutamine synthetase within the cells

(58) enabling glutamine addicted breast cancer cells to rely heavily on exogenous glutamine. The resulting glutamate produced by the tumor cells is exported out of the cell by Xc-cystine/glutamate antiporter (*SLC7A11*), which promotes aggressiveness and invasiveness of breast cancer (60), suggesting that GLS (specifically GAC) is an important drug target.

In breast cancer, GLS has been shown to be highly expressed in HER2-positive and triple negative breast cancers (TNBC). Not surprisingly, Kim et al showed that patient samples representing these breast cancer subtypes have higher levels of glutamine consumption and glutaminolysis compared to luminal subtypes (44). To further validate the importance of glutaminolysis in breast cancer cell viability, Lampa and colleagues investigated the role of GLS as a therapeutic target in TNBC using GLS specific shRNA constructs and glutaminase inhibitor CB-839 as a pharmacological tool. They demonstrated that GLS knockdown in glutamine-dependent human TNBC cell lines led to a decrease in downstream metabolites and significant cell growth inhibition (24). Additional metabolomics analysis of 270 clinical breast cancer tissues and 97 normal breast tissues revealed an elevated glutamate to glutamine ratio in breast cancer samples due to increase GLS1 expression (61). Increased glutamate levels in breast tumors have been associated with invasiveness and drug resistance, correlating with increased risk of recurrence. For this reason, the increased ratio of glutamate to glutamine may represent another biomarker that could help to stratify patients' treatment with specific glutamine inhibitors.

While much has been shown about GLS in different cancers, the role of GLS2 is still not fully understood. Some studies have enumerated the role of GLS2 as a tumor suppressor while others have suggested GLS2 as a tumor promoter whose upregulation contributes to cancer cell survival. Lui Juan and colleagues showed that GLS2 is a downstream target gene of p53 and increased expression of GLS2 significantly reduced liver tumorigenesis by inhibiting anchorage-

independent growth of hepatocellular carcinoma cells (HCC) and the growth of HCC xenograft tumors (62). However, GLS2 has also been shown to support tumor growth and promote ionizing radiation resistance in cervical cancer (63), indicating the role of GLS2 in cancer may be context dependent and requires further studies.

Regulation of Glutaminase in Cancer

Like most biological processes, glutaminolysis is well regulated in normal cells. The MYC oncogene is a transcription factor that is frequently dysregulated in human cancers. MYC regulates the expression of multiple genes involve in diverse processes including cellular metabolism, differentiation, vasculogenisis, cell adhesion, cell growth, apoptosis, and DNA damage responses (64). MYC regulates glutamine metabolism by upregulating *GLS*, glutamine synthase (*GLUL*), *GLUD* and aminotransferases and the glutamine transporters *SLC1A5* and *SLC38A5* (65–67) (Figure 1.3). MYC promotes *GLS* expression indirectly by repressing the transcription of miR-23a and miR-23b. Other signaling pathways like c-JUN, GSK3α/β, and mTORC1/S6K1 upregulate *GLS* directly or indirectly (reviewed in (67)). *GLS* can also be regulated by hypoxia-inducible factor 1 (HIF1) both at the mRNA and protein expression (68). Studies from our lab provide evidence that the receptor tyrosine kinase (RTK) EphA2 regulates glutamine metabolism through the EphA2-Rho-glutaminase pathway in a breast cancer mouse model driven by activated HER2/ErbB2 (MMTV-NeuT). EphA2 RTK promotes glutamine metabolism by activating the transcriptional coactivators YAP and TAZ. Once activated, YAP/TAZ binds to TEAD4 transcription factor to upregulate *GLS* and *SLC1A5* genes thereby promoting glutaminolysis in cancer (69,70).

Alternatively, GLS2 is regulated differently from GLS. Studies have shown that GLS2 is regulated by the tumor suppressor p53 (71,72). Members of the p53 family, TAp63 and TAp73

also regulate GLS2 (73,74). Taking together, targeting glutamine metabolism is warranted for therapeutic drug development.

Targeting Glutaminolysis in Cancer

The diverse roles played by glutamine in tumor metabolism present an opportunity for targeting glutamine metabolism for cancer therapy, especially in the glutamine-addicted HER2-positive and triple negative breast cancers. Although advances in targeted therapy have improved the survival of ER^+/PR^+ and HER2 patients, long-term response rates are limited due to acquired resistance. Because no oncogenic drivers have been identified in TNBC, therapeutic options for most of these patients are very limited and prognosis remains poor. , Immunotherapies are beginning to be used in TNBCs patients, however, strategies are needed to identify patients who will benefit from these therapies (75). Additionally, efforts are needed to reduce immune-related toxicity, and cost on these patients.

The first strategy to target glutamine metabolism would involve inhibiting the transporters to block the import of glutamine. The small molecule inhibitor of ASCT2, gamma-l-glutamyl-p-nitroanilide (GPNA), has been proven to be effective in glutamine-dependent cancers (51). However, due to toxicity to other healthy cells that rely on glutamine and lack of specificity, GPNA could not be used in the clinic (76,77). Recently, a new ASCT2 inhibitor, V-9302, was discovered and has proven potent in blocking glutamine transport. Using the V-9302 inhibitor in murine models resulted in decreased cancer cell growth and proliferation, increased cell death, and increased oxidative stress, thereby contributing to anti-tumor responses both *in vitro* and *in vivo* (78).

In addition, as the rate-limiting step in glutaminolysis, GLS is a suitable target in cancer therapy. Indeed, several approaches have been employed to target glutaminase (Figure 1.2) including small molecule analogues, such as, 6-diazo-5-oxo-L-norleucine (DON), compound 968, BPTES, CB-839, JHU-083 and LL202. DON is a glutamine antagonist which binds covalently to the enzyme active site and blocks glutamine-dependent enzymes (GLS and glutamine amido-transferases) involved in *de novo* nucleotide biosynthesis, amino acid synthesis and hexosamine production in tumor cells (67,79–81). DON exhibited a degree of anti-proliferative effects in pre-clinical studies involving *in vitro* assays and xenograft animal models. However, DON use and development was discontinued due to dose-limiting neurotoxicity, gastrointestinal toxicity and myelosuppression (82). To diminished the toxicity of DON, a novel prodrug, JHU-083, was discovered which selectively blocks glutaminase activity (83). Being a pro-drug, JHU-083 itself is inactive. JHU-083 is converted either in the plasma by plasma esterases or intracellularly by cathepsin, which is more highly expressed in the tumor compared to normal tissues (84). Overall, DON and JHU-083 are pleiotropic and have effects on other metabolic pathways such as glycolysis.

Unlike DON and JHU-083, Compound-968, BPTES, and CB-839 target glutaminase without affecting other glutamine metabolism reactions. Compound-968 belongs to the family of benzophenanthridinone and it can allosterically inhibit GAC. This drug binds to the monomeric forms of GAC and prevents the formation of the active GAC tetramer (85). Compound-968 is specific to GLS however, it shows limited potency in the presence of the inorganic phosphates that promote GLS activation by tetramerization (85). BPTES blocks GLS in an uncompetitive fashion by causing a conformational change upon binding to KGA and GAC, trapping these isoforms in an inactive tetramer form (86,87). BPTES suppresses tumor growth both *in vitro* and *in vivo* in various cancers including breast cancer. However, BPTES is not the appropriate candidate for GLS inhibition because of its poor solubility and bioavailability (88).

Due to the limited potency of Compound-968 and the low solubility of BPTES, the efforts of developing new pharmacological inhibitors for GLS, and especially GAC, is necessary. CB-839 is an analogue of BPTES that inhibits both the GAC and KGA glutaminase splice variants but not GLS2 (88). Unlike the other glutaminase inhibitors, CB-839 exhibits low nanomolar potency in biochemical and cellular assays and has good oral bioavailability (89). In pre-clinical studies, CB-839 has been shown to inhibit the growth of several cancers including lymphoma and non-small cell lung cancer (90). Furthermore, CB-839 is able to inhibit proliferation of triple negative breast cancer cells but not ER^+ cells both *in vitro* and *in vivo* (88,89). Although CB-839 monotherapy has been well tolerated and demonstrated evidence of efficacy in a subset of patients with solid tumors, CB-839 has only yielded 15% of stable disease in TNBC patients (91). To achieve a durable effect of CB-839, clinical trials combination with chemotherapies in different solid cancers including TNBC are underway (ClinicalTrials.gov identifiers NCT03428217, NCT04265534, NCT03875313, NCT03057600).

Most recently, a novel macrocyclic inhibitor, LL202, was developed which binds GLS with high affinity and targets GLS allosterically with an IC_{50} value of 6nM. LL202 blocks glutamine metabolism by increasing ROS level and have a similar *in vivo* antitumor activity as CB-839 (92).

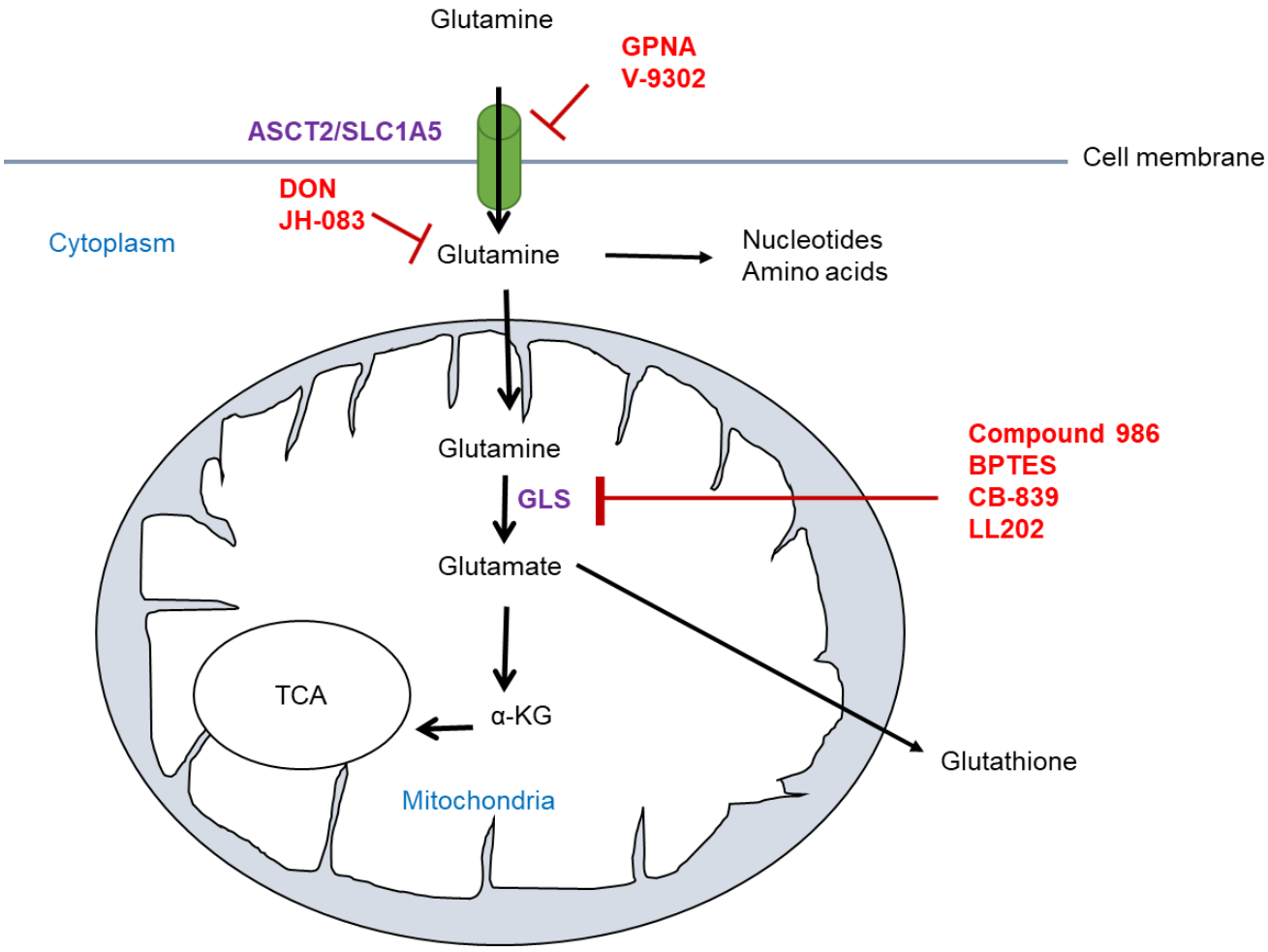

Figure 1.2: Summary of glutaminolysis inhibition in cancer cells. Glutamine is imported through the transporters ASCT2 to be used in the glutaminolysis pathway. The inhibitors in red indicates their various targets.

Blood Vessel Formation

The inner walls of blood vessels are coated by endothelial cells. These cells enable the exchange of nutrients and oxygen between the bloodstream and the surrounding tissues. Blood vessels form from de novo vasculogenesis, which requires precursor cells (angioblasts) to differentiate into endothelial cells, or angiogenesis, which is sprouting of pre-existing blood vessels (93,94). Angiogenesis is a complex, well-regulated process. Both processes of blood vessel formation are observed in the embryo; however, in adults, new blood vessels primarily develop in response to physiological stimulus through angiogenesis. Physiological situations during which new blood vessels form include the cycling of the ovary, wound healing and in the placenta during pregnancy. Dysregulation of angiogenesis can lead to pathological conditions including ocular diseases, inflammatory disorders and cancer (95,96).

One important stimuli of angiogenesis which is required in both normal and tumor blood vessels is the vascular endothelial growth factor (VEGF). The VEGF gene is upregulated by other growth factors including platelet-derived growth factor (PDGF), fibroblast growth factor (FGF), epidermal growth factor (EGF), tumor necrosis factor (TNF), transforming growth factor-beta (TGF-β) and interleukin-1 (IL-1) (97). In addition to the above growth factors, hypoxia is also an inducer of VEGF. The VEGF protein family comprises of five members: VEGF-A, VEGF-B, VEGF-C, VEGF-D and placental growth factor (PlGF). These proteins signal through three receptor tyrosine kinase; VEGFR-1 (FLT1), VEGFR-2 (KDR/FLK1) and VEGFR-3 (FLT4) (98) (Figure 1.3) that are located on the surface of endothelial cells. VEGF-A, which preferentially binds to VEGFR2, is the main inducer of angiogenesis and activates pro-angiogenic signaling resulting in migration and survival of the endothelial cells (97,98).

Angiogenesis

Angiogenic sprout is promoted by the protrusion of highly motile tip cells and continues with stalk cells lagging behind as the sprout continue to elongate (99). Tip cells are highly polarized and rich in cell surface receptors and molecules that destroy the basement membrane and extracellular matrix degradation. Stalk cells however, are highly proliferative. They trail behind tip cells ensuring tube and branches, and lumen formation (100). Crosstalk between tip and stalk cells depends on VEGF and Notch signaling, where VEGF induces tip cell migration while Notch controls tip cell selection (101–103). Binding of VEGF to VEGFR-2 or VEGF-C/D to VEGFR-3 induce a signal transduction cascade which promotes expression of the Notch receptor ligand DLL4 resulting in high Notch signaling activation. This activated Notch signaling contributes to sprouting angiogenesis by differentially regulating the levels of VEGFR-1 and VEGFR-2 in stalk cells (104–106).

Once the new blood vessels are formed, they undergo a maturation phase which involves the enhancement of tight junctions and the recruitment of perivascular cells (107). Endothelial cells secrete Platelet-derived growth factor (PDGF) which signal through the PDGFR to recruit pericytes to the newly formed blood vessels enabling stability to the vessels. Vascular maturation by pericytes coverage have being associated with the Ang-Tie receptor system (107,108). The Tie/Ang signaling system is made up of Angiopoietin ligands 1-4 and two Tie tyrosine kinase receptors (Tie-1 and -2). Pericytes express Ang-1 which bind to Tie-2 on endothelial cells. Ang-2 is expressed both by endothelia and smooth muscle cells and has an antagonistic effect which can cause loss of pericytes to the ECs.

Another interesting signaling pathway in angiogenesis is the Eph receptor tyrosine kinase pathway. Eph proteins belong to a superfamily of receptor tyrosine kinases which are

subdivided into either subclass- A or subclass-B. They were first identified in neural development guiding axons to their targets, and subsequently found to be involved in human cancers (109) and other biological processes. The ligands for Eph proteins, ephrins, are tethered to neighboring/adjacent cell membranes and could either signal through forward or reverse signaling (110). Amidst the plethora roles of Ephs and ephrins in vascular development, tissue-border formation, cell migration, axon guidance, their roles have also been described in tumor growth and neovascularization. For example, blockade of EphA2 using soluble recombinant fusion proteins inhibited in vivo tumor angiogenesis and progression (111–113). EphA receptors promote tumor growth and also have a role in the endothelium, thereby making them a potential tumor therapeutic targets (112,114).

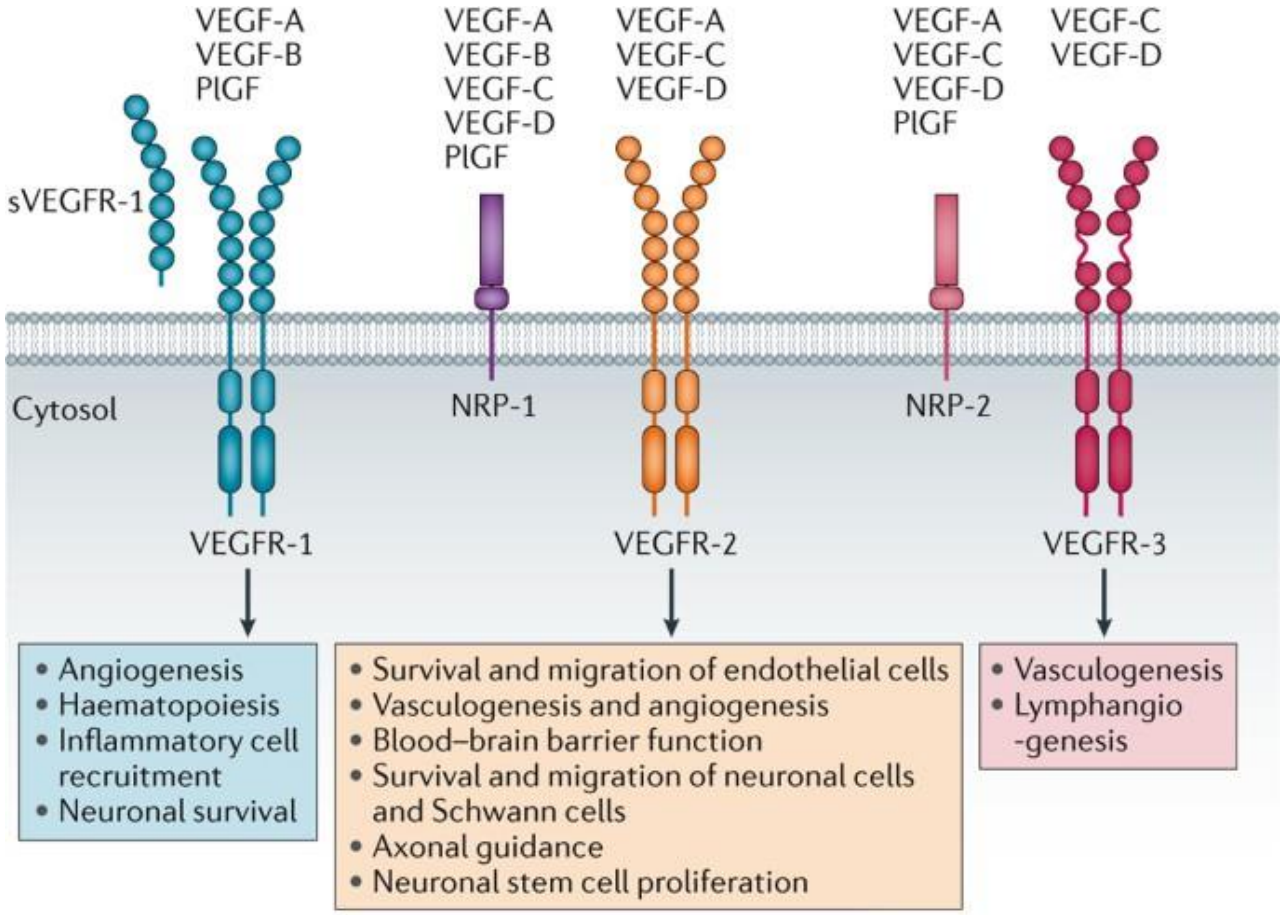

Figure 1.3: Different vascular endothelial growth factor isoforms and their binding receptors. Ligands: VEGF (also known as VEGF-A), VEGF-B, VEGF-C, VEGF-D and placental growth factor (PlGF). Receptors: VEGFR-1, VEGFR-2 and VEGFR-3 and the co-receptors neuropilin-1 (NRP-1) and NRP-2 (Reviewed in Lange et al. *Nature Reviews Neurology*, 2016

Tumor Angiogenesis

Growing tumors acquire nutrients and oxygen through diffusion. However, for solid tumors to grow beyond $2mm^3$ in diameter, they require a vascular system (115). Judah Folkman, also known as "The Father of Angiogenesis", in 1971 hypothesized that tumor growth was angiogenesis dependent. He stipulated that inhibition of angiogenesis could be a therapeutic strategy for solid malignant tumors (6). This suggested that anti-angiogenesis could hold the tumor in a non-vascularized state to restrict the tumors from nutrients, oxygen, and promote shrinkage and eventually death of the tumor (Figure 1.4). Tumor blood vessels are characterized by being morphologically abnormal and structurally dysfunctional. Compare to normal blood vessels, tumor vessels are tortuous, leaky, irregular and form chaotic networks (116). The endothelia cells that line tumor blood vessels are irregular in shape and are disorganized. These ECs also have weak junctions promoting trans-migration. In addition, pericytes coverage is lost in tumor vasculature hence resulting in poor stability.

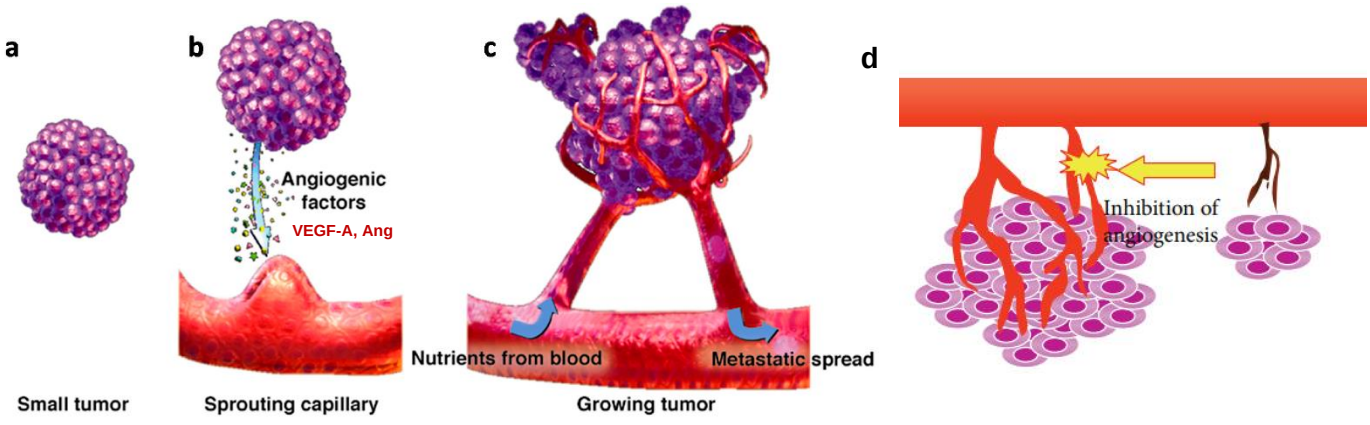

Figure 1.4: Formation of tumor angiogenesis from a small tumor (a), sprouting vessels (b), to growing tumor (c). Tumor blood vessels can be targeted using anti-angiogenesis (d). (Adapted from Loizzi et al. *Int. J. Mol. Sci.* 2017)

The chaotic nature of tumor blood vessels promotes a hostile tumor microenvironment due to poor oxygen delivery and the removal of waste resulting to a hostile hypoxic milieu. The hypoxic medium promotes cells that are in cable to withstand the harsh environment to escape hence promoting tumor progression and metastasis (117,118). Additionally, the lack of mural cell coverage on tumor blood vessels have been associated with metastasis in human cancers (119). Furthermore, abnormal tumor blood vessels prevent the delivery of drugs into the tumor parenchyma. Based on Folkman's hypothesis, antiangiogenic drugs inhibit the blood vessels and at the same time renders drug delivery difficult. In addition, the hypoxic milieu has been linked to radiation and chemotherapy resistance in breast cancer (120). Understanding the concept that abnormal tumor blood vessels result when pro-angiogenic factors outweighs the anti-angiogenic factors, Rakesh Jain hypothesized that using judicious dose of anti-angiogenic drugs would "normalize" tumor vasculature (121) (Figure1.5).

Tumor Vessel Normalization

The concept of tumor vessel normalization can be defined as re-establishing the balance between pro- and anti-angiogenic factors created during angiogenic switch. This new paradigm has indeed been validated in mouse studies which have shown that blocking VEGF/VEGFR2 using either bevacizumab (a monoclonal antibody targeted against VEGF) or DC101 (a rat monoclonal antibody targeted against mouse VEGFR2) normalized the vasculature and hence decreased interstitial fluid pressure, microvessel density and improved intratumoral perfusion (122–124). Other genetic and pharmacological strategies have been shown to promote vessel normalization to improve drug delivery and immune cell infiltration (125–128).

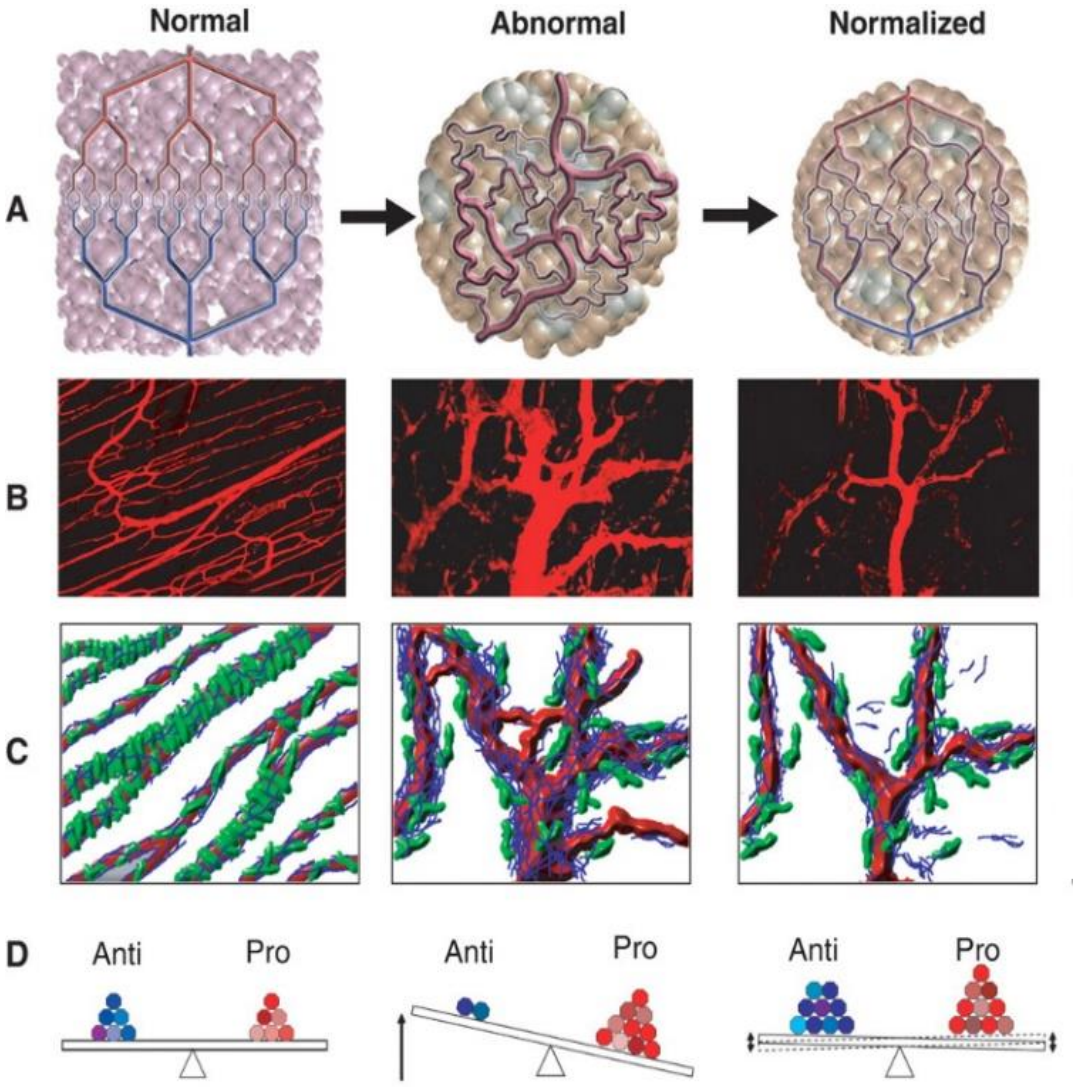

Figure 1.5: Proposed concept of tumor vessel normalization in response to antiangiogenic therapy. A and D Steps from normal to abnormal and normalized bloods vessel maintained by the perfect balance of pro-and antiangiogenic molecules. B and C showing vascular normalization induced by antiangiogenic treatment and pericytes (green) coverage from normal to normalized vessels. (Adapted from references 11 and 12)

Because leukocytes circulate through the hematogenous vasculature (129) abnormal tumor blood vessels often impair tumor infiltration of lymphocytes, which may contribute to tumor immune evasion. Increasing data suggest that tumor vessel normalization may enhance the efficacy of immunotherapy, not only by improving delivery of immune checkpoint inhibitors (ICIs) to tumors, but also by promoting new lymphocyte infiltration (130–136). Therefore, therapeutic strategies that improve vessel normalization may synergize with ICIs to improve treatment response and patient outcome. Indeed, anti-VEGF antibody increased lymphocyte infiltration and enhanced the effectiveness of adoptive immunotherapy in a B16 tumor model (137) (29). Subsets of infiltrating immune cells, including Th1 cells and eosinophils have been shown to enhance blood vessel normalization (128,138) and further attraction of infiltrating lymphocytes. Thus, immune-vascular crosstalk may mediate a feedback loop of vascular normalization and reprogramming of anti-tumor immunity.

Metabolism in Endothelial and Tumor Endothelial Cells

Glucose Metabolism

Like cancer cells, vascular ECs also reprogram their metabolism for rapid proliferation (99). The main energy provider is through the glycolysis pathway. This results in ~75-85% of ATP production (139,140). Similar to cancer cells, ECs utilize glucose under aerobic conditions resulting to lactate production (140–142). Studies have confirmed that glucose metabolism is essential for EC functionality and upkeep as inhibiting glycolysis using 2-deoxy-D-glucose promotes ECs cytotoxicity. Again, pharmacological inhibition or genetic loss of phosphofructokinase-2/fructose-2,6-biphosphatase 3 (PFKFB3) hinders ECs proliferation,

migration and sprouting (140,142,143). In addition to energy production, ECs use glucose metabolism in the pentose phosphate pathway to yield nicotinamide adenine dinucleotide phosphate (NADPH) and ribose-5-phosphate (R5P). These molecules are necessary for antioxidant defense and nucleotide biosynthesis (35).

Tumor endothelial cells (TECs) line the inner walls of tumor blood vessels. Like normal endothelial cells (NECs), TECs are hyper-glycolytic for ATP production and still maintains functional mitochondria. The hyper-glycolytic phenotype is observed due to increased expression of glucose transporter GLUT1 and the glycolytic activator PFKFB3. Inhibition of PFKFB3 in TECs promoted tumor vessel normalization and decrease tumor metastasis while promoting chemotherapy drug delivery (13,144).

Fatty Acid Metabolism

ECs utilize fatty acid metabolism to support their proliferation, differentiation and permeability. Like other cells where the mitochondria serve as the energy powerhouse, ECs use the mitochondria as a biosynthetic hub. Fatty acid derived carbons are source for production of the amino acid aspartate and deoxyribonucleotides use in DNA synthesis (145). Carnitine palmitoyltransferase 1a (CPT1a) is the rate-controlling enzyme of fatty acid oxidation. This enzyme links carnitine to long chain fatty acyls so they can be imported into the mitochondria. Once in the mitochondria, fatty acids are metabolized through beta-oxidation to yield acetyl-CoA which in turns enters the TCA cycle for energy production (146). Endothelial-specific inhibition of CPT1a has resulted to vascular sprouting defects in vivo and ablation of EC proliferation in vitro (145). Fatty acid metabolism regulates EC membrane stiffness by modulating the lipid

composition. Unlike glycolysis, which controls EC proliferation and migration, EC fatty acid metabolism controls only EC proliferation (139,140,145,146).

Compared to NECs, TECs also increase lipid production by upregulating fatty acid synthase (FASN), the rate-limiting enzyme in the FA synthesis pathway (147). Additionally, pharmacological inhibition of FASN with cerulenin and orlistat impairs lymphatic ECs viability, proliferation and migration which contributed to decrease melanoma cancer spread (148). Lymphatic ECs are not necessarily TECs, but these studies suggest that targeting fatty acid metabolism in TECs is a therapeutic potential which remains to be exploited.

Glutamine Metabolism

In addition to glucose and FA metabolism, a growing body of evidence shows that glutamine metabolism also contributes to EC proliferation, providing carbons for biomass production that is required for EC proliferation (9,14,141). Glutamine metabolism is also required for angiogenesis by contributing to the TCA cycle anaplerosis and redox homeostasis. Pharmacological inhibition or EC-specific deletion of glutaminase (GLS), blocked EC proliferation and migration (9,14). The withdrawal of glutamine from culture medium also had a similar effect. However, with the addition of asparagine in glutamine-depleted medium, EC function and protein synthesis was restored (14,32).

Glutaminolysis is important for vessel development and homeostasis in vivo. For example, pharmacological blockade of glutaminase using CB-839 in vivo suppressed pathological ocular angiogenesis (14). One mechanism of regulating glutamine metabolism in ECs is through the transforming growth factor-β (TGF-β) and Raf-MEK-ERK signaling pathways (149). Glutaminolysis is enhanced within NECs upon infection with Kaposi's sarcoma virus, rendering

these cells dependent on glutamine metabolism for survival, suggesting that glutamine may play an important role in tumor endothelial cells (150). However, there is a gap of knowledge on the role of glutamine metabolism in TECs. In this dissertation I sought to examine the role of glutaminnolysis in TECs on mammary tumor growth and progression.

Anti-angiogenic Drugs for Cancer Therapy

Disrupting the process required by tumors to grow is critical thereby making tumor angiogenesis an attractive target for cancer treatment. Cancer patients have benefited from Aanti-angiogenic drugs, however, because of resistance, insufficient efficacy and even toxicity, the responses from these drugs are not durable. In this section, the use of targeted angiogenic drugs in a clinical setting will be discussed (Figure 1.6) as well as how EC metabolism can be leveraged as an anti-angiogenic target.

Bevacizumab (Avastin) is a humanized anti-VEGF-A monoclonal antibody. Binding of bevacizumab blocks VEGF-A from binding to VEGFR1 and VEGFR2. When used as a single therapy, bevacizumab failed to improve patients' overall survival (OS) (121); however, in combination with chemotherapy, it was able to increase progression free survival and/or OS in several solids tumors including metastatic colorectal cancer, non-small cell lung cancer (NSCLC), Glioblastoma multiforme (GBM), and breast cancer (151–153).

Ziv-aflibercept (Zaltrap) is a recombinant fusion protein where key domains of human VEGFR1 and VEGFR2 are fused to the Fc portion of human IgG1. It blocks VEGF-A, B and PIGF ligands from binding to VEGFR1 and VEGFR2 receptors. It is being used in combination with 5-

fluorouracil, leucovorin, and irinotecan (FOLFIRI) in metastatic colorectal cancer patients after progression with oxaliplatin-containing regimen (154–156).

Ramucirumab (IMC-1121B) is a monoclonal antibody which targets the extracellular domain of VEGFR2 blocking VEGF-A from binding to its receptor. The regimen either as a single dose or in combination with paclitaxel is use in patients with metastatic gastric, metastatic colorectal cancer, and gastroesophageal junction cancer after progression on fluoropyrimidine or platinum-containing protocols. It is also used in addition with erlotinib as a first-line metastatic EGFR-mutated NSCLC regimen (154,156–158)

In addition to monoclonal antibodies targeting either the VEGF or the VEGF receptors, preclinical and clinical studies with small molecule inhibitors to block angiogenesis are ongoing. Sorafenib and sunitinib are tyrosine kinase inhibitors that target primarily the VEGFR2 receptor (159) . Sorafenib is used in renal cell cancer (RCC), hepatocellular cancer (HCC) and thyroid cancer while sunitinib is used in RCC, pancreatic neuroendocrine tumors, and gastrointestinal stromal tumors (GIST). Regorafenib is a TKI that blocks VEGFR1-3, KIT (platelet-derived growth factor receptor-β) and fibroblast growth factor receptor (FGFR) and is used in colorectal cancer (CRC), HCC and GIST tumors (160). Additional small molecule inhibitors are described in Table 1.2.

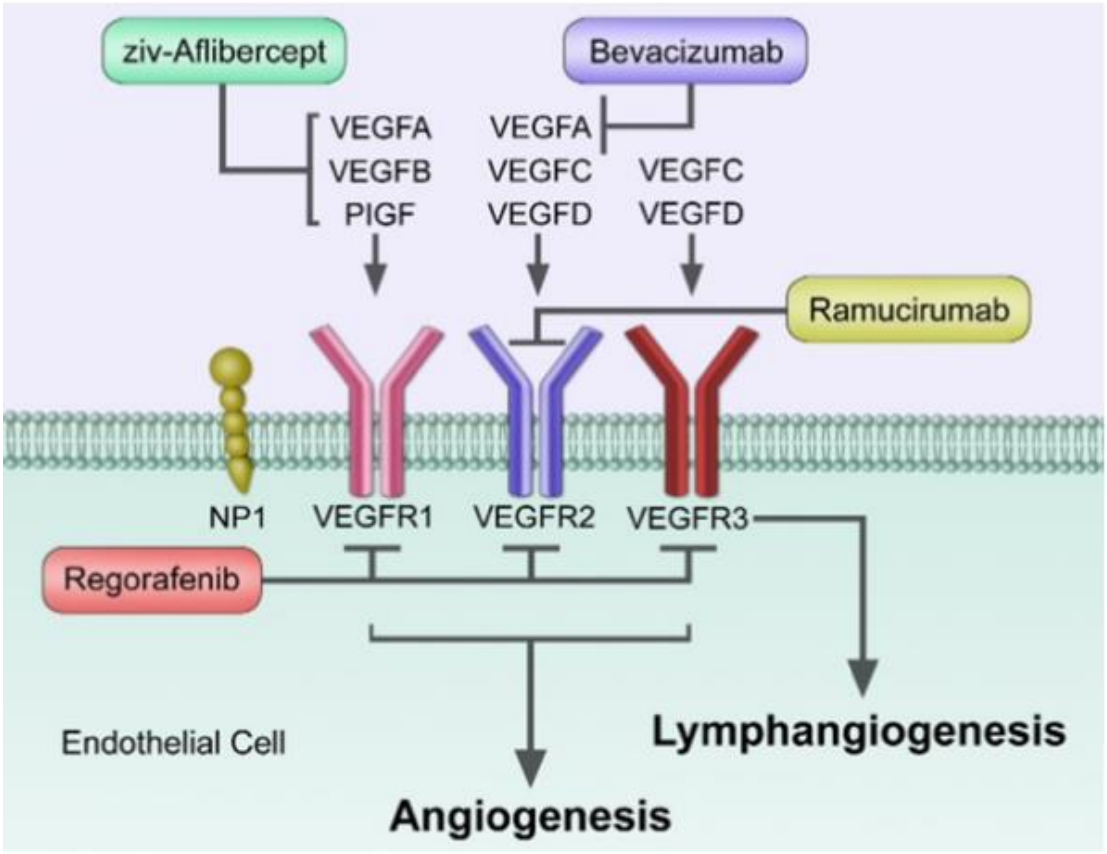

Figure 1.6: Mechanism of action of antiangiogenic drugs tarting either the ligands (VEGF-A, B, PIGF) or the receptors VEGFR-1-3 (Reviewed in Clarke et al. *Cancer Treatment Reviews* 2014)

Table 1.2: Anti-angiogenic Drugs Use in Cancer Treatment

Drug	Cancer	Mechanism	Company	Approval date
Bevacizumab (Avastin)	mCRC, NSCLC, RCC, GBM, Ovarian cancer, cervical cancer	Monoclonal anti-VEGF antibody	Genentech	Feb 26, 2004
Ziv-Aflibercept (Zaltrap)	mCRC	Recombinant fusion protein again VEGF	Sanofi and Regeneron Pharmaceuticals	Aug 3, 2012
Ramucirumab (Cyramza)	mCRC, gastric cancer, NSCLC, and HCC	Monoclonal anti-VEGFR2 antibody	Eli Lily and Company	April 21, 2014
Sorafenib (Nexavar)	RCC, HCC and thyroid cancer	TKI against VEGFRs, PDGFRs,	Bayer	December 20, 2005
Sunitinib Malate (Sutent)	RCC, pancreatic and GIST	TKI against VEGFRs, PDGFRs, CSFR1, FLT3 and RET	Pfizer	Jan 26, 2006; May 20, 2011; Nov 16, 2017
Regorafenib (Stivarga)	GIST, CRC, and HCC	TKI against VEGFRs, PDGFRs, RAF, FGFR1 KIT and RET	Bayer	September 27, 2012

Vandetanib (Caprelsa)	Medullary thyroid cancer	TKI against VEGFRs, EGFR and RET	AstraZeneca	April 6, 2011
Axitinib (Inlyta)	Advanced RCC	TKI against VEGFRs, and c-Kit	Pfizer	Jan 27, 2012
Cabozantinib (Cometriq)	Metastatic medullary thyroid cancer	TKI against VEGFRs, KIT, TRKB, FLT-3, AXL, RET	Exelixis	Nov 29, 2012

Limitations of Anti-angiogenic Therapy

Targeting VEGF/VEGFRs represented a great breakthrough in cancer patients. However, durable and complete response are rare with this treatment option. However, therapeutic resistance remains the major challenge, due in part to the heterogenous nature of tumor vasculature. Another mechanism of resistance results from several different pathways being activated upon the inhibition of VEGF/VEGFR signaling pathway trying to compensate for the blockade (161,162). Additionally, tumors are able to become vascularized using non-angiogenic methods, including vascular mimicry (formation of vascular-like structures by non-vascular cells), vessel co-option (hijacking existing vasculature of non-tumor cells in the surrounding and migrate along these vessels) and intussusception (splitting of preexisting vessels into daughter vessels)(162–164).

In addition to resistance mechanism, use of anti-angiogenic therapies are limited by adverse effects. Compared to conventional chemotherapy, these side effects are very different because the drugs function differently. The most common toxicity observed are hypertension, proteinuria, headaches, intestinal bleeding, clots in the arteries and poor wound healing (154,165–167). With toxicity and safety issues, it can be speculated that targeting the VEGF/VEGFR signaling pathway is not the best approach for future development of targeted tumor vasculature therapies. Instead, targeting the mechanisms exploited by tumor endothelial cells may be preferential. This dissertation will explore if tumor endothelial cell glutamine metabolism may represent a therapeutic option to target angiogenesis in tumors.

Summary and Thesis Project

Breast cancer and metastatic disease continue to be a significant cause of cancer mortality in women worldwide. In spite of advances in cancer research and treatment options, resistance to targeted therapies is increasing in cancer patients. Thus, it is imperative to investigate molecular mechanisms that promote breast cancer progression and metastasis as measures to better target the disease and improve patient outcomes. Deregulation of cellular energetics and tumor angiogenesis are hallmarks of cancer in which extensive research has been performed to improve therapeutic options. Targeting tumor angiogenesis was initially considered to be a sound treatment strategy aimed to block tumor blood vessels and shrink tumors by restricting nutrient delivery. Anti-angiogenic molecules have been successful in pre-clinical studies; however, limited or no efficacy has been observed clinically. This is, in part, due to tumors switching to alternative angiogenic routes or increased metastatic progression in patients.

The tumor vasculature is morphologically and functionally abnormal. These blood vessels are leaky, tortuous, irregular, heterogeneous in shape and size, and form chaotic network. Tumor blood vessels are lined by endothelial cells, but these are disorganized, irregular in shape and are associated with fewer pericytes compared to normal vessels. With the shortcomings of anti-angiogenic drugs in the clinic, exploration of other mechanisms to better target tumor angiogenesis are necessary. One such concept that has evolved is tumor vessel normalization (TVN), which aims to remodel the chaotic tumor blood vessels to restore their structure and function. This dissertation aims to explore targeting glutamine metabolism of endothelial cells as a new way to induce tumor vessel normalization and reduce breast tumor growth and metastasis.

In Chapter II, I describe the material and methods used in the studies presented in Chapter III and Chapter IV. Chapter III presents data showing the effect of vascular endothelial GLS deletion in primary tumor growth and metastasis in a model of breast cancer. This chapter further shows the role of endothelial GLS in tumor angiogenesis and in vascular integrity and function. In Chapter IV, I discus implications, future directions and limitations of this thesis. Chapters III and IV are primarily data modified from a publication in Cancer Research Communication, with some additional data not included in the manuscript (Ngwa et al. 2022).

CHAPTER II

MATERIALS AND METHODS

Animals: All animal care and experimental procedures were performed under protocols approved by Vanderbilt University's Institutional Animal Care and Utilization Committee (IACUC). All mice used in this study were immunocompetent and housed in a non-barrier animal facility. $GLS^{fl/fl}$ (C57BL/6) mice were generated as described previously (168) and provided by Dr. Jeff Rathmell (Vanderbilt University, Nashville, TN). CDH5-Cre^{ER} mice (C57BL/6) were originally generated in Dr. Ralf Adam's laboratory (Max Planck Institute, Münster, Germany) and provided by Dr. Hong Chen (Boston Children's Hospital, Harvard Medical School, Boston, Massachusetts, USA).

Genotyping: Animals were genotyped for Cre and floxed *GLS* alleles. Ear biopsy samples were digested at 55^0C overnight in 100ul BBK buffer (500mM KCl, 100mM Tris-HCL (pH 8.3), 1% Gelatin (Cat# 7765, Sigma-Aldrich), 0.1mg/ml Proteinease K (Cat# 740506, Clonetech), 0.45% IGPEAL, 0.45% Tween-20). The samples were heated at 105^0C for 15min and quickly vortexed and centrifuged at 21000 x g for 1min. One micro litter of genomic DNA was added to a 25ul of PCR reaction mix containing 12.5ul of oneTag Quick-Load 2x Master Mix (Cat# M0486L, New England Biolabs), 0.5ul forward/0.5ul reverse primers and 10.5ul molecular grade water. Genotyping primers for amplifying Cre (Forward: ACCTGAAGATGTTCGCGATTATCT;

Reverse: ACCGTCAGTACGTGAGATATCTT) and GLS (Forward: TAAGATCTGTGGCTGGTCTTCCAGG; Reverse: ACAATGTACCTGAGGGAGTTGACAGG)

were purchased from Integrated DNA Technologies (Coraville, IA) (Figure 2.1). To delete GLS specifically in the endothelium (GLS^{ECKO}), Tamoxifen (#B5965, ApexBio) was reconstituted in sunflower seed oil (#S5007, Sigma-Aldrich) at 15 mg/ml, and a dose of 2mg/kg was administered to 6-8-weeks old mice by intraperitoneal injection for 5 consecutive days.

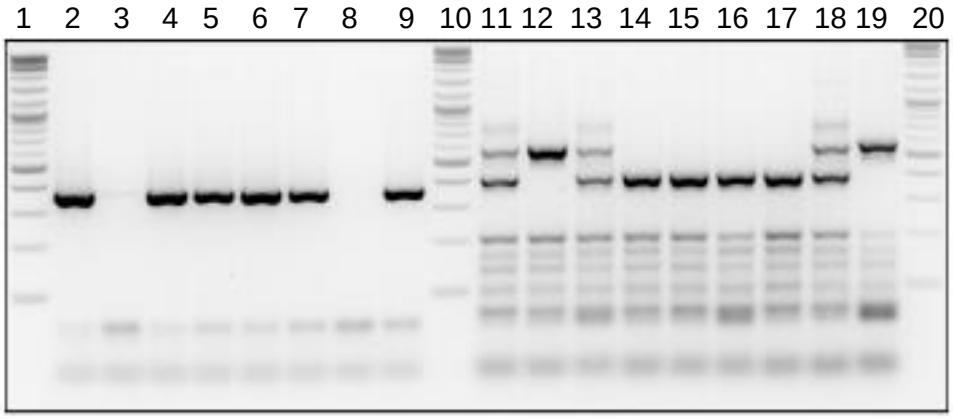

Figure 2.1: Genotyping of Ve-Cad:$Cre^{+/-}$ and $GLS^{f/f}$ by agarose gel electrophoresis. Lanes 1, 10 and 20 are 1Kb DNA ladder. Lanes 2-8 are Ve-Cad:$Cre^{+/-}$ and Lane 9 is a positive Cre control. Lanes 11-18 are GLSf/f lanes and lane 19 is a positive GLSf/f

Cell lines and cell culture: Mouse mammary cancer cell line E0771 was provided by Dr. Barbara Fingleton (Vanderbilt University) and cultured in Dulbecco's modified Eagle's medium (DMEM) (Corning #10-013-CV) supplemented with 10% fetal bovine serum (FBS) and 100 U/ml penicillin and streptomycin. MMTV-PyMT cells were first isolated (169) and provided by Dr. Rebecca Cook (Vanderbilt University) and were cultured in the same condition as above. All tumor cells were maintained at low passages after thaw and cells identities were confirmed by morphology, growth rate, cell signaling, in comparison with phenotypes described in the literature(26,170). All cells were regularly tested for mycoplasma contamination.

Endothelial cells isolation and culture from tumor bearing mice: Murine pulmonary microvascular endothelial cells were isolated from 1–3-month-old mice after tamoxifen treatment to assess GLS deletion in the endothelium. In some experiments, ECs was isolated in tumor bearing WT (GLS floxed mice) by perfusing the lungs with PBS and trypsin (**Figure 2.2**). The cells were cultured for 3-4 days in complete EGM-2 medium containing 100 U/ml penicillin and streptomycin and seeded on 0.1% gelatin -precoated culture plates. The cells were washed with PBS and passage once in complete medium before transducing with Ad-CMV-iCre (Cat # 1045) or Ad-CMV-control (Ad-CMV-null, #1300) (Vector BioLabs) for 24hr in 0.2% serum EBM-2 medium.

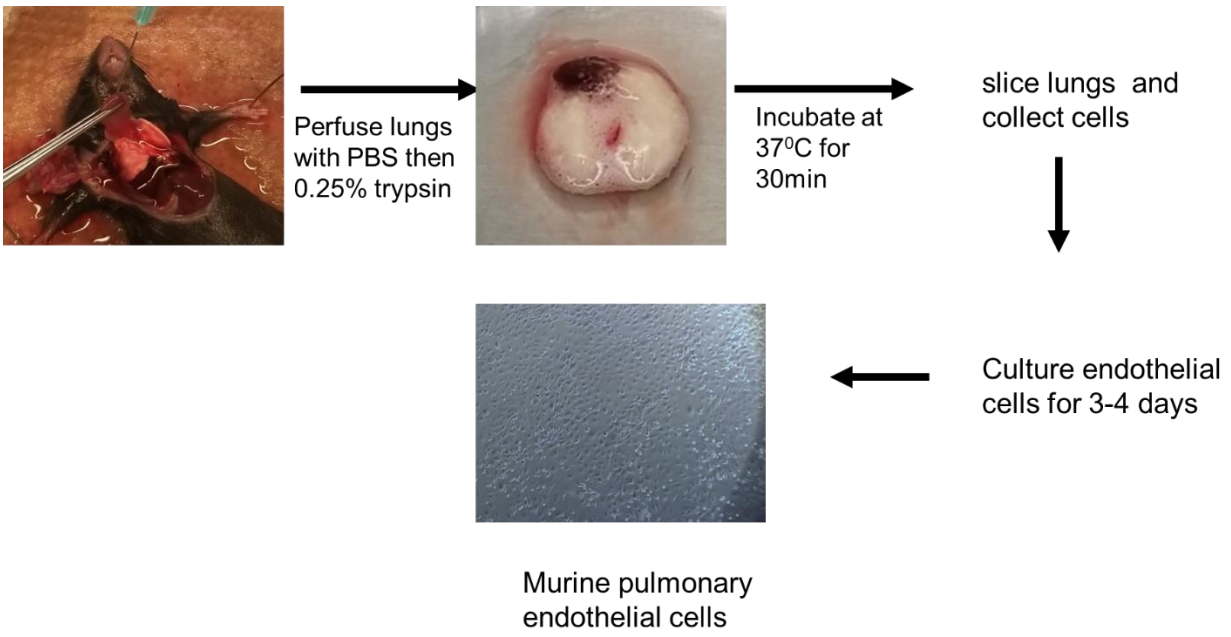

Figure 2.2 Endothelial cells isolation and culturing from mouse lungs.

Tumor model and Metastasis: For orthotopic models, E0771 cells (2.5 x 10^5) or MMTV-PyMT (5 x 10^5) in 1:1 Matrigel/medium were implanted into the #4 inguinal mammary fat pads of 6-8 weeks old female $GLS^{fl/fl}$ (WT) and CDH5-Cre^{ER}/$GLS^{fl/fl}$ treated with tamoxifen (GLS^{ECKO}). Starting on day 7, primary tumors were monitored by measuring the length (L) and width (W) every other day using a digital caliper. Tumor volume (V) was calculated using the formula ($V=LxW^2x0.5$).

For metastasis studies, E0771 cells were implanted into WT and GLS^{ECKO} mice as described above. Lungs from WT and GLS^{ECKO} were harvested on day 21 and fixed in 10% neutral buffered formalin before H&E staining. 5 sections per lung were cut at 100µm apart and metastases numbers were analyzed in a rasterized manner on 10x magnification fields. To examine lung nodules, E0771 cells implanted in WT and GLS^{ECKO} mice were resected on day 14 post -implantation and the lungs harvested on day 20 post-resection after perfusing the lungs with India ink (15% India ink, 85% dH_2O, 3 drops NH_4OH/100ml, SKU # STIIN25, Statlab). India ink injected lungs were washed in tap water and placed in fresh Fekete's solution (95% ethanol, 37% formaldehyde, glacial acetic acid) overnight (171). White tumor nodules against black lung background were counted in a blind fashion.

Immunofluorescence: Tumor cryosections were prepared as previously described (172). Tumor samples were immediately frozen in OCT compound (#50-363-579, Fisher Scientific) and kept at -80 degrees until they were further processed. 6-10µm sections were cut on Leica Cryostat CM1950. Cryosections were fixed in cold acetone for 10 minutes at room temperature followed by two washes with PBS. The sections were incubated in 3% H_2O_2 diluted in methanol for 10minutes at room temperature followed by two washes with PBS 5minutes each. Samples

were blocked with 2.5% goat serum (#G9023, Sigma-Aldrich) in PBS for 1 hour at room temperature. The following antibodies were used for immunofluorescence on cryosections: CD31 (1:100, #102501, Biolegend), α-SMA (1:100, #M085129-2, Dako), NG2 (1:100, #AB5320, Sigma-Aldrich), and GLS (1:100, #12855-1-AP, Proteintech). Apoptosis or proliferation were assessed by incubating samples with antibodies against cleaved caspase-3 (1:100, #9664, Cell Signaling Technology) or Ki-67 (1:100, #14-5698-80, eBioscience) respectively (Figure 2.3). All primary antibodies were incubated overnight at 4 degrees, followed by secondary antibodies for 1 hour at room temperature. Secondary antibodies used were goat-anti-rat–Alexa Fluor 594 (#A-11007; Invitrogen), goat-anti-mouse–Alexa Fluor 488 (#A-11001; Invitrogen), goat-anti-rabbit-Alexa Fluor 488 (#A-11006, Invitrogen) and goat-anti rabbit-Alexa Fluor 594 (# A-11012, Invitrogen**)**. Unless indicated, all secondary antibodies were used at 1:500 dilution. The α-SMA staining was performed using mouse on mouse Elite Peroxidase kit (#PK-2200, M.O.M, Vector Laboratories) to reduce background. Tumor sections were mounted using SlowFade Diamond antifade reagent containing DAPI (#S36963, Molecular Probes). Images were taken by an Olympus inverted fluorescence microscope and processed by using the Cellsens Dimension software program. Six to10 random fields (10x or 20x magnification) were taken per tumor section and analyzed using the NIH Image J software.

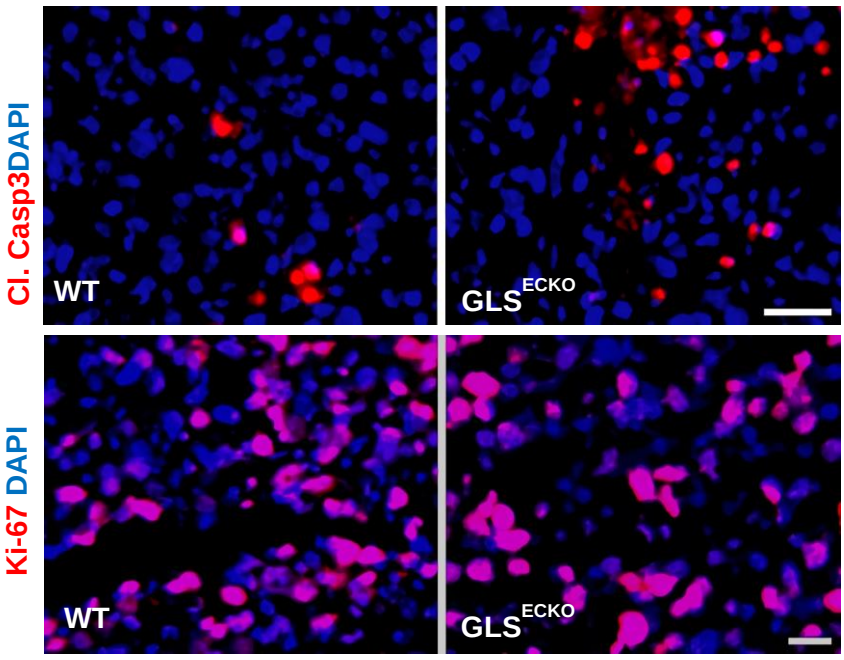

Figure 2.3: Loss of GLS in the endothelium increases apoptosis but not cell proliferation. (A) Representative immunofluorescence images of cleaved-caspase 3 (red) and DAPI (blue) in WT versus GLS^{ECKO} tumors. Scale bar: 50 µm. (B) Representative immunofluorescence images of Ki-67 (red) and DAPI (blue) in WT versus GLS^{ECKO} tumors. Scale bar: 20 µm.

Immunohistochemistry: Tumor sections were subjected to immunohistochemistry staining as previously described (1), Briefly tissue sections were fixed in acetone and incubated with 10% H_2O_2 in methanol. The sections were blocked with 2.5% goat serum and incubated at 4°C overnight with leptin antibody (1:100; #AF498-SP, R&D systems). Following several washes, samples were incubated with biotinylated anti-goat IgG antibody (H+L) (BA-9400-1.5, Vector laboratories) for 1 hr at room temperature, followed by streptavidin peroxidase reagents (#51-75477E, BD Pharmingen), liquid diaminobenzidine (DAB) (#00-2014, Invitrogen), and counter

stained with hematoxylin. Stained sections were mounted with Cytoseal XYL, and images of at least five fields of view were obtained using an Olympus inverted fluorescence microscope (40×) (Figure 2.4).

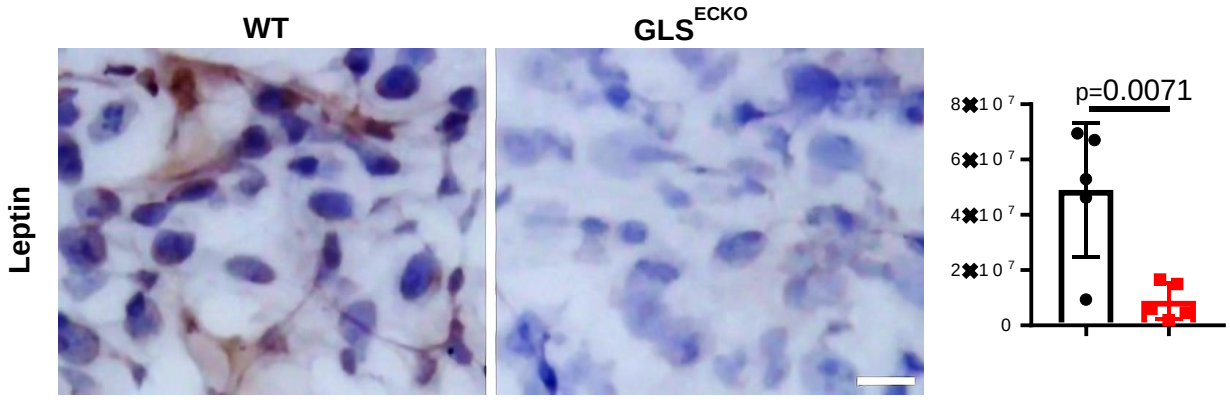

Figure 2.4: Cytokine array was performed which showed decrease leptin expression in tumor sections of GLS^{ECKO} compared to WT. Here is a representative immunohistochemistry images and quantification showing decrease leptin expression. n=5 mice per group. Scale bar: 50 µm

Tumor hypoxia and blood vessel perfusion assays: To assess tumor hypoxia, E0771 cells were implanted into WT and GLS^{ECKO} mice as described above. On day 21 post implantation, hyproxyprobe 100ul (14ng/ml, Item# HP2-100Kit, Burlington, MA) was injected intravenously for 2hrs before tumors were harvested. CD31 staining on cryosections were performed as described above. Hypoxia region was determined by assessing pimonidazole positive area per field in each tumor sample using Image J software. For vessel perfusion analysis, E0771 tumor-bearing mice were injected intravenously with 100µl of Tomato Lectin (#DL-1174, Vector Laboratories) ten minutes before tumors were harvested and processed for CD31 staining as described above. The perfused area was defined as a percentage of Lectin^{+}CD31+ of the total

$CD31^+$ area using Image J. Five to 10 random fields (20x magnification) were taken per tumor section and analyzed using the NIH Image J software.

Treatment of E0771 tumors with chemotherapeutic agents and GLS inhibitor: To examine the effect of vascular GLS deletion in response to chemotherapy, E0771 cells were implanted into WT and GLS^{ECKO} mice as described above. On day 21 post implantation, tumor bearing mice were treated with Doxorubicin HCl (5mg/kg, NDC 63323-883-05, Fresenius Kabi, USA) via retro-orbital injection (I.V). Tumors were harvested 10 minutes later. Doxorubicin (DOXO) is autofluorescent and was analyzed in conjunction with CD31 as described above to examine tumor drug delivery. To evaluate antitumor effect in a separate cohort of animals, tumor-bearing mice received cisplatin (Cpt) (4mg/kg, intraperitoneal injection) every other day for a total of seven doses starting on day 11. Lungs from these mice were perfused and fixed in 10% neutral buffer formalin and sections stained with H&E to analyze lung metastasis. 5 sections per lung were cut at 100µm apart. To inhibit GLS pharmacologically, a separate cohort of wild type female C57BL6 mice at age 7 weeks were inoculated with E0771 (2.5 x 10^5 cells). The mice were randomized on day 7 and treated with either vehicle or CB-839 (50mg/kg, #HY-12248, MedChemExpress) by i.p injection before treating with cisplatin (4mg/kg) or PBS starting on day 11. Tumor volumes were measured with a digital caliper and calculated as length x $width^2$ x 0.5.

Leptin Treatment of E0771 tumor-bearing mice: To examine the effect of vascular GLS deletion in response to exogeneous leptin treatment, E0771 cells were implanted into WT and GLS^{ECKO} mice as described above. On day 9 post tumor inoculation, mice were randomized and treated daily with either PBS or recombinant leptin 1mg/kg (L3772-1MG, Sigma-Aldrich) through i.p injection until day 24 before the mice were sacrificed on day 25. Tumor volume change was

calculated as [(V_{final}-$V_{initial}$)/$V_{initial}$]: where V_{final} = volume on last day of treatment; $V_{initial}$ = volume on first day of treatment. Tumor sections were cryo-sectioned to examine CD31 co-stained with α-SMA. Five to 10 random fields (20x magnification) were taken per tumor section and analyzed using the NIH Image J software.

Cytokine array: Cytokine antibody array analysis of 62 different targets (Table 2.1) was performed on tumor lysates from WT (n=2) and GLS^{ECKO} (n=2) using the Mouse Cytokine Array G3 (Cat: AAM-Cyt-G3-4, RayBiotech) according to manufacturer's protocol. Brief, tumors were homogenized in 1× lysis buffer and centrifuged to collect supernatants. 100 µg of proteins from each sample were analyzed. Fluorescence quantification of glass microarrays was obtained by a laser scanner (GenePix4000B; Axon Instruments). All raw cytokine array intensity data were normalized to the mean intensity of the WT according to the instructions. Each sample was analyzed as duplicate.

Table 2.1 Mouse Cytokine Antibody Array G-Series 3 Map

	A	B	C	D	E	F	G	H	I	J	K	L	M	N
1	POS1	POS2	POS3	NEG	NEG	Axl	BLC	CD30L	CD30	CD40	CRG-2	CTACK	CXCL16	CCL11
2	POS1	POS2	POS3	NEG	NEG	Axl	BLC	CD30L	CD30	CD40	CRG-2	CTACK	CXCL16	CCL11
3	CCL24	FASLG	CX3CL1	G-CSF	GM-CSF	IFN-γ	IGFBP3	IGFBP5	IGFBP6	IL-1α	IL-1β	IL-2	IL-3	IL-3 Rβ
4	CCL24	FASLG	CX3CL1	G-CSF	GM-CSF	IFN-γ	IGFBP3	IGFBP5	IGFBP6	IL-1α	IL-1β	IL-2	IL-3	IL-3 Rβ
5	IL-4	IL-5	IL-6	IL-9	IL-10	IL-12 p40/p70	IL-12 p70	IL-13	IL-17A	KC	Leptin R	Leptin (OB)	LIX	SELL
6	IL-4	IL-5	IL-6	IL-9	IL-10	IL-12 p40/p70	IL-12 p70	IL-13	IL-17A	KC	Leptin R	Leptin (OB)	LIX	SELL
7	XCL1	MCP1	MCP5	M-CSF	MIG	MIP-1α	MIP-1γ	MIP-2	MIP-3β	MIP-3α	PF4	SELP	RANTES	SCF
8	XCL1	MCP1	MCP5	M-CSF	MIG	MIP-1α	MIP-1γ	MIP-2	MIP-3β	MIP-3α	PF4	SELP	RANTES	SCF
9	SDF-1α	TARC	TCA-3	TECK	TIMP1	TNF-α	sTNFR1	sTNFR2	THPO	VCAM1	VEGF-A	NEG	NEG	NEG
10	SDF-1α	TARC	TCA-3	TECK	TIMP1	TNF-α	sTNFR1	sTNFR2	THPO	VCAM1	VEGF-A	NEG	NEG	NEG

Western blot: For immunoblotting, precleared lysates were electrophoresed by SDS–polyacrylamide gel electrophoresis and transferred to nitrocellulose membranes, which were blocked for 1 hour in 5% nonfat dry milk. Membranes were incubated with GLS primary antibody dilution at 1:1000 (#12855-1-AP, Proteintech) overnight, followed by incubation with secondary antibody for 1 hour at room temperature, and imaged using LI-COR Odyssey. Measured proteins were normalized using tubulin as a control.

ELISA: Whole tumor lysates from WT and GLS^{ECKO} were homogenized under cold conditions. The homogenate was centrifuge for 10min at 15000x g at 4^0C, and the supernatant was collected. The supernatant was directly used for leptin quantification using the mouse/rat leptin

enzyme-linked immunosorbent assay (ELISA) kit (#MOB00B, R&D Systems, Minneapolis, MN, USA), according to the manufacturer's instructions.

Glutamate assay: Intracellular glutamate concentrations were determined in duplicate using the glutamate assay kit (MAK004-1KT, Sigma-Aldrich) according to the manufacturer's instructions and as previously described (174). ECs isolated from $GLS^{fl/fl}$ mice were treated with Ad-CMV-control (WT) or Ad-CMV-iCre (GLS^{ECKO}) as described above in 0.2% serum EBM-2 medium. The cells were fed with complete medium after 24hrs for an additional 24hrs. ECs were then starved from glutamine for 24hrs and were stimulated with L-glutamine (2.5mM) in EBM-2 medium supplemented with 0.2% FBS for 30 min. Glutamate concentrations were calculated from known standards, and all data are normalized based on baseline values.

qRT-PCR assay: Total RNA was isolated and reversely transcribed using the RNeasy kit (Qiagen, #74104) and iScript, respectively, according to the manufacturer's instructions. qPCR was performed using the SYBR Green PCR Master Mix (#4368706, Thermo Fisher) on StepOne system (Applied Biosystems). Each condition was assayed in triplicate. Relative quantification was obtained by comparative CT method and relative mRNA expression was normalized to Acta2 housekeeping gene. The primer sequences used for each gene are as follows: mouse *gls*, forward: 5'- GTACAGTCTCTGTGGCTTGG -3' and reverse: 5'-CAGTTAGCGGCTCATTCAC -3'; mouse *leptin*, forward: 5'- TGCTGCAGATAGCCAATGAC-3' and reverse: 5'-AGTAGAGTGAGGCTTCCAGGA-3'; mouse leptin receptor, forward: 5'-ACACTGTTAATTTCACACCAGAG-3'; and reverse: 5'-TGGATAAACCCTTGCTCTTCA-3'; mouse pigment epithelium-derived factor (PEDF), forward: 5'-AGGACATGAAGCTACAGTCGTTGTT-3' and reverse: 5'-CTCGAAAGCAGCCCTGTGTT-3';

acta2, forward: 5'-TGACGCTGAAGTATCCGATAGA-3; reverse: 5'-GTACGTCCAGAGGCATAGAGG-3'. Quantitation was performed using the $\Delta\Delta C_t$ method.

RNA Sequencing: RNA was extracted from control (WT) or GLS-deleted ECs (GLS^{ECKO}) using the Direct-zol RNA Miniprep Kit (Zymo Research, Irvine, CA) according to manufacturer's instructions. RNA sequencing was performed by BGI Americas (Cambridge, MA) using the DNBSEQ platform. Rraw data was filtered to remove reads with high rates of unknown bases, low quality reads, and reads of adapter sequences. Clean reads were aligned to the reference genome (Mus musculus, version GCF_000001635.26_GRCm38.p6) using HISAT and aligned to reference genes using BowTie2. All analysis was performed using the Dr. Tom platform (BGI). Briefly, differentially expressed genes (DEG) between WT and GLS^{ECKO} endothelial cells were identified using DESeq2 (q value < 0.05), followed by Kyoto Encyclopedia of Genes and Genomes (KEGG) gene enrichment analysis of DEG's. To profile the entire transcriptome in WT and GLS^{ECKO} endothelial cells, gene set enrichment analysis was performed against all KEGG pathways. For both analytical enrichments, all significant pathways (q<0.05) are shown.

Flow cytometry: Tumors were dissociated in RPMI-1640 media (Corning #MT10040CV) supplemented with 5% FBS, 1 mg/ml collagenase IA (Sigma-Aldrich #C9891), and 0.25 mg/ml DNase I (Sigma-Aldrich #DN25) for 30 minutes at 37°C followed by filtering the digested tissue through a 70-µm strainer. Red blood cells were lysed using ACK Lysis Buffer (KD Medical #RGF-3015) and samples washed with PBS before staining with Ghost Dye Violet V510 (Tonbo Biosciences #13-0870) to exclude dead cells. After washing with buffer (0.5% BSA, 2mM EDTA in PBS), samples were blocked in anti- CD16/32 mouse Fc block (Tonbo Biosciences #70-0161) and cell surface proteins were analyzed using antibodies against: CD45, TCRβ, CD4, CD8a,

CD25, CD69, CD44, CD62L, and/or CD107a. Intracellular staining for GZMB, IFN-γ, IL-4 and IL-17A, was accomplished using a Cytofix/Cytoperm solution kit (BD, 554714) on paraformaldehyde-fixed cells, according to the manufacturer's protocol. The following markers were used to define cell populations: T cells: $CD45^{+}TCR\beta^{+}$; NK cells: $CD45^{+}TCR\beta^{-}NK1.1^{+}$; Macrophage: $CD45^{+}CD11b^{+}Ly6G^{-}F4/80^{hi}$; M1-like macrophages: $MHCII^{hi}CD206^{-}$; M1-like macrophages: $MHCII^{lo}CD206^{+}$; M-MDSC: $CD45^{+}CD11b^{+}Ly6C^{hi}Ly6G^{-}$; PMN-MDSC: $CD45^{+}CD11b^{+}Ly6C^{-}Ly6G^{hi}$. Fluorescence minus one (FMO) sample were included in the gating controls when needed using splenocytes or tumor cell suspensions. Flow cytometry data was obtained on a BD Fortessa FACSDiva software and analyzed using FlowJo software v10.6.1. Figure 2.5 and Table 2.2 show the gating strategy and antibodies used in flow panels are detailed in Table 2.3.

Statistical analysis: Prism software was used to statistically analyze the results. Student's t test was used to compare two experimental groups. One or two-way ANOVA were used when comparing multiple experimental groups simultaneously: a significant ANOVA test shows that there was a significant difference among the groups and was corrected with either a Tukey's, Dunnett's or Sidak's Multiple Comparison Test. Error bars represent standard error of the mean (SEM) and alpha was set at 5%.

Table 2.2: Gating strategies use in flow cytometry analysis

Cell population	Gating strategy
CD45 Immune cells	Lymphocytes, single cells, live cells, $CD45^+$
TCRβ T cells	$CD45^+$, $TCR\beta^+$
CD8 T cells	$CD45^+$, $TCR\beta^+$, $CD4^-$, $CD8a^+$
CD4 T cells	$CD45^+$, $TCR\beta^+$, $CD4^+$, $CD8a^-$
NK cells	$CD45^+$, $TCR\beta^+$, $NK1.1^+$
Macrophages	$CD45^+$, $CD11b^+$, $Ly6G^-$, $F4/80^{hi}$
M1-like Macrophages	$CD45^+$, $CD11b^+$, $Ly6G^-$, $F4/80^{hi}$, $MHCII^{hi}$, $CD206^-$
M2-like Macrophages	$CD45^+$, $CD11b^+$, $Ly6G^-$, $F4/80^{hi}$, $MHCII^{lo}$, $CD206^+$
M-MDSC	$CD45^+$, $CD11b^+$, $Ly6C^{hi}$, $Ly6G^-$
PMN-MDSC	$CD45^+$, $CD11b^+$, $Ly6C^-$, $Ly6G^{hi}$

Table 2.3. Antibodies used in flow cytometry

Target	Fluorophore	Source	Dilution
CD4	PE/Dazzle-594	Biolegend #100455	1:500
CD8	VioletFluor 450	BD #560471	1:250
CD11b	FITC	BD # 557396	1:250
CD45	APC-Cy7	BD#557659	1:500
CD107a	PE	BD #558661	1:300
Ly6C	PE-Cy7	eBioscience #25-5932-80	1:1000
Ly6G(Gr1)	PerCP-Cy5.5	Biolegend #127615	1:500
TCR-β	PerCP-Cy5.5	Tonbo #65-5961	1:250
F4/80	APC	eBioscience # 17-4801-82	1:250
Nk1.1	APC	Tonbo #205941-U025	1:200
Granzyme B	PE	Invitrogen #12-8898-82	1:20
IFNγ	APC	BD #554413	1:50
IL-4	FITC	eBioscience #11-7042-82	1:20
MHC Class II (IA/IE)	RedFluro710	Biolegend #107622	1:1000
CD206	PE	Biolegend #141705	1:1000
Ghost	V510	Tonbo #13-0870-T100	1:1000

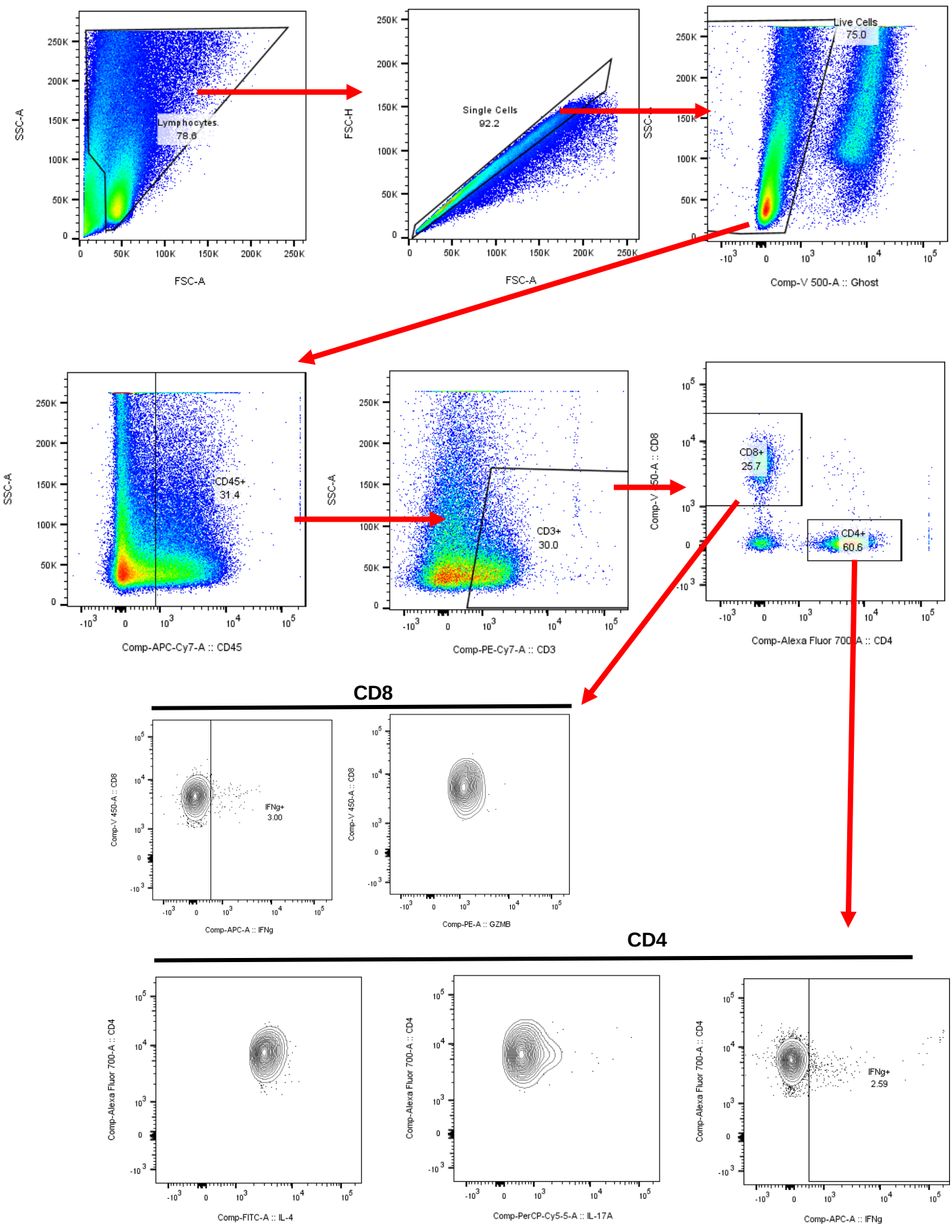
SSC-A
FSC-A
Lymphocytes
78.6
FSC-H
Single Cells
92.2
Live Cells
75.0
Comp-V 500-A :: Ghost
CD45+
31.4
Comp-APC-Cy7-A :: CD45
CD3+
30.0
Comp-PE-Cy7-A :: CD3
CD8+
25.7
CD4+
60.6
Comp-Alexa Fluor 700-A :: CD4
CD8
IFNg+
3.00
Comp-V 450-A :: CD8
Comp-APC-A :: IFNg
Comp-PE-A :: GZMB
CD4
Comp-Alexa Fluor 700-A :: CD4
Comp-FITC-A :: IL-4
Comp-PerCP-Cy5-5-A :: IL-17A
IFNg+
2.59

Figure 2.5: Flow cytometry gating strategy for T cells and activation markers. Initial gating was performed on lymphocytes, then doublets were eliminated. The single live cells were selected followed by total immune cells (CD45+). CD3+ were gated followed by CD4+ and CD8+. Activation markers were then gated from the respective CD4 or CD8 parent cells.

CHAPTER III

LOSS OF VASCULAR ENDOTHELIAL GLUTAMINASE INHIBITS TUMOR GROWTH AND METASTASIS, AND INCREASES SENSITIVITY TO CHEMOTHERAPY

The data presented in this chapter are being accepted for publication with the same title in Cancer Research Communications, 2022. Some words and figures have been edited for this dissertation.

Summary

Glutamine is the most abundant non-essential amino acid in blood stream; yet it's concentration in tumor interstitium is markedly lower than that in the serum, reflecting the huge demand of various cell types in tumor microenvironment for glutamine. While many studies have investigated glutamine metabolism in tumor epithelium and infiltrating immune cells, the role of glutamine metabolism in tumor blood vessels remains unknown. Here, we report that inducible genetic deletion of glutaminase (GLS) specifically in host endothelium, GLS^{ECKO}, impairs tumor growth and metastatic dissemination *in vivo*. Loss of GLS decreased tumor microvascular density, increased perivascular support cell coverage, improved perfusion, and reduced hypoxia in mammary tumors. Importantly, chemotherapeutic drug delivery and therapeutic efficacy were improved in tumor-bearing GLS^{ECKO} hosts or in combination with GLS inhibitor, CB-839. Mechanistically, loss of GLS in tumor endothelium resulted in decreased leptin levels, and exogenous recombinant leptin rescued tumor growth defects in GLS^{ECKO} mice. Together, these data demonstrate that inhibition of endothelial glutamine metabolism normalizes tumor vessels, reducing tumor growth and metastatic spread, improving perfusion, reducing hypoxia, and

enhancing chemotherapeutic delivery. Thus, targeting glutamine metabolism in host vasculature may improve clinical outcome in patients with solid tumors.

Significance

This study demonstrates a crucial role for glutamine metabolism in tumor endothelium, which may be exploited therapeutically to induce vascular normalization and improve drug delivery in solid tumors.

Introduction

The vasculature of a solid tumor is characterized by tortuous, leaky and chaotic networks of irregular endothelial cells (ECs) and reduction in perivascular support cells. Through impaired nutrient delivery and increased hypoxia, this dysfunctional network promotes tumor metastasis and resistance to therapy (8,142,175–177). Like cancer cells, tumor vascular endothelial cells are highly proliferative and require nutrients to support their rapid growth. Glucose metabolism has been shown to be critical in tumor endothelial cells (13,142). Targeting PFKFB3 to inhibit endothelial glycolysis promoted tumor vessel normalization, increased drug delivery and decreased metastasis (13). In addition to glycolysis, normal endothelial cells also depend on glutamine metabolism for proliferation and migration (9,14); however, the role of glutaminolysis in tumor endothelium remains to be determined. This is particularly important, as inhibitors of glutamine metabolism that potentially impact multiple cell types in the tumor microenvironment are in various stages of clinical trials.

Glutamine provides nitrogen for biosynthesis of nucleotides and amino acids, serves as a mitochondrial substrate, and fuels lipid biogenesis (50). Cells readily convert glutamine to

glutamate by glutaminase 1 and 2 (GLS1/ GLS2), the rate limiting step of glutaminolysis. High expression of *GLS1* (GLS) is associated with poor prognosis in human cancers (38,178). In addition, glutamate, a metabolite of GLS, is a precursor of glutathione, a major cellular antioxidant. Glutamine is also the source of a-ketoglutarate, which serves as a substrate for dioxygenases that modify proteins and DNA for epigenetic regulation (4). While the role of glutamine metabolism has been defined for tumor cells and a number of immune cells (24,26,88), little is known about glutamine metabolism in tumor blood vessels. Here, we assessed if targeting GLS in vascular ECs affects pathologic angiogenesis, tumor blood vessel structure and function, and tumorigenesis and metastasis, as GLS2 is expressed at low level in endothelial cells (10).

To understand the role of vascular endothelial GLS in tumor vasculature, we utilized an inducible transgenic mouse model to delete GLS specifically in the endothelium (GLS^{ECKO}) using an inducible endothelial-specific Cre. The specificity of the promoter has been previously documented (179). We showed that vascular endothelial GLS is required for tumor angiogenesis, tumor growth and metastasis. Our data reveal that GLS loss in endothelium decreases angiogenic sprouting while promoting tumor vessel normalization. GLS^{ECKO} tumors with normalized blood vessels displayed an increase in drug delivery and enhanced anti-tumor effect of chemotherapy. Mechanistically, we discovered a functional link between GLS and expression of leptin, a key regulator of metabolic homeostasis. Together, these data demonstrate a crucial role for glutamine metabolism in tumor endothelium, which may be exploited therapeutically to induce vascular normalization and improve drug delivery in solid tumors.

Results

Loss of Vascular Endothelial Glutaminase Reduces Breast Cancer Growth and Metastasis

To investigate the role of GLS in tumor vasculature, we crossed C57BL/6 mice harboring floxed *GLS* alleles ($GLS^{fl/fl}$, referred to as WT) with C57BL/6 mice expressing tamoxifen-inducible Cre recombinase (Cre^{ER}) under the control of the *Cdh5*/vascular endothelial-cadherin (VE-Cad) gene promoter. Following tamoxifen treatment, EC-specific loss of GLS mice (referred to as GLS^{ECKO}) were generated (Fig 3.1A). GLS^{ECKO} mice were viable and healthy before and following tamoxifen treatment, suggesting that GLS is not required for the survival of vascular endothelial cells in adult animals.

To induce Cre activity and delete endothelial GLS, 6-8 weeks old female mice were injected with tamoxifen daily for five consecutive days. E0771 tumor cells or cells derived from the mouse mammary tumor virus driven polyoma virus middle T antigen transgenic model (MMTV-PyMT) (169) were then orthotopically implanted into mammary fat pad of GLS^{ECKO} and WT control mice. Loss of GLS was confirmed by qRT-PCR and western blot analysis in isolated lung microvascular endothelial cells (Fig 3.1B), as well as co-localization of anti-GLS and anti-CD31 immunofluorescence in tumor sections (Fig 3.1C). Functionally, GLS deletion reduces intracellular glutamate concentration (Fig 3.1D). Endothelial GLS loss resulted in a moderate but consistently significant decrease in primary tumor volume over time (Fig 3.1E) and tumor weight at harvest (Fig 3.1F). Furthermore, the percentage of cleaved caspase 3 positive cells increased significantly (Fig 3.1G) reflecting apoptosis in GLS^{ECKO} tumors while there was no change in the percentage of Ki-67 positive cells (Fig 3.1H). In the MMTV-PyMT model, we also observed

decrease in primary tumor volume and tumor weight when GLS was deleted in the endothelium (Fig. 3.1I and J).

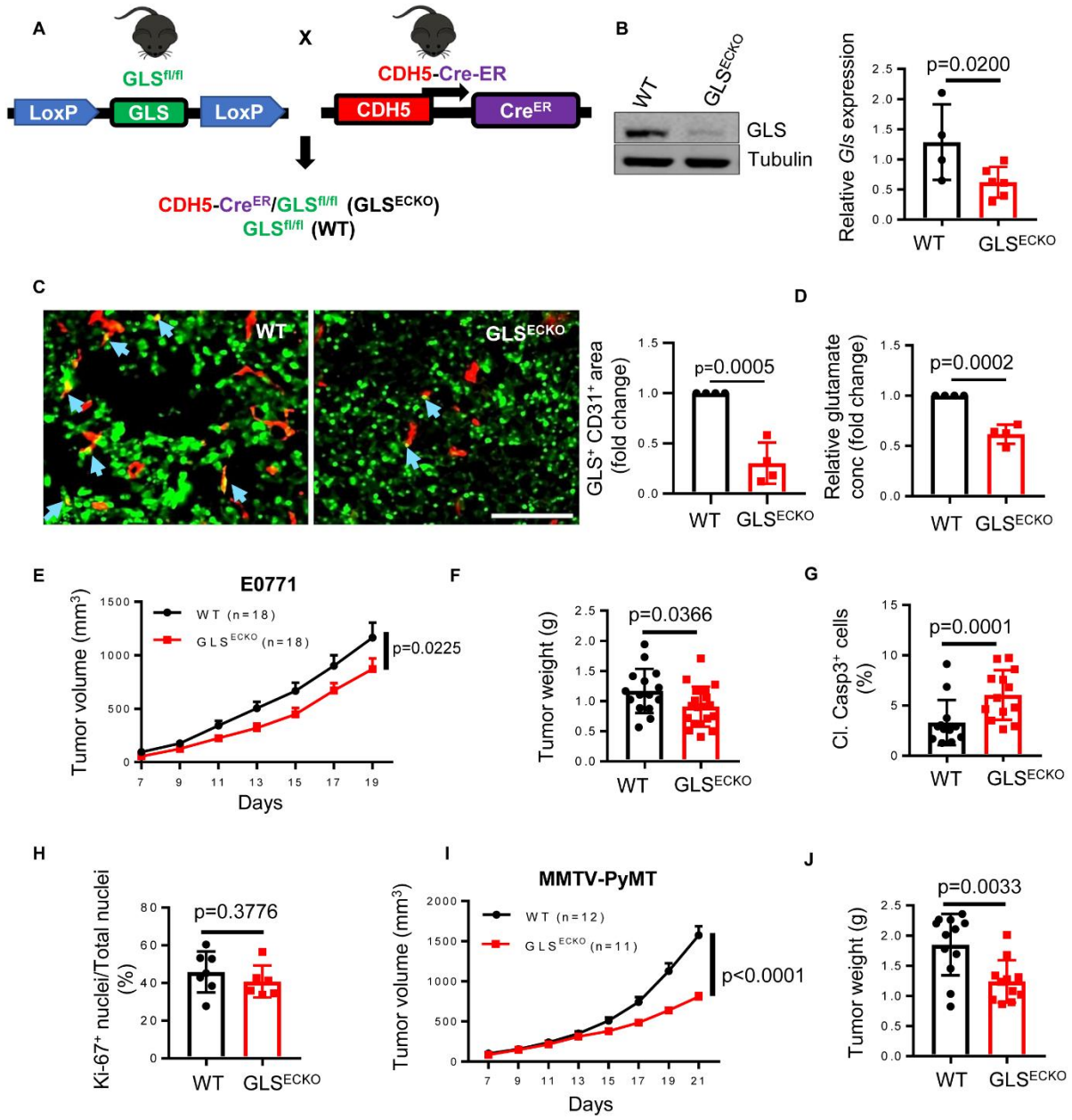
A
GLS^fl/fl
LoxP
GLS
LoxP
X
CDH5-Cre-ER
CDH5
Cre^ER
CDH5-Cre^ER/GLS^fl/fl (GLS^ECKO)
GLS^fl/fl (WT)
B
WT
GLS^ECKO
GLS
Tubulin
Relative Gls expression
p=0.0200
WT
GLS^ECKO
C
WT
GLS^ECKO
GLS+ CD31+ area (fold change)
p=0.0005
D
Relative glutamate conc (fold change)
p=0.0002
E
E0771
Tumor volume (mm3)
WT (n=18)
GLS^ECKO (n=18)
p=0.0225
Days
F
Tumor weight (g)
p=0.0366
G
Cl. Casp3+ cells (%)
p=0.0001
H
Ki-67+ nuclei/Total nuclei (%)
p=0.3776
I
MMTV-PyMT
Tumor volume (mm3)
WT (n=12)
GLS^ECKO (n=11)
p<0.0001
Days
J
Tumor weight (g)
p=0.0033

Figure 3.1: Loss of vascular endothelial glutaminase reduces breast cancer growth. (**A**) A schematic for inducible EC-specific GLS knockout model (GLS^{ECKO}). (**B**) Western analysis and qRT-PCR of mouse lung microvascular ECs showing GLS loss in GLS^{ECKO} samples. (**C**) Dual immunofluorescence images and quantification showing GLS (green) in $CD31^{+}$ (red) blood vessels of E0771 tumors grown in WT versus GLS^{ECKO} mice (n=4 mice per group; Scale bar: 200µm). Light blue arrows, GLS^{+} tumor ECs. (**D**) Intracellular glutamate concentration measured from lung microvascular ECs isolated from GLS f/f mice and treated with Ad-control (WT) or Ad-Cre (GLS^{ECKO}). (**E**) E0771 tumor growth curves (n=18). p=0.0255, two-way ANOVA with Sidak's multiple comparisons correction test. (**F**) End-stage E0771 tumor weight in WT and GLS^{ECKO} mice (n=15-18). (**G**) Cleaved-caspase quantification in WT versus GLS^{ECKO} E0771 tumors (n=10-13 mice per group). (**H**) Ki-67 quantification in WT versus GLS^{ECKO} E0771 tumors (n=6 -7 mice per group). (**I**) MMTV-PyMT tumor growth curves (n=11-12), p=0.0001, two-way ANOVA with Sidak's multiple comparisons correction test. (**J**) End-stage MMTV-PyMT tumor weight in WT and GLS^{ECKO} mice (n=11-12). All data are presented as mean ± SEM from 2 or 3 independent experiments. P values of **B**, **C**, **D**, **F**, **G**, **H** and **J** were determined by two-tailed unpaired Student's t-test.

We assessed lung metastasis at the end of studies, three weeks after E0771 tumor implantation. There were no surface metastatic lesions observed; however, serial section (n=5/lung) of lungs revealed that the numbers of microscopic metastases in WT mice was significantly greater than that detected in GLS^{ECKO} mice (Fig 3.2A-3.2C). Additionally, we examined the area of each metastatic lesion but did not observe any significant difference between WT or GLS^{ECKO} mice, suggesting that loss of GLS in the host vasculature may reduce dissemination of cells to the lung rather than impact outgrowth of tumor cells once they arrive at the lungs. To be rigorous, we repeated these studies with a modified approach, removing primary tumors at day 14 and assessing lung surface metastatic lesions 20 days following tumor resection (Fig 3.2D). WT mice displayed significantly more visible metastatic lung nodules compare to those in GLS^{ECKO} animals (Fig 3.2E and 3.2F). Collectively, these results showed that loss of GLS in the host endothelium inhibited primary tumor growth and lung metastasis.

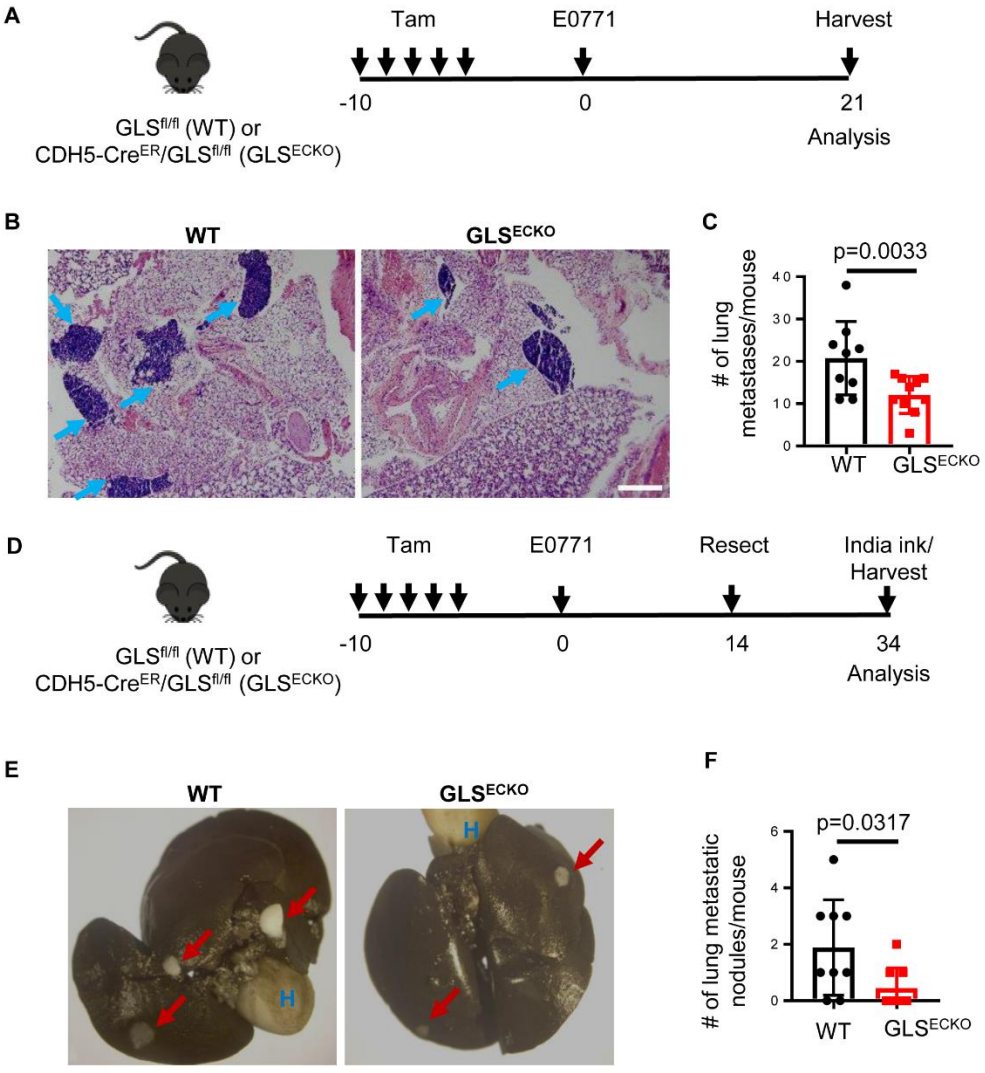

Figure 3.2: Loss of vascular endothelial glutaminase reduces breast cancer metastasis. (**A**) A schematic diagram showing the experimental procedure of tamoxifen treatment (5x: 5 times) and E0771 mammary fat pad implantation. (**B**) Representative histological images of H&E-stained lung sections from WT and GLS^{ECKO} mice (n=9-10). Scale bar: 200µm. Blue arrows denote lesions. **(C)** Quantification of metastatic lung lesions per mouse in WT versus GLS^{ECKO} (n=9-10 mice per group). **(D)** A schematic diagram showing the experimental procedure of tamoxifen treatment (5 times), E0771 mammary fat pad implantation, resection, and India ink Injection. **(E)** Representative images of India-ink-infused lungs from WT versus GLS^{ECKO} mice following primary tumor resection. Red arrows indicate metastatic foci. H (blue) indicates the position of heart. **(F)** Quantification of metastatic nodules in lungs of WT versus GLS^{ECKO} (n=9 mice per group). Data in panels **C** and **F** are presented as mean ± SEM from 2 or 3 independent experiments. P values were determined by two-tailed unpaired Student's t-test.

Endothelial GLS Deletion Reduces Tumor Vascular Density and Normalizes Tumor Vessels

To determine the impact of endothelial GLS deletion specifically on vasculature, we first assessed vascular density and maturation in multiple organs in adult animals without tumors. We did not observe significant differences between WT and GLS^{ECKO} mice in the vasculature of mammary gland, lung, kidney, and liver (Fig 3.3A-D). To investigate if GLS loss affects tumor vasculature, we analyzed tumor sections from tumors harvested two to three weeks after implantation. Compared to those from WT animals, tumors derived from GLS^{ECKO} mice had reduced microvascular density as measured by CD31 staining, suggesting that loss of GLS in the endothelium reduces angiogenic sprouts in tumors (Fig 3.4A). To assess tumor vessel integrity, CD31 positive vessels were co-stained with pericyte markers, alpha smooth muscle actin (α-SMA) or NG2. We observed that $\alpha\text{-SMA}^{+}$ or $NG2^{+}$ pericyte coverage on tumor vessels was significantly increased in GLS^{ECKO} tumors (Fig 3.4B and 3.4C), indicative of tumor vessel maturation and structural integrity.

We next evaluated tumor vessel functionality by tracing intravenously injected fluorescently labeled lectin (FITC-Lectin) as a measure of vessel perfusion. Lectin perfused vessel areas were markedly elevated in tumors of GLS^{ECKO} hosts compared to those of WT host (Fig 3.4D). Further, we examined hypoxic areas in the tumor tissue by intravenously injecting pimonidazole hydrochloride, a bioreductive chemical probe which becomes activated at low oxygen conditions (180), into E0771 tumor-bearing WT and GLS^{ECKO} mice. We observed a decrease in hypoxic tumor areas in GLS^{ECKO} E0771 tumors compared to WT tumors (Fig 3.4E), suggesting that GLS^{ECKO} tumors were less hypoxic than the WT. Taken together, these data suggest that endothelial GLS loss leads to tumor vessel normalization.

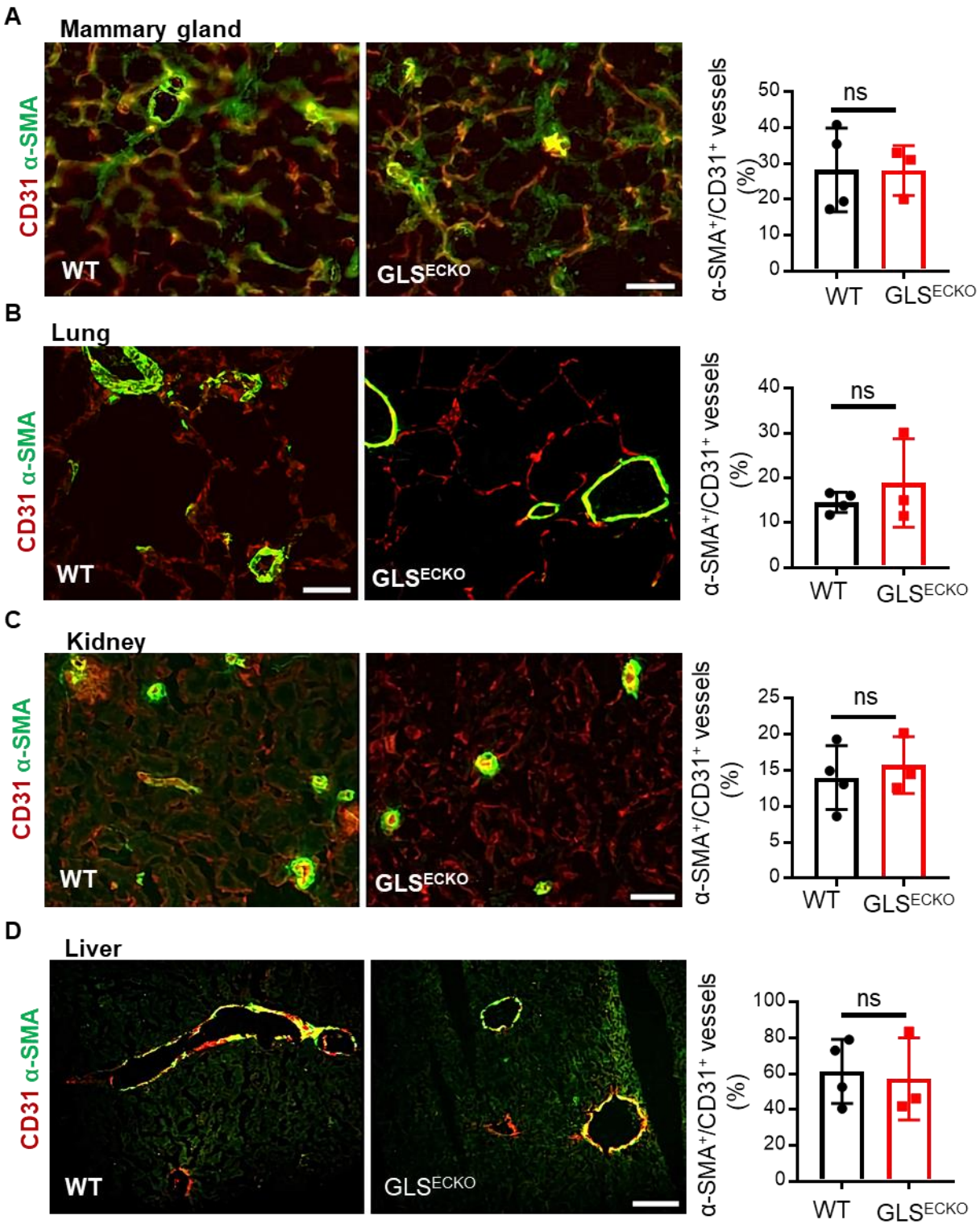

Figure 3.3: Loss of GLS in tumor-free endothelium does not affect the vasculature of adult animals. WT and GLS^{ECKO} mice were treated with tamoxifen for 5 consecutive days to induce EC-specific loss of GLS. One week following the last tamoxifen treatment, the mammary gland (**A**), Lungs (**B**), Kidneys (**C**) and Liver (**D**) were harvested and co-stained with CD31 (red) and α -SMA (green) to assess vascular integrity. n=3-4 mice per group. Scale bar: 50 µm (**A**, **B**, **C**) and 100 µm (**D**).

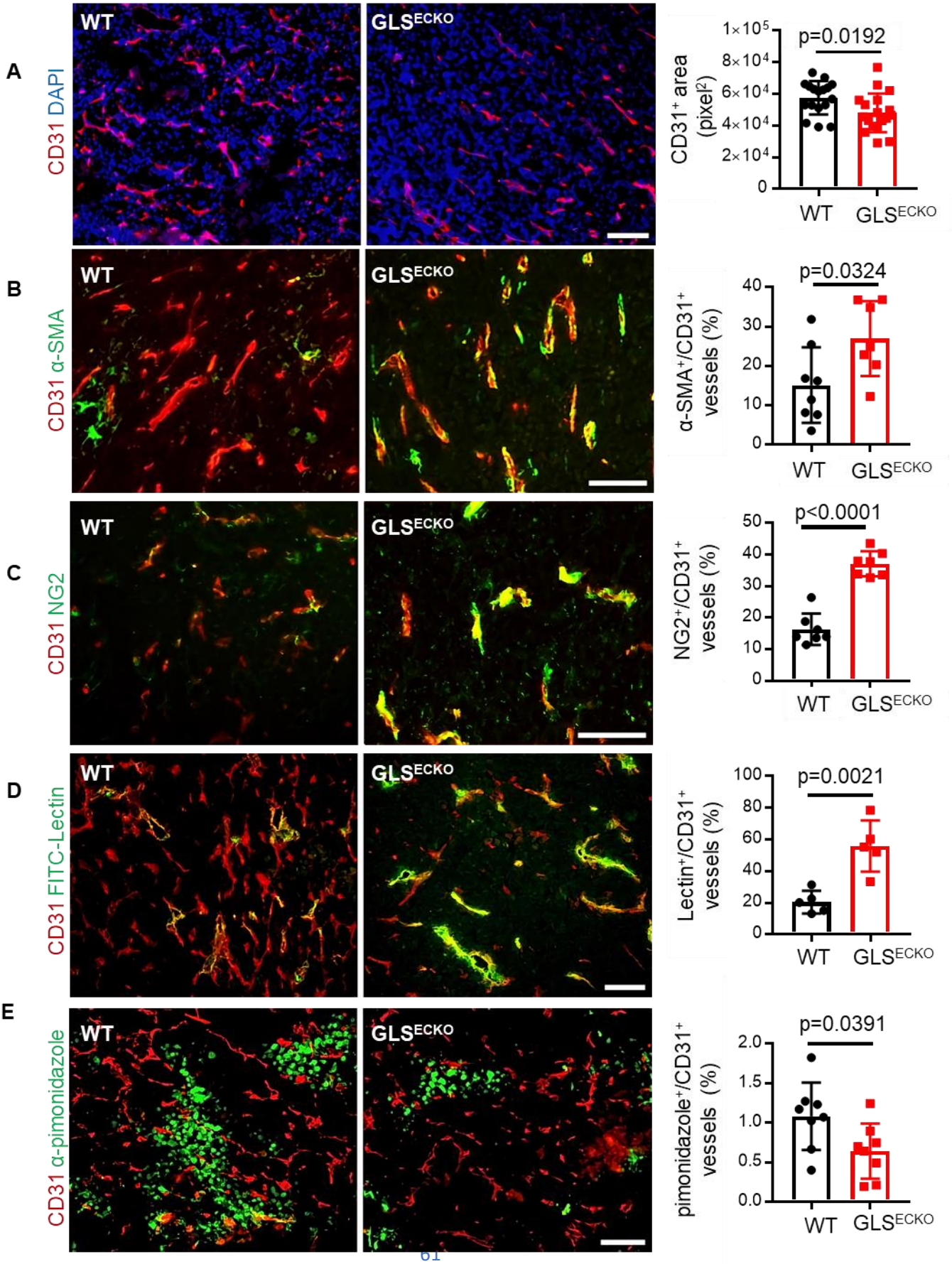
A
CD31 DAPI
WT
GLSECKO
CD31+ area (pixel2)
1×10^5
8×10^4
6×10^4
4×10^4
2×10^4
0
p=0.0192
WT
GLSECKO
B
CD31 α-SMA
WT
GLSECKO
α-SMA+/CD31+ vessels (%)
40
30
20
10
0
p=0.0324
WT
GLSECKO
C
CD31 NG2
WT
GLSECKO
NG2+/CD31+ vessels (%)
50
40
30
20
10
0
p<0.0001
WT
GLSECKO
D
CD31 FITC-Lectin
WT
GLSECKO
Lectin+/CD31+ vessels (%)
100
80
60
40
20
0
p=0.0021
WT
GLSECKO
E
CD31 α-pimonidazole
WT
GLSECKO
pimonidazole+/CD31+ vessels (%)
2.0
1.5
1.0
0.5
0.0
p=0.0391
WT
GLSECKO

Figure 3.4: Endothelial GLS deletion reduces tumor vascular density and normalizes tumor vessels. **(A)** Representative immunofluorescent images and quantification of $CD31^+$ vessels (red), DAPI (nuclei, blue) in E0771 tumors harvested from WT control and GLS^{ECKO} mice (n=10-12 mice per group). Scale bar: 100µm. **(B)** Representative immunofluorescent images and quantification of pericyte coverage (α-SMA; green) on tumor vessels (red). Pericyte coverage is presented as percentage of $\alpha\text{-SMA}^+/CD31^+$ blood vessels (yellow), (n=7-8 mice per group). Scale bar: 100µm. **(C)** Representative immunofluorescent images and quantification of pericyte coverage on tumor vessels using NG2 marker (green). n=7 per group. Scale bar: 50µm. **(D)** Representative immunofluorescent images and quantification of tumor vessel perfusion. Functional blood vessels were assessed by perfusion of FITC-lectin (green) in $CD31^+$ tumor blood vessels (red). Vessel perfusion is presented as percentage of $Lectin^+$ area within the $CD31^+$ vessels (n=5 per group). Scale bar: 100µm. **(E)** Representative immunofluorescent images and quantification of $pimonidazole^+$ hypoxic regions within E0771 tumors. Hypoxia area was assessed by injecting hydroxyprobe into tumor-bearing mice. Hypoxic regions (green) and $CD31^+$ blood vessels (red) are shown within the tumor (n=8 mice per group). Scale bar: 100 µm. All data are presented as mean ± SEM from 2 or 3 independent experiments. P values were determined by two-tailed unpaired Student's t-test.

Decreased Leptin in GLS^{ECKO} Tumors and Leptin Treatment Rescued Tumor Growth Defects in GLS^{ECKO} Mice

Tumor vessel normalization was previously shown to enhance the number and effector functions of infiltrating lymphocytes (172,181,182). However, we detected neither significant changes in tumor infiltrating $CD8^+$ cytotoxic T cells or $CD4^+$ T helper cells nor differences in NK cells, macrophages, or MDSCs between WT and GLS^{ECKO} in E0771 tumors (Fig 3.5). As a first step to determine the molecular mechanism underlying the effect of GLS deficiency on tumor growth phenotypes, E0771 tumor lysates harvested from WT or GLS^{ECKO} mice were assessed for changes in cytokine and chemokine production. While several cytokines appear to increase to varying degrees, we found that leptin was the only factor that is decreased in GLS^{ECKO} tumors (Fig 3.6A). Notably, this decrease in leptin (Lep) was accompanied by an increase in leptin receptor (LepR), suggesting that leptin signaling may be altered in GLS^{ECKO} tumors (Fig 3.6A). The decrease of leptin and increase of leptin receptor in GLS^{ECKO} tumors was further confirmed by quantitative RT-PCR analyses on isolated tumor cells (Fig 3.6B). Further validation of Lep in whole tumor lysate by ELISA with additional independent tumor samples showed that the levels of leptin were significantly decreased in tumors derived from GLS^{ECKO} mice relative to WT mice (Fig 3.6C). Consistent with cytokine array data and ELISA results, we also detected a reduction in leptin staining in the GLS^{ECKO} tumors compared to WT tumors by immunohistochemistry on tumor sections. Together, these results suggest that loss of GLS in tumor endothelium affects leptin levels in tumors.

Leptin is a protein hormone that primarily functions to regulate appetite and energy expenditure (183–186). The leptin-leptin receptor signaling is also known to play a critical role in cancer progression, including cell proliferation, metastasis, angiogenesis, and chemoresistance (187–

190). We reasoned that increased leptin receptor expression in tumors from GLS^{ECKO} mice may render these tumors sensitive to leptin treatment. To test this hypothesis and to determine if tumor growth is dependent on leptin, E0771 tumors were implanted into tamoxifen-treated mice, and the tumor-bearing animals were administered with recombinant leptin or vehicle controls (Fig 3.6D). Addition of leptin rescued defective tumor growth in GLS^{ECKO} hosts, compared with those treated with vehicle controls (Fig 3.6E and 3.6F). Additionally, leptin treatment reverses the vascular normalization phenotype in GLS^{ECKO} tumors (Fig 3.6G and 3.6H). Collectively, these data suggest that endothelial GLS deletion reduces tumor growth, at least in part, through reduced leptin levels, consistent with previously described important roles of leptin in breast cancer (187,191).

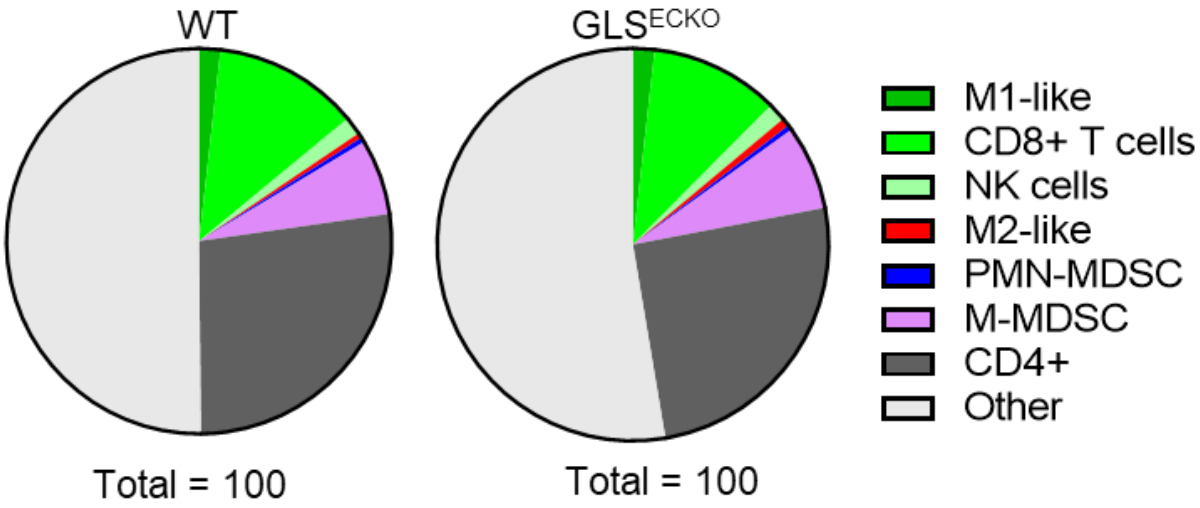

Figure 3.5: Percentages of different cell types within the E0771 tumors are presented in the pie chart.

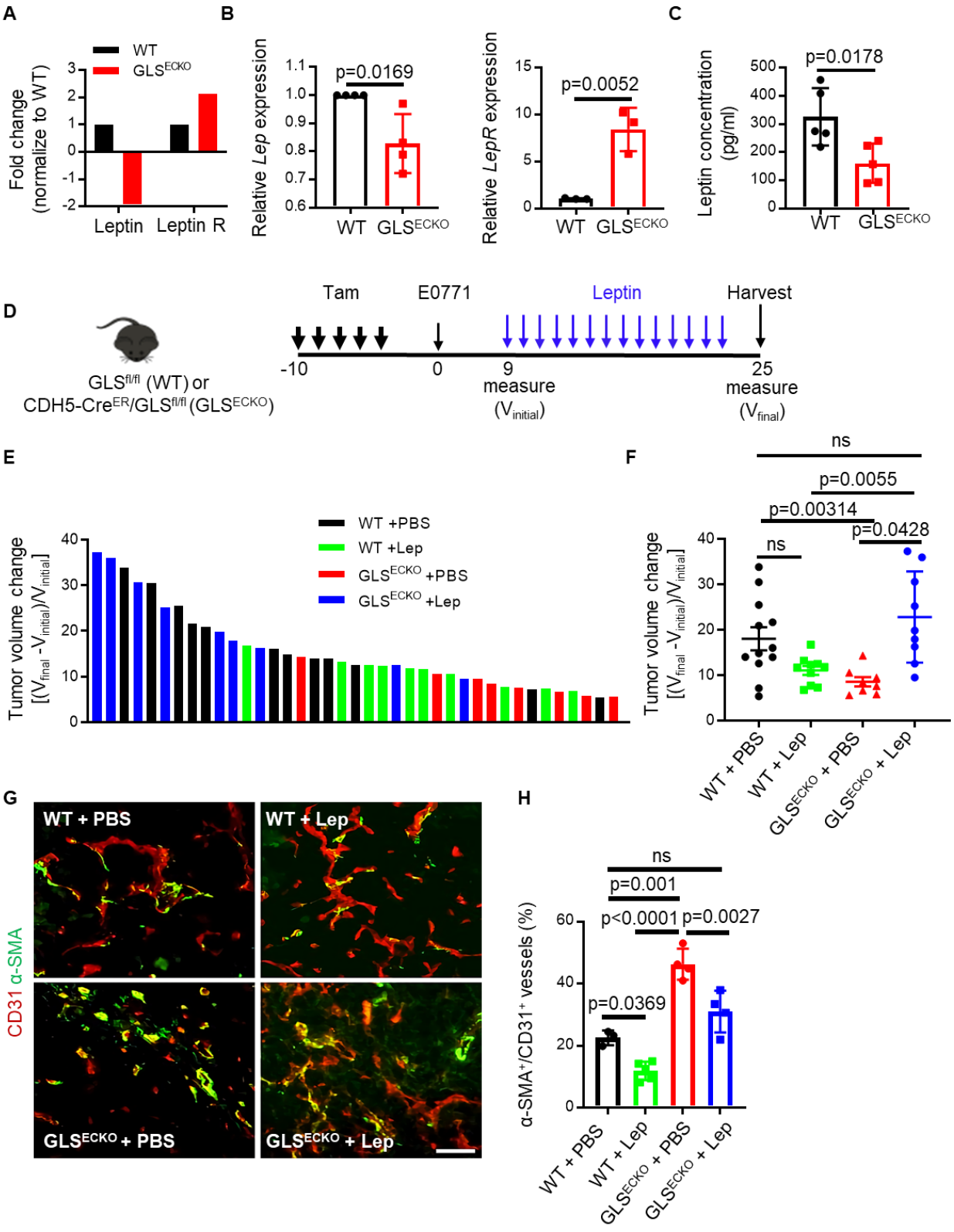
A
WT
GLS^ECKO
Fold change (normalize to WT)
Leptin
Leptin R
B
Relative Lep expression
p=0.0169
WT
GLS^ECKO
Relative LepR expression
p=0.0052
C
Leptin concentration (pg/ml)
p=0.0178
D
GLS^fl/fl (WT) or CDH5-Cre^ER/GLS^fl/fl (GLS^ECKO)
Tam
E0771
Leptin
Harvest
-10
0
9 measure (V_initial)
25 measure (V_final)
E
WT +PBS
WT +Lep
GLS^ECKO +PBS
GLS^ECKO +Lep
Tumor volume change [(V_final -V_initial)/V_initial]
F
ns
p=0.0055
p=0.00314
p=0.0428
WT + PBS
WT + Lep
GLS^ECKO + PBS
GLS^ECKO + Lep
G
WT + PBS
WT + Lep
GLS^ECKO + PBS
GLS^ECKO + Lep
CD31 α-SMA
H
α-SMA+/CD31+ vessels (%)
p=0.001
p<0.0001
p=0.0027
p=0.0369

Figure 3.6: Leptin treatment rescues tumor growth defects in GLS^{ECKO} mice. (**A**) Cytokine array showing differentially expressed leptin and Leptin receptor in WT versus GLS^{ECKO} E0771 tumor lysates. (**B**) Leptin and Leptin receptor mRNA expression was measured by qRT-PCR (n=3-4) in E0771 tumor cells isolated from WT versus GLS^{ECKO} mice. (**C**) Leptin ELISA from whole tumor lysates of WT versus GLS^{ECKO} (n=5 mice per group). (**D**) A schematic diagram of experimental design with E0771 tumor allograft and leptin treatment (1mg/kg). (**E**) Tumor volume change of WT and GLS^{ECKO} mice treated with leptin or PBS control (n=8-13) calculated as [(V_{final}-$V_{initial}$)/$V_{initial}$]. V_{final} = volume on last day of treatment; $V_{initial}$ = volume on first day of treatment. (**F**) Quantification of tumor volume change. (**G**) Representative images and quantification of α-SMA^{+}CD31^{+} vessels, showing tumor vessel normalization reversal following leptin treatment. (Scale bar: 50μm). All data are presented as ± SEM. P values were determined by two-tailed unpaired Student's t-test (**B** and **C**), One-way ANOVA with Tukey's multiple comparisons test (**F**

Loss of Endothelial GLS Promotes Delivery of Chemotherapeutic Agents

Based on the significant increase in tumor vessel perfusion observed in GLS^{ECKO} hosts, we assessed the impact of endothelial GLS loss on chemotherapeutic drug delivery. Doxorubicin (DOXO) was initially used because its autofluorescence property enables direct monitoring of the drug's penetration into the tumor. DOXO was intravenously injected three weeks following inoculation of E0771 tumors into WT and GLS^{ECKO} mice (Fig 3.7A). We observed an increase in DOXO accumulation in GLS^{ECKO} tumor sections compared to their WT control counterparts, suggesting improved delivery of the chemotherapeutic drug in GLS^{ECKO} tumors (Fig 3.7B). Because DOXO has been shown to be less potent in triple-negative breast cancer PDX and E0771 models than platinum-based therapies (173,192,193), we examined the antitumor effect of cisplatin chemotherapy in GLS^{ECKO} tumor model (Fig 3.7C). As expected (173), tumor growth was significantly reduced by loss of GLS in tumor endothelium or cisplatin (Cpt) treatment of WT animals (Fig 3.7D). However, a combination of GLS deletion in host vessels with cisplatin administration further decreased tumor growth relative to WT tumor growth (approximately 4-fold at day 25) (Fig 3.7D). H&E sections from the lungs of these mice also showed reduced metastatic lung lesions in GLS^{ECKO} mice treated with cisplatin compared to GLS^{ECKO} animals (Fig 3.7E and 3.7F). Taken together, these findings demonstrate that loss of GLS in the endothelium enhances the delivery and efficacy of chemotherapy.

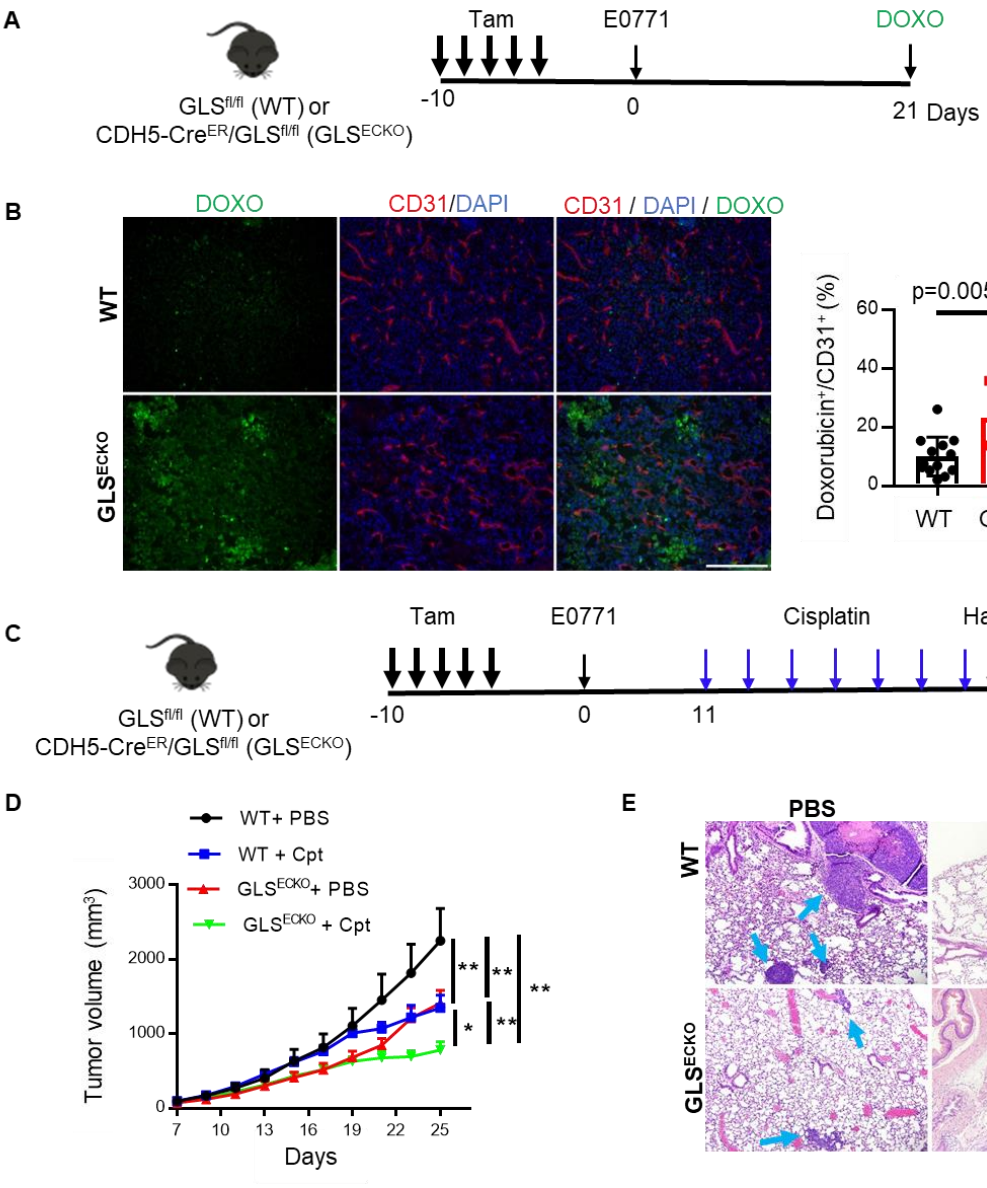
A
Tam
E0771
DOXO
GLSfl/fl (WT) or
CDH5-CreER/GLSfl/fl (GLSECKO)
-10
0
21 Days
B
DOXO
CD31/DAPI
CD31 / DAPI / DOXO
WT
GLSECKO
p=0.0055
Doxorubicin+/CD31+ (%)
60
40
20
0
WT
GLSECKO
C
Tam
E0771
Cisplatin
Harvest
GLSfl/fl (WT) or
CDH5-CreER/GLSfl/fl (GLSECKO)
-10
0
11
25 Days
D
WT+ PBS
WT + Cpt
GLSECKO+ PBS
GLSECKO + Cpt
Tumor volume (mm3)
3000
2000
1000
0
7
10
13
16
19
22
25
Days
**
**
**
*
**
E
PBS
Cpt
WT
GLSECKO

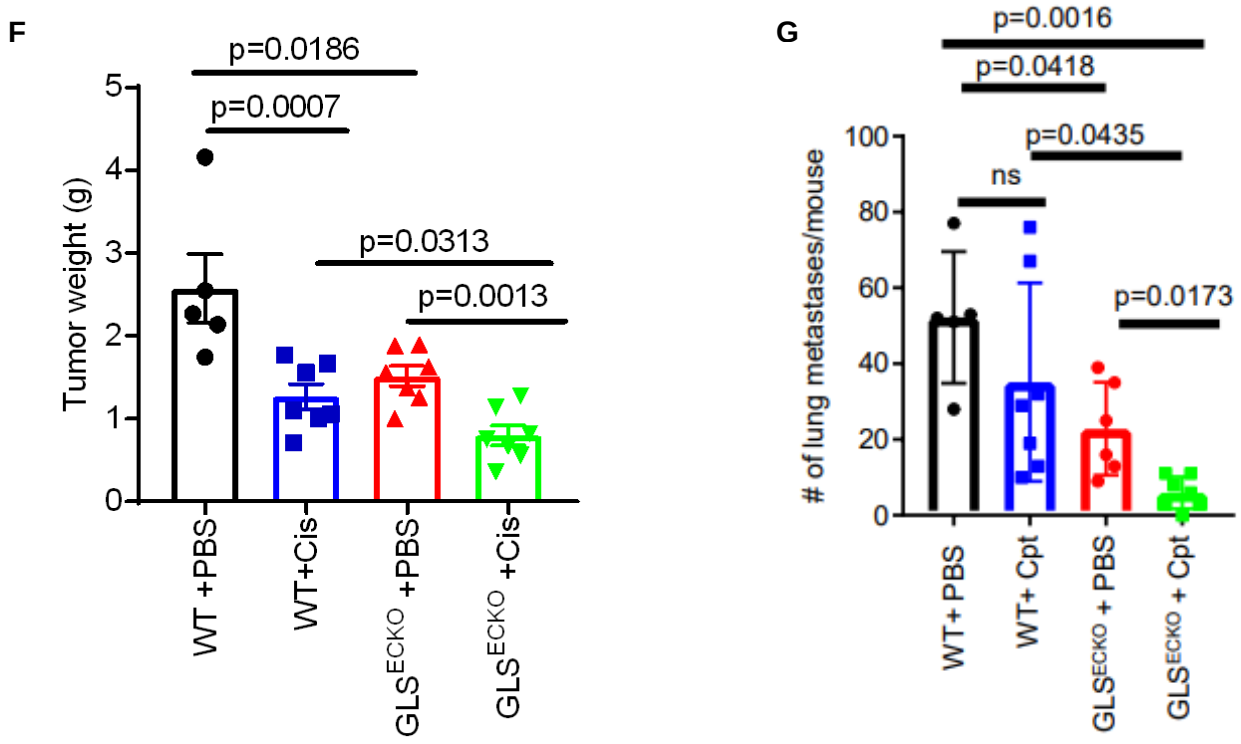

Figure 3.7: Loss of endothelial GLS enhances the efficacy of chemotherapeutic agents. (**A**) A schematic diagram showing the experimental procedure of tamoxifen (Tam) treatment (5 times), tumor implantation and doxorubicin (DOXO) treatment. **(B)** Representative images and quantification of doxorubicin autofluorescence in E0771 tumors grown in WT versus GLS^{ECKO} mice (n=13-14 mice per group). The doxorubicin^{+} area (DOXO green) is presented as a percentage of total nuclei, $DAPI^{+}$ (blue). Scale bar: 200µm. **(C)** A schematic diagram showing the experimental procedure of tamoxifen treatment (5 times), tumor inoculation, and Cisplatin (Cpt) treatment. **(D)** Growth curve of E0771 tumors grown in WT versus GLS^{ECKO} mice treated with either vehicle control (PBS) or Cisplatin (Cpt), n=6-7 mice per group. $^{**}P \leq 0.01$. $^{*}P \leq 0.05$. **(E)** Representative histological images of H&E-stained lung sections of Cisplatin and control treated WT and GLS^{ECKO} tumors (n=6-7 mice per group). Blue arrows indicate metastatic foci. Scale bar: 200µm. **(F)** End-stage E0771 tumor weight in WT and GLS^{ECKO} mice treatment groups (n=5-7) represented in **D**. **(G)** Quantification of lung metastases in WT or GLS^{ECKO} mice treated with cisplatin tumor implantation and cisplatin treatment represented in **E**. All data are presented as mean ± SEM from 2 or 3 independent experiments. P values were determined by two-tailed unpaired Student's t-test (**B**), two-way ANOVA with Tukey's multiple comparison test (**D, F** and **G**). $^{**}P \leq 0.01$. $^{*}P \leq 0.05$.

Pharmacological Inhibition of GLS Enhance Efficacy of Chemotherapeutic Agents

To investigate clinical relevance of GLS inhibition in the tumor blood vessels, we tested if pharmacologic inhibition of GLS can improve efficacy of chemotherapy. E0771 tumor cells were implanted into wild type C57BL/6 female mice. When tumors grew to approximately 60mm^3 (day 7), mice were randomized and treated with vehicle or CB-839 (50mg/kg) by i.p. injection every day for 16 days (Fig 3.8A). On day 11, animals were further randomized to receive either PBS or cisplatin (Cpt) (4mg/kg) every other day for a total of 6 doses. CB-839 monotherapy did not significantly reduce tumor growth but a combination of CB-839 and cisplatin significantly inhibited tumor growth greater than either CB-839 or cisplatin treatment alone (Fig 3.8B), suggesting that pharmacological inhibition of GLS enhances efficacy of chemotherapy, which may be leveraged to improve clinic outcome in glutamine-addicted tumors.

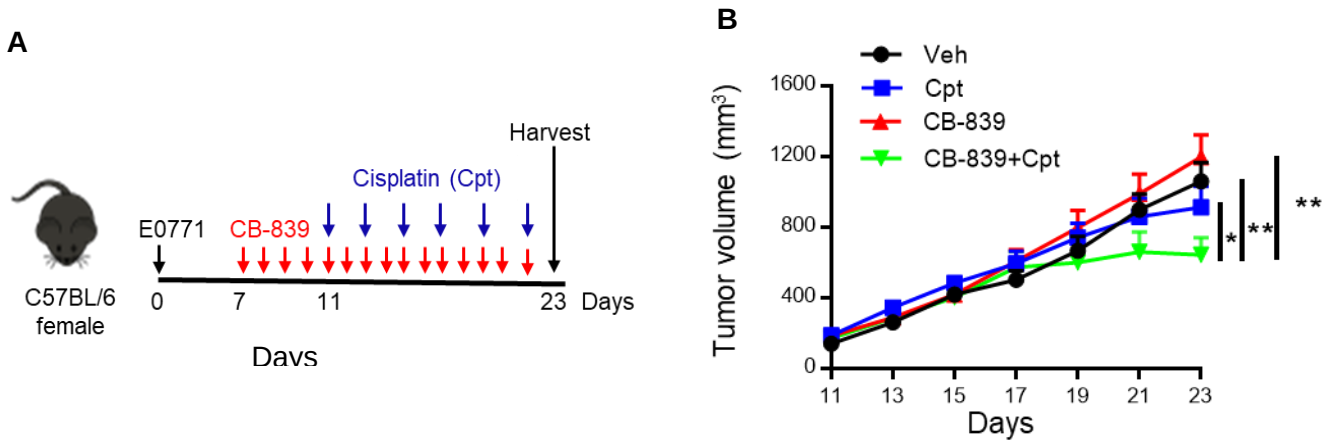

Figure 3.8: CB-839 treatment on WT mice improve drug delivery. (A) A schematic diagram showing the experimental procedure of tamoxifen treatment, tumor inoculation, CB-839 and Cisplatin (Cpt) treatment. **(B)** Growth curve of E0771 tumors upon treatment with vehicle (Veh), CB-839 (50mg/kg by i.p, daily), and Cisplatin (4mg/kg by i.p, every other day), alone or in combination with CB839 (n=6-7 per group). All data are presented as mean ± SEM from 2 independent experiments. P values were determined by two-way ANOVA with Tukey's multiple comparison test. $^{**}P \leq 0.01$. $^{*}P \leq 0.05$.

Discussion

Rapidly growing tumors require blood vessels to supply oxygen and nutrients to meet their bioenergetic and biosynthetic requirements. Cancer cells secrete angiogenic factors that promote the proliferation of tumor vascular endothelial cells, resulting in a tortuous, leaky and chaotic networks of endothelial tubes (125,194). This angiogenic process is an energy and biomass-demanding process (100). Indeed, proliferating angiogenic sprouts in tumors favor glycolysis over OXPHOS, upregulating GLUT-1 and LDH-A, and PFKFB3, all of which are key glycolytic regulators in endothelial cells (142,195). Inhibition of PFKFB3 either genetically or pharmacologically normalized tumor blood vessels, leading to suppression of tumor metastasis and improvement of drug delivery (13). Glutamine is also required for normal endothelial cell proliferation, migration, and sprouting (9,14), but its role in tumor vasculature remains unclear. Given that GLS2 expression levels are low in ECs (16) , we focused on the effects of GLS1 (GLS). We showed that loss of GLS in tumor endothelium inhibited vascular density, improved perivascular cell coverage, enhanced tissue perfusion, and reduced tumor hypoxia, leading to reduced tumor growth and metastasis and improvement of drug delivery. These data highlight the important role of glutamine in tumor blood vessel and inhibition of glutamine metabolism in the tumor vasculature may sensitize tumors to various therapeutic agents.

We demonstrated that GLS loss in tumor endothelium leads to decreased leptin but increased leptin receptor levels in E0771 tumors. In addition to its traditional role in regulating appetite and energy expenditure, leptin signaling is implicated in promoting tumor cell proliferation and migration (196–198). Although adipose cells are known to be major source of leptin (199,200), it is currently unclear how glutamine metabolism in EC precisely regulates leptin production within the mammary tumor microenvironment. In addition to leptin produced by tumor cells, we speculate that interaction between endothelial cells and adipose cells in the tumor

microenvironment accounts for dysregulation of leptin. This is based on our observation that the defective tumor growth phenotype was only observed when tumor cells were injected into the mammary fat pad, but not when the tumor cells were implanted subcutaneously with LLC and B16F10 cell lines (Figure 4.3). The reciprocal increase in leptin receptor in GLS^{ECKO} tumors may represent a compensatory response to decreased leptin level, possibly enhancing the sensitivity of tumors to leptin treatment. Indeed, administration of exogenous recombinant leptin rescued tumor growth defects and reverses the vascular normalization phenotype in GLS^{ECKO} mice, suggesting that leptin is one mechanism through which endothelial glutamine metabolism controls tumor growth.

The tumor microenvironment is a diverse landscape, containing tumor cells, immune cells, endothelial cells, and fibroblasts, among others (201). Normalization of tumor blood vessels has been recognized recently to recruit tumor infiltrating lymphocytes and enhance antitumor immune responses (128,138,172,202). Although loss of GLS in tumor endothelium normalized tumor vessels, we did not observe consistent changes in lymphocyte numbers or effector function within the time frame in our model systems. Previous studies demonstrated a positive feedback loop between CD4+ Th1 cells and vessel normalization, involving cell-cell interaction, cytokine production and pericyte maturation and coverage (181). Our data do not exclude the possibility of a role of endothelial GLS in regulating recruitment and function of tumor infiltrating lymphocytes. However, it is conceivable that in addition to tumor vessel normalization, other cytokines or factors in the microenvironment may be required for immunostimulatory reprogramming in cancer.

Addiction to glutamine in many tumors led to targeting glutamine metabolism as a means to therapeutically treat these aggressive tumors. For example, the GLS inhibitor CB-839 is

undergoing clinical trials for numerous solid tumors. Although as a single agent CB-839 has limited efficacy, our results indicate that targeting endothelial GLS genetically leads to tumor vessel normalization and increased drug delivery. Thus, CB-839 may be a good candidate for combination therapy with chemotherapeutic agents or immune checkpoint inhibitors. Indeed, our data show that CB-839 improves efficacy of cisplatin antitumor effect. Given the complex interplay between oncogenic signaling and metabolic rewiring among different cell types in the tumor microenvironment, elucidating how glutamine metabolism in endothelial cells impacts tumor growth is of great importance and could provide opportunities for therapeutic intervention.

CHAPTER IV

CONCLUSIONS AND FUTURE DIRECTIONS

Conclusions

Tumor cells alter their metabolism to incorporate sufficient nutrients into biomass production, balance redox status, and generate sufficient energy to support the rapid and uncontrolled proliferation. The theory that altered metabolism is a characteristic of cancer was made in 1920 by Otto Warburg, who observed that tumor cells consume large quantities of glucose and produce lactate even in the presence of oxygen. In addition to glucose, cancer cells have been found to exploit lipid and glutamine metabolism as sources of carbon and nitrogen to support biosynthesis, energetics and cellular homeostasis to support growth. Since these discoveries, several studies have attempted to target metabolic pathways as a treatment option for cancer. However, clinical success has been limited due to the fact that normal cells and tissues use the same enzymes and metabolic pathways. Therefore, to exploit cancer metabolism for therapeutic development, it is important to first identify the pathways that support cancer progression.

A plethora of research has been conducted targeting the aforementioned pathways in cancer cells, but recent approaches have begun to examine how metabolism in the tumor microenvironment contributes to tumor progression. Notably in the tumor vasculature, inhibition of endothelial glucose metabolism has improved vessel function leading to better perfusion and delivery of chemotherapy. In this dissertation, I investigated the role of vascular endothelial glutaminase in tumor growth, tumor vessel normalization, metastasis and drug delivery. I provided evidence that loss of GLS in the host vasculature normalizes tumor vessels to

decrease breast cancer primary growth and metastasis. Further analysis showed loss of GLS in the endothelium decreased tumor cell leptin, and administration of exogenous leptin reverses the growth and normalization phenotypes. Finally, targeting GLS both genetically and pharmacologically improves the antitumor effect of chemotherapy. The work presented in this dissertation is, to the best of my knowledge, the first to look at the role of glutamine metabolism in the tumor vasculature. These findings suggest that GLS inhibitors may improve therapeutic efficacy for existing cancer treatments in solid tumors, including chemotherapy or immunotherapy.

The work presented here has improved our understanding of the role of vascular endothelial glutaminase in breast cancer progression and metastasis. At the same time, it has opened up exciting questions as potential points for future investigations (Figure 4.1). In this chapter, I discuss these open questions, as well as the therapeutic implications of my findings, and limitations of the presented work.

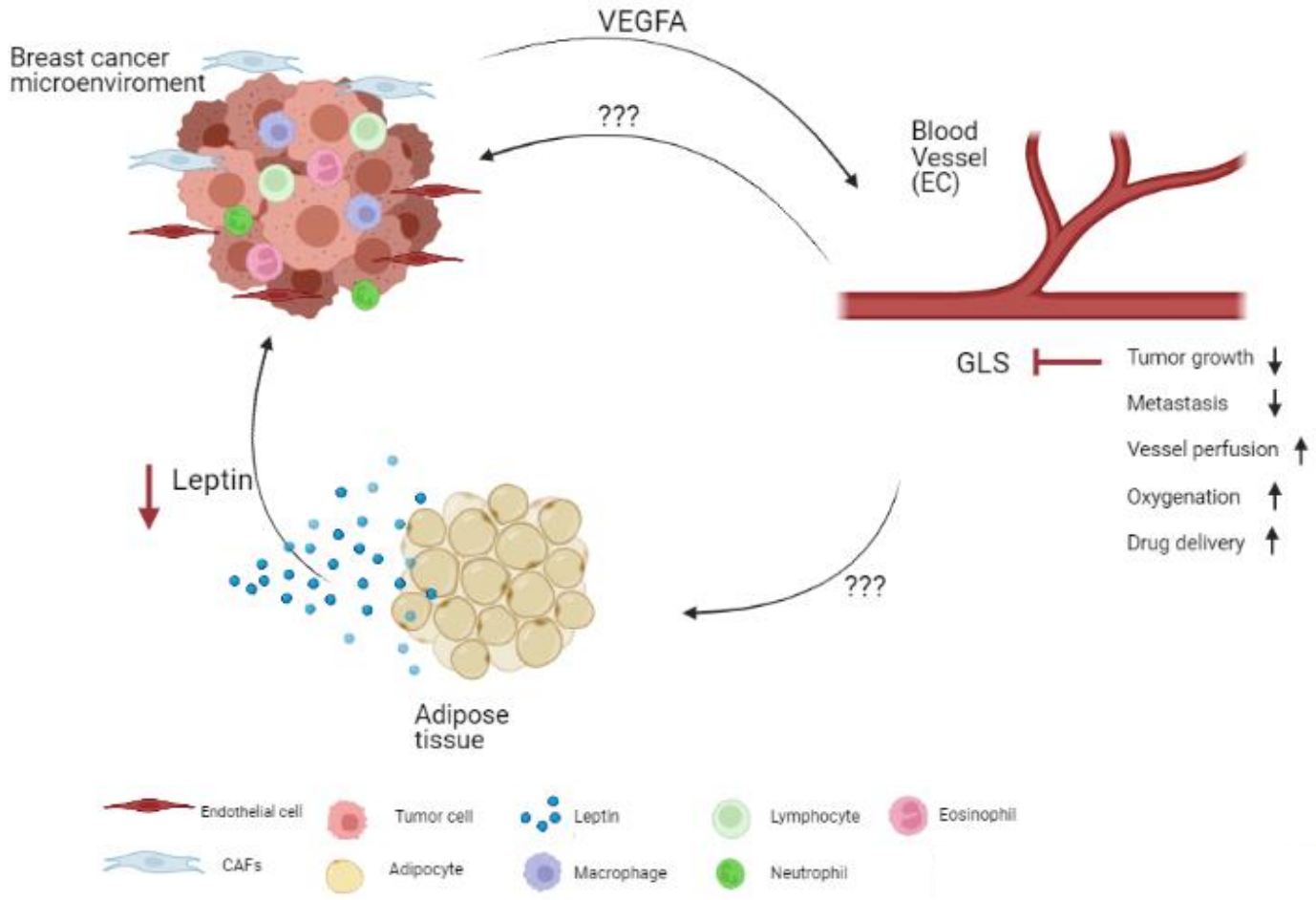

Figure 4.1: Proposed model of endothelial GLS deletion in breast tumor vasculature (Created in BioRender.com)

Future Directions

1. Open Questions

How does loss of GLS in the endothelium affect leptin secretion in the tumor cells?

I show that loss of endothelial GLS decreased leptin but increased leptin receptor (LepR) expression in tumors. While leptin is primarily secreted by adipose tissue, it can also be produced by breast cancer cells to initiate signaling through the leptin receptor (LepR) on tumor cells (203). Both in vitro and in vivo experimental models have shown that leptin supports tumor cell proliferation and survival through activation of the JAK/STAT, MAPK, and PI3K/AKT signaling cascades (203,204) (203). Additional crosstalk with growth factors and inflammatory factors can amplify these pro-tumor impacts (205). High expression of leptin and LepR are common in high grade breast cancers and have been linked with an increased risk of metastasis (206,207). Therefore, the reduction in leptin expression in response to endothelial GLS deletion may have profound impacts on tumor cell survival and metastatic potential.

The exact mechanism of how GLS loss in the endothelium decreased tumor cell leptin is unclear, but alterations in the tumor microenvironment may strongly contribute. It has been reported that hypoxia significantly increased leptin expression in breast cancer through HIF-1α (Figure 4.2A) (208). Indeed, I observe that vessel normalization phenotype in the GLS^{ECKO} tumors decreases hypoxia, which could potentially lead to decreased HIF-1α-dependent leptin expression. The leptin promoter harbors eight hypoxia-responsive elements (HRE) including the core HIF-1α binding motif 5'-RCGTC-3'. It remains to be tested if the decrease in hypoxia observed also decreased HIF-1α expression and further reduction in leptin expression by either HIF-1α CHIP-seq, immunofluorescence or western blot. If HIF-1α decreased in GLS^{ECKO}, then

constitutively activation of HIF-1α in GLS^{ECKO} would show a reverse phenotype. Similar studies may be extended to adipocytes, as it has been shown that hypoxia induces leptin expression and secretion in human adipocytes (Figure 4.2B) (209). Hypoxia-mediated changes to leptin expression by adipocytes may explain my findings that a tumor growth defect in GLS^{EKCO} animals was observed when cancer cells were implanted in the mammary fat pad but not subcutaneously (Figure 4.3).

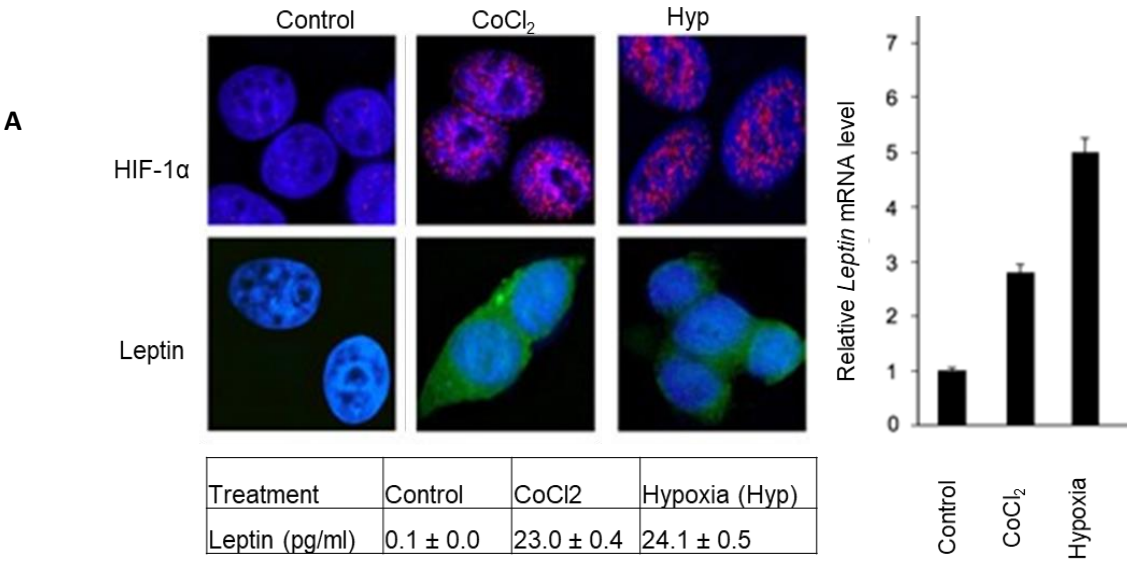

Treatment	Control	CoCl2	Hypoxia (Hyp)
Leptin (pg/ml)	0.1 ± 0.0	23.0 ± 0.4	24.1 ± 0.5

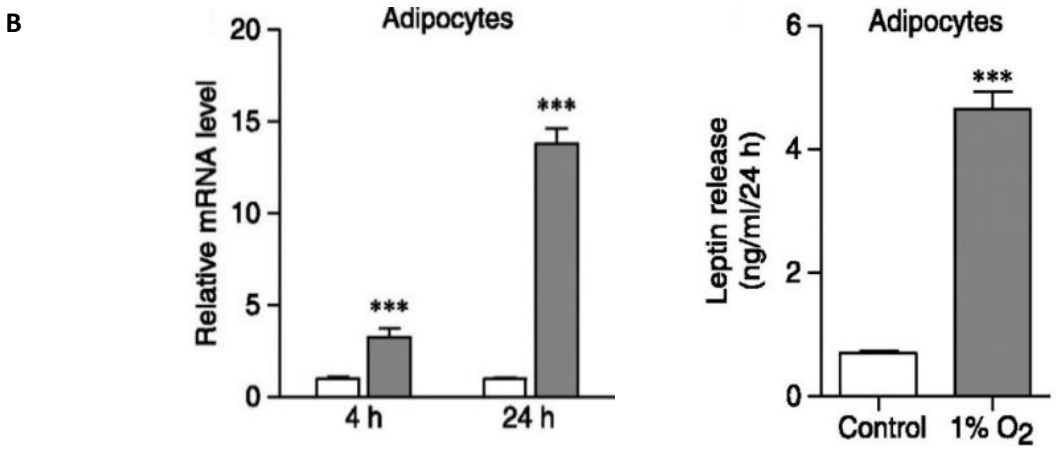

Figure 4.2: CoCL2 and hypoxia increase HIF-1α which in turn induce leptin mRNA and protein expression. A) MCF-7 cells were treated for 16 hours with CoCl2 (hypoxia inducer) or hypoxia (Hyp). HIF-1α (red) and leptin (green) increase relative with increase hypoxia. B) Adipocytes were exposed in hypoxia and nomoxia at 4 and 24 hour and leptin mRNA and protein levels were measured. (Adapted from reference Cascio et al. *Oncogene* 2008)

In addition to directly decreasing leptin signaling in tumor cells, the hypoxia reduction in GLS^{ECKO} tumors may also support further vessel normalization. RNA-seq on tumor cells isolated from GLS^{ECKO} or control WT tumors showed that endothelial GLS does not have a broad impact on the E0771 tumor cell transcriptome as only one gene, *Serpinf1/Pedf* (pigment epithelium-derived factor), was differentially expressed (Figure 4.4A). PEDF is a non-inhibitory member of the SERPIN family of serine protease inhibitors (210–214) that is commonly downregulated in human cancers including breast adenocarcinoma (215). *PEDF* expression is negatively regulated in part through HIF-1α in response to hypoxia (216). Therefore, increased *Pedf* expression in GLS^{ECKO} tumor cells, which was confirmed by qRT-PCR (Figure 4.4B), may be a consequence of reduced hypoxia in the tumor microenvironment. Of note, this glycoprotein carries a number of additional activities, including a potent anti-angiogenic function that blocks VEGF-induced angiogenesis and vascular permeability (217,218). Given that the activities of PEDF can block these important factors in tumor vascular dysfunction, increased *Pedf* expression in GLS^{ECKO} tumors has the potential to further improve vascular normalization (219). Interestingly, PEDF has also been reported to block leptin-induced angiogenesis in endothelial cells (220), suggesting that these observed changes in *Pedf* and *leptin* expression may act synergistically to improve vessel function. Therefore, PEDF is a potential candidate to play a key role in angiogenesis inhibition and vessel normalization in GLS^{ECKO} tumors. Further, by identifying the receptor through which PEDF signals in tumor cells and ablating this signaling pathway either by administering an anti-PEDF or blocking the receptor could lead to the reversal phenotype in GLS^{ECKO}. These studies open up the exciting opportunity for future investigation of the signaling loop among hypoxia, leptin and PEDF in the interplay of tumor cells, vascular endothelial cells, and adipocytes.

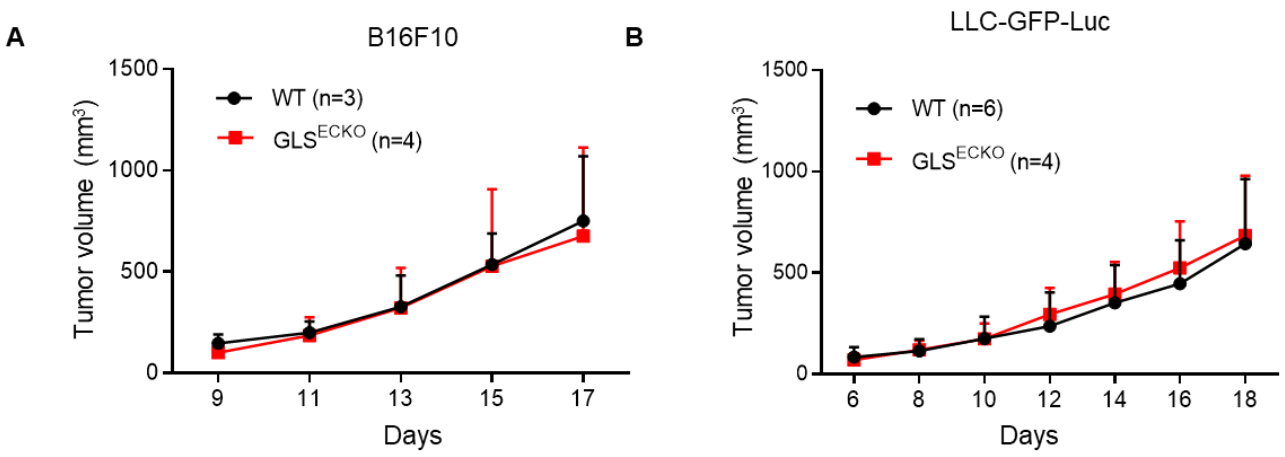

Figure 4.3: Loss of GLS in the endothelium does not affect subcutaneous tumor growth of (A) B16F10 melanoma and (B) LLC-GFP-Luc lung cancer models.

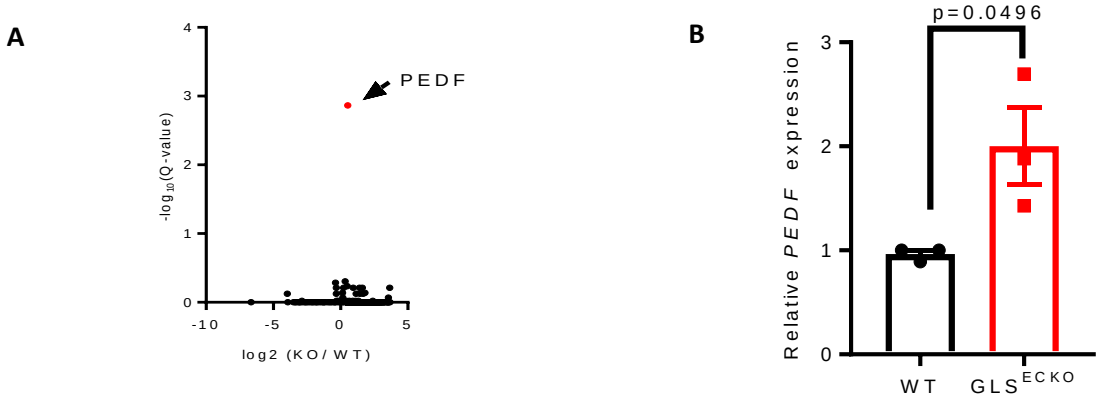

Figure 4.4: RNA-seq showing PEDF secretion from tumor cells isolated from WT vs GLS^{ECKO}. E0771 tumors were isolated from WT vs GLS^{ECKO} (**A**) and confirmed by RT-PCR (**B**).

What role does other metabolic pathways contribute to the observed phenotype in this study?

Tumor vascular endothelial cells are rapid proliferating cells that alter their metabolism to keep up with their rapid growth. Glucose, glutamine and fatty acid metabolisms are all utilized by these cells. The work presented herein showed that like glucose metabolism (13), tumor endothelial cells also use glutamine metabolism to support tumor growth. Deletion of GLS in the endothelium resulted in a consistent, although moderate, decrease in primary tumor growth in murine breast cancer models. Knowing that two variants of glutaminase (GLS/GLS1 and GLS2) are present in mammalian cells, I focused on *GLS* as *GLS2* expression in normal endothelial cells is low (14). RNA-seq data of endothelial cells demonstrated that loss of GLS in the host vasculature has an impact on the endothelial cell transcriptome (Figure 4.5). Even though expression of angiogenesis genes such as *VEGFA*, *VEGFR2* and *TEK* did not change, RNA-seq data indicated that genes involved in metabolic pathway are significantly altered, suggesting that loss of this glutamine metabolism gene leads to a switch to other metabolic pathways.

Among these metabolic changes, oxidative phosphorylation stands out as an upregulated pathway in GLS^{ECKO} ECs. It's been shown that oxidative phosphorylation (OXPHOS) and fatty acid oxidation (FAO) are key biochemical pathways involved in cellular energetics (221). FAO provides reducing equivalents to OXPHOS pathway through complex I and complex III and therefore making FAO a suitable pathway to investigate. Considering the increase in OXPHOS, it can be speculated that FAO is one metabolic pathway that compensates for the loss of endothelial GLS. One could evaluate this possibility by targeting carnitine palmitoyltransferase 1 (CPT1), the enzyme that constitutes the rate-limiting step of FAO. CPT1 converts long-chain DCA species to their respective long-chain acyl-carnitines to be transported into the mitochondria (145,222), and loss would prevent these ECs from utilizing exogenous fatty acids

hence reduce tumor growth. Alternatively, the Seahorse flux analyzer could be used to examine ROS levels in GLS^{ECKO} and further confirm if these cells are using FAO.

It has been known for a long time that nutrient sensing is important to sustain normal and tumor cell growth and proliferation. The mammalian target of rapamycin complex 1 (mTORC1) is the key nutrient sensor in the cell, given that its activation is controlled by growth factors, amino acids and stress. Growth factors alone cannot attain mTORC1 maximal activities without amino acids supplementation, suggesting amino acids are a key component of mTORC1 activation (223,224). In environments enriched with amino acids, mTORC1 localizes to the lysosomal membrane where it becomes activated (225). RNA-seq analysis of GLS^{ECKO} ECs revealed gene set enrichment of the lysosome pathway (Fig 4.5B). The lysosome is the main organelle containing digestive enzymes to degrade proteins and other macromolecules, which can serve to supplement amino acids during stress or starvation (226). Enrichment of lysosomal pathways suggest that the loss of GLS may be affecting lysosomal abundance or function and could further indicate altered mTORC1 activation (227). It would be interesting to investigate if mTORC1 signaling is affected in ECs lacking GLS, and whether this is in response to changes in amino acid or nutrient availability. This is specifically exciting as work from the lab has shown that loss of Raptor/mTORC1 in ECs promoted tumor vessel normalization to decrease tumor growth and metastasis (172), as well as altering fatty acid transportation across tumor endothelium (manuscript in preparation).

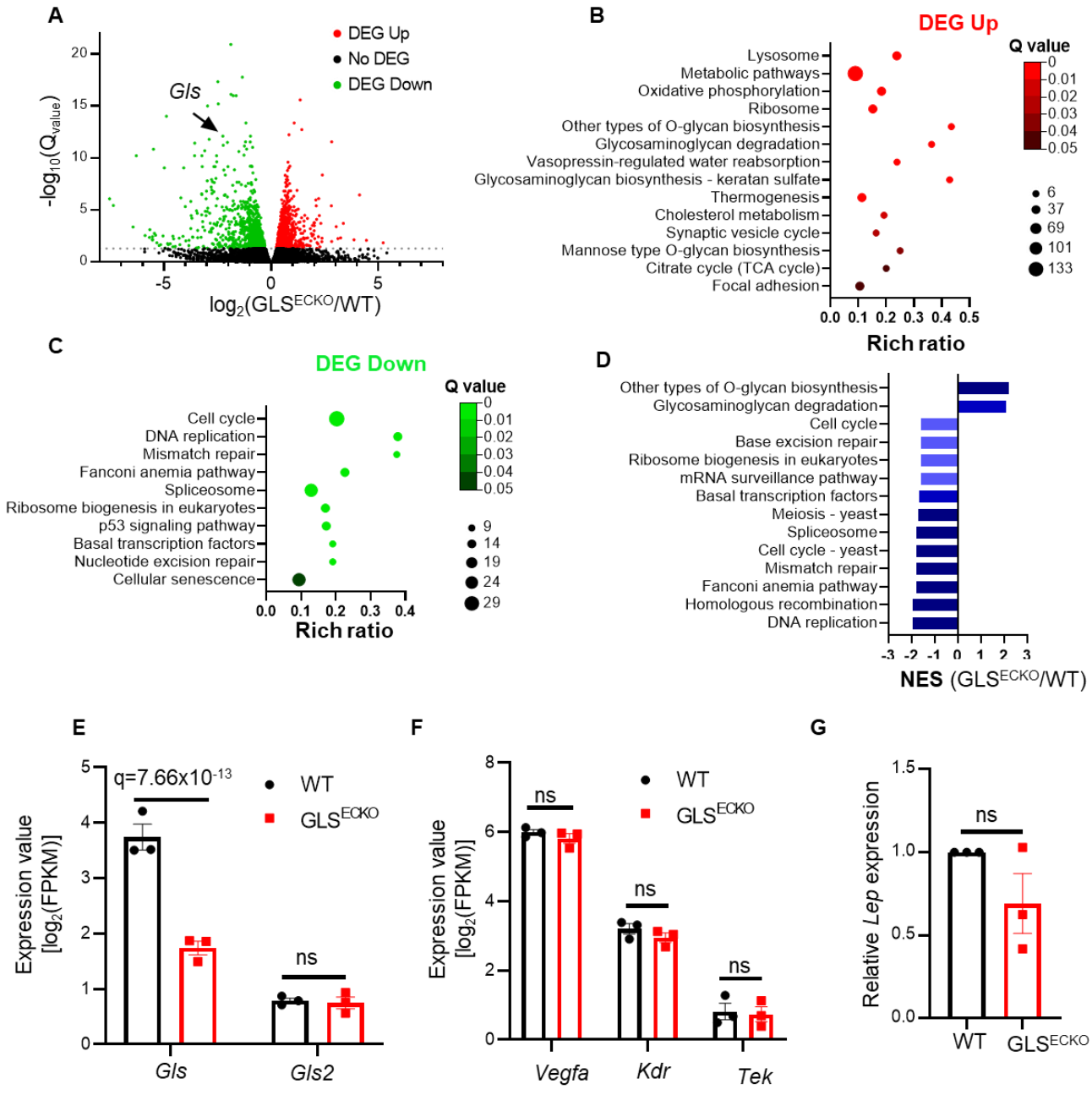
A
DEG Up
No DEG
DEG Down
Gls
-log10(Qvalue)
log2(GLSECKO/WT)
B
DEG Up
Q value
Lysosome
Metabolic pathways
Oxidative phosphorylation
Ribosome
Other types of O-glycan biosynthesis
Glycosaminoglycan degradation
Vasopressin-regulated water reabsorption
Glycosaminoglycan biosynthesis - keratan sulfate
Thermogenesis
Cholesterol metabolism
Synaptic vesicle cycle
Mannose type O-glycan biosynthesis
Citrate cycle (TCA cycle)
Focal adhesion
Rich ratio
C
DEG Down
Q value
Cell cycle
DNA replication
Mismatch repair
Fanconi anemia pathway
Spliceosome
Ribosome biogenesis in eukaryotes
p53 signaling pathway
Basal transcription factors
Nucleotide excision repair
Cellular senescence
Rich ratio
D
Other types of O-glycan biosynthesis
Glycosaminoglycan degradation
Cell cycle
Base excision repair
Ribosome biogenesis in eukaryotes
mRNA surveillance pathway
Basal transcription factors
Meiosis - yeast
Spliceosome
Cell cycle - yeast
Mismatch repair
Fanconi anemia pathway
Homologous recombination
DNA replication
NES (GLSECKO/WT)
E
q=7.66x10-13
WT
GLSECKO
ns
Expression value [log2(FPKM)]
Gls
Gls2
F
WT
GLSECKO
ns
Expression value [log2(FPKM)]
Vegfa
Kdr
Tek
G
ns
Relative Lep expression
WT
GLSECKO

Figure 4.5: RNA seq analysis of WT and GLS KO endothelial cells. Murine pulmonary microvascular endothelial cells (MPMECs) were isolated from GLS f/f mice and transduced with either Ad-Cre or Ad-control. Deletion of GLS in MPMECs was confirmed by western blot analysis. RNAs were isolated from either WT (Ad-control) or GLS^{ECKO} (Ad-Cre) endothelial cells and sent to BGI Inc. for sequencing and analysis using the Dr. Tom software. **(A)** Volcano plot of differentially expressed genes (DEG) in GLS^{ECKO} versus WT. Red and green dots mark the upregulated and downregulated genes respectively in GLS^{ECKO} compared to WT (n= 3 per group, FDR q-value < 0.05). **(B-C)** Bubble chart showing KEGG enrichment analysis of DEGs up **(B)** and DEGs down **(C)** comparing GLS^{ECKO} with WT. Circle size represents the gene number while circle color represents the value of $-\log_{10}(q_{value})$. **(D)** The mean normalized enrichment score (NES) of the gene set enrichment analysis (GSEA) comparing to GLS^{ECKO} to WT are represented by each bar. NES <0 and NES >0 represent downregulation and upregulation of specified pathways in GLS^{ECKO} versus WT respectively. **(E-G)** Expression values of Gls2, Vegfa, Kdr (Vegfr2), Tek (Tie2), and Leptin (Lep) in GLS^{ECKO} compared to WT. ns, not significant.

How does loss of GLS in the endothelium contribute to the immune profile of the tumor microenvironment?

Just like nutrients and oxygen, immune cells also require a functional vessel network to enter different tissues. Tumor associated endothelial cells (TECs) produce low levels of adhesion molecules such as vascular cell adhesion protein 1 (VCAM1) and intercellular adhesion molecule protein 1 (ICAM1), a process known as endothelial anergy. This process can have significant impacts on anti-tumor immune responses through reduced trafficking of immune cells into the tumor parenchyma (228), leading to immunologically cold tumors that are a critical challenge for immune checkpoint treatment. In addition to reversing the abnormal and dysfunctional features of the tumor vasculature as summarized in Chapter 1, tumor vessel normalization has been leveraged to promote immune cell infiltration. Indeed, vessel normalization through deletion of regulator of G protein signaling 5 (*Rgs5*) or the mTORC1 component Rptor resulted in spontaneous infiltration of CD8+ cells that was able to prolong survival of tumor bearing mice (126,172). Improved lymphocyte infiltration can also have

positive effects on the vasculature, as Tian et al. showed that CD4+ T cells activation promoted vessel normalization and further CD8+ cell infiltration (181). All of these studies prove that improved vasculature can turn cold tumors hot to further improve responses to immune checkpoint blockades treatment (229).

As shown in Chapter III and IV, I investigated whether loss of endothelial GLS promotes immune infiltration. I examined a number of factors, including infiltration of lymphocytes, T cell activation, and presence of immunosuppressive populations but did not observe significant changes in the tumor models discussed in this dissertation (Figure 3.4 and 4.6). However, cytokine array data showed many chemokines changing at varying levels in the GLS^{ECKO} E0771 tumor lysates, indicating that another phenotype may be required in addition to normalization for these cells to perform their function properly. Given that I did not observe any substantial or consistent changes in T cell populations or their functional state in these models, T cell suppression or the lack of tumor specific antigen cannot be ruled out.

Although I focused on T lymphocytes in this work, other immune cells in the innate and adaptive immune system were never explored to the same level as the T cells. Indeed, the cytokine array showed an increase in other molecules like interleukin-5 (IL-5) and eotaxin-2 (CCL-24) in GLS^{ECKO} tumors (Fig 4.7). IL-5 plays a central role in the differentiation, growth, activation of eosinophils (230) while CCL-24 induces chemotaxis of eosinophils to the allergenic site upon binding to the chemokine receptor CCR3 (231). In the context of tumors, these molecules have also been shown to induce eosinophils recruitment (232,233). While eosinophils can have multiple roles in the tumor microenvironment (234), they have also been shown to increase CD8+ T cell recruitment while also promoting vessel normalization (138). In GLS^{ECKO} MMTV-PyMT tumors, there was no change in the number of eosinophils but more carried the activation marker CD69 (Fig 4.7). Because I observed more activated eosinophils in GLS^{ECKO} tumors, it

would be important to follow up with functional studies on this cell population in the TME. Using a Siglec-F neutralizing antibody to deplete eosinophils might provide more clarity on their role in the TME and/or other immune cells of these GLS^{ECKO} tumors, particularly whether they are cytotoxic or regulatory in this model.

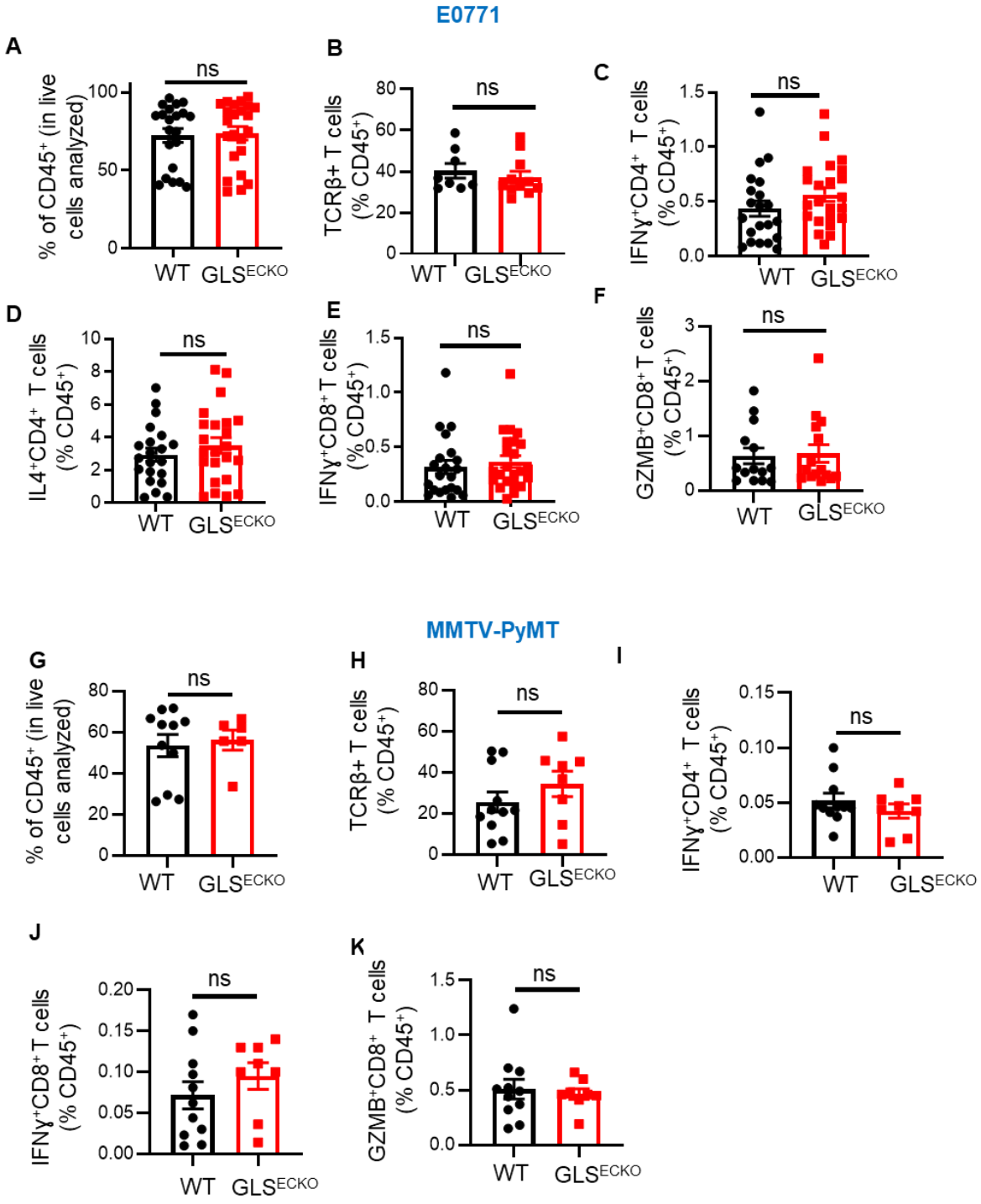
E0771
A
% of CD45+ (in live cells analyzed)
ns
WT
GLSECKO
B
TCRβ+ T cells (% CD45+)
C
IFNγ+CD4+ T cells (% CD45+)
D
IL4+CD4+ T cells (% CD45+)
E
IFNγ+CD8+ T cells (% CD45+)
F
GZMB+CD8+ T cells (% CD45+)
MMTV-PyMT
G
H
I
J
K

Figure 4.6: Endothelial GLS deletion does not appear to affect tumor infiltrating immune cells. E0771 tumors (**A-F**) or PyMT tumors (**G-K**) were harvested from WT or GLS^{ECKO} mice. Tumor infiltrating immune cells were quantified by flow cytometric analyses, including CD45^{+} cells (**A** and **G**), T cells (**B** and **H**), Th1 and Th2 CD4 T cells (**C, D,** and **I**), IFNɣ$^{+}$ and GZMB^{+} CD8 T cells (**E, F, J**, and **K**). All data are presented as mean ± SEM from 2 of 3 independent experiments. ns, not significant as determined by two-tailed unpaired Student's t-test.

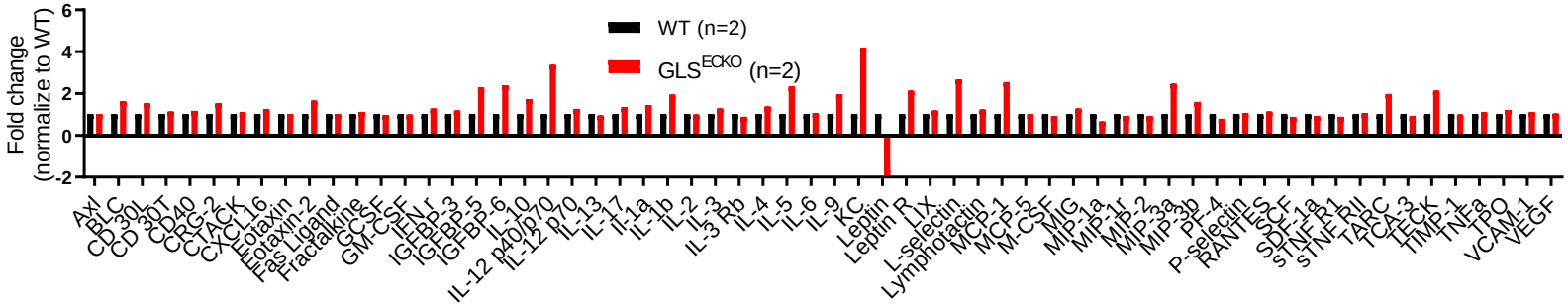

Figure 4.7: Cytokine array showing differentially expressed proteins in WT versus GLS^{ECKO} tumor lysates, including Leptin and Leptin receptor.

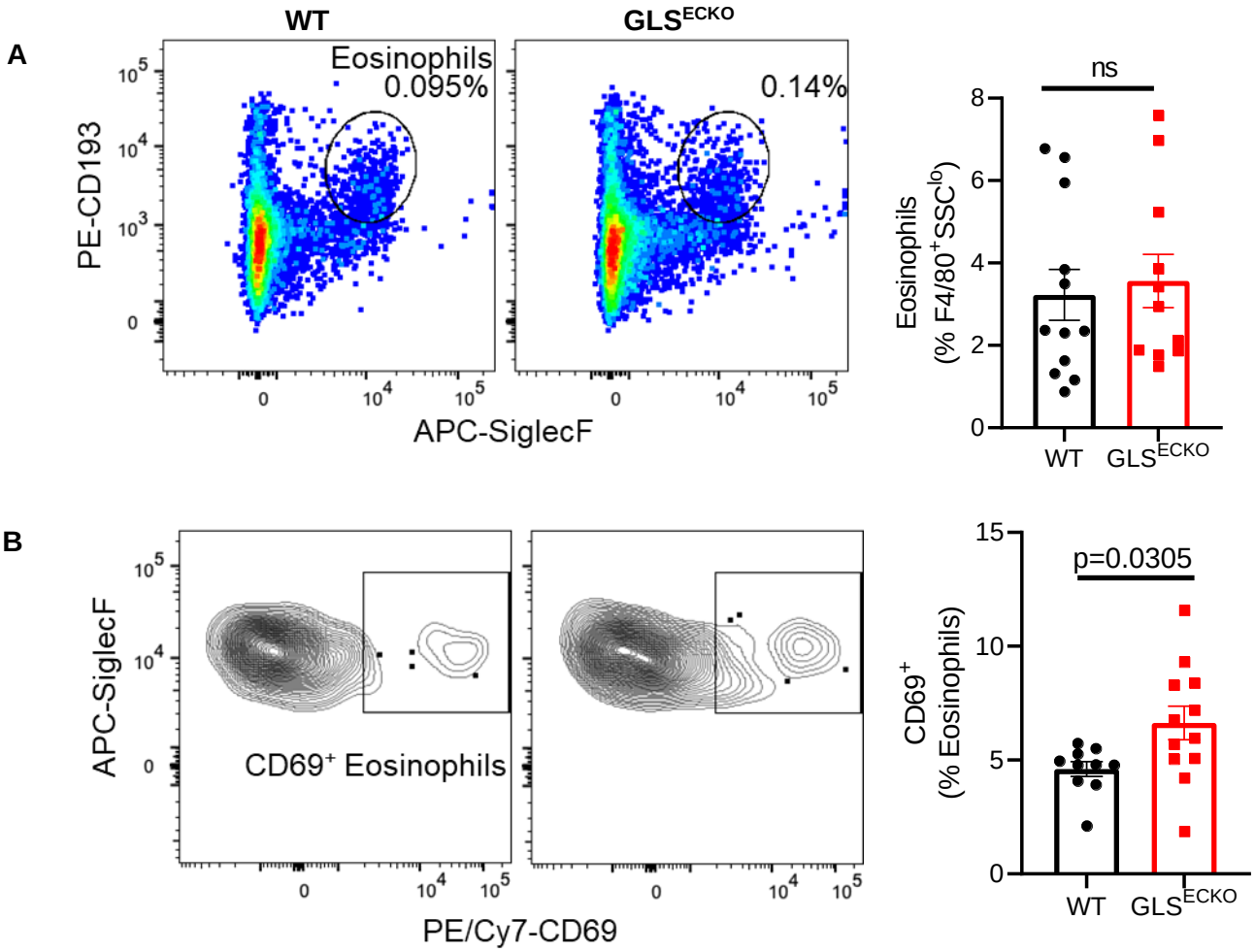

Figure 4.8: Endothelial GLS deletion does not appear to affect eosinophil tumor infiltrating but activation is increased in GLS^{ECKO}. PyMT tumors were harvested from WT or GLS^{ECKO} mice. **A**) Infiltrating eosinophils and **B**) eosinophil activation were quantified by flow cytometric analyses.

Is the microbiome playing a role on the immune phenotype?

It has been well established that the gut microbiome plays a role in the development and maturation of the immune system (235,236). The human gut microbiota contains trillions of organisms, comprised of bacteria, viruses, fungi and protozoan. As the most dominant group in the microbiome, bacterial cells outnumber cells present in the human body by approximately 10 fold (236). Of note, the gut microbiota not only regulate the local intestinal immune system but have an enormous effect on systemic immune responses (237). For example germ-free mice demonstrated multiple defects in their immune systems and were prone to infections compare to non-sterile mice (238). In addition to their impact on immune system development, microbiota can also promote tumor development. Production of LPS by the microbiome is able to induce tumor cell proliferation and survival in hepatocellular carcinoma (HCC) cells, through the LPS receptor TLR4 (239,240). The gut microbiota also regulates estrogen metabolism, and altering microbiome diversity may have significant effects on the availability of estrogen, a key driver of ER+ breast cancer (241). Obesity has been shown to change microbiota diversity to increase circulating deoxycholic acid (DCA) and promote HCC development (242). DCA has also been observed at relatively high levels in the plasma of postmenopausal breast cancer patients, suggesting that the gut microbiomes could be targeted as a potential therapy in some breast cancer patients (243).

Indeed, depleting the microbiome using oral antibiotics significantly reduced tumor burden in pancreatic, colon, and melanoma tumor models (244). In this same study, the authors showed that depleting the microbiome in Rag-1 knockout mice, which lack mature B and T cells, did not inhibit tumor growth. Specifically, depletion of the microbiome in immunocompetent mice increased interferon gamma production, but decreased expression of the pro-tumorigenic cytokines IL-17A and IL-10, in T cells (244). Another study showed that the gut metabolite bile

acid promoted accumulation of natural killer T cells in HCC through induction of CXCL16 expression in liver sinusoidal endothelial cells (245). Together, these studies suggest that the microbiome may alter immune responses in the tumor microenvironment. One of the surprising findings from my work was the lack of any T cell phenotype observed in response to vessel normalization (Fig 4.6). Therefore, it remains to be tested if endothelial GLS also regulates the gut microbiome to counteract the potential benefit of vessel normalization on immune responses in the tumor microenvironment. It is important to note due to the fact that increases in interferon-gamma-producing CD4+ and CD8+ T cells were observed early in this work. However, the interferon-gamma response was not observed following a mouse housing change, which can impact the microbiome (246) (Fig 4.9). Future studies may evaluate this possibility by either depleting the microbiome using oral antibiotics in GLS^{ECKO} tumor bearing mice or raising the mice in a completely sterile environment.

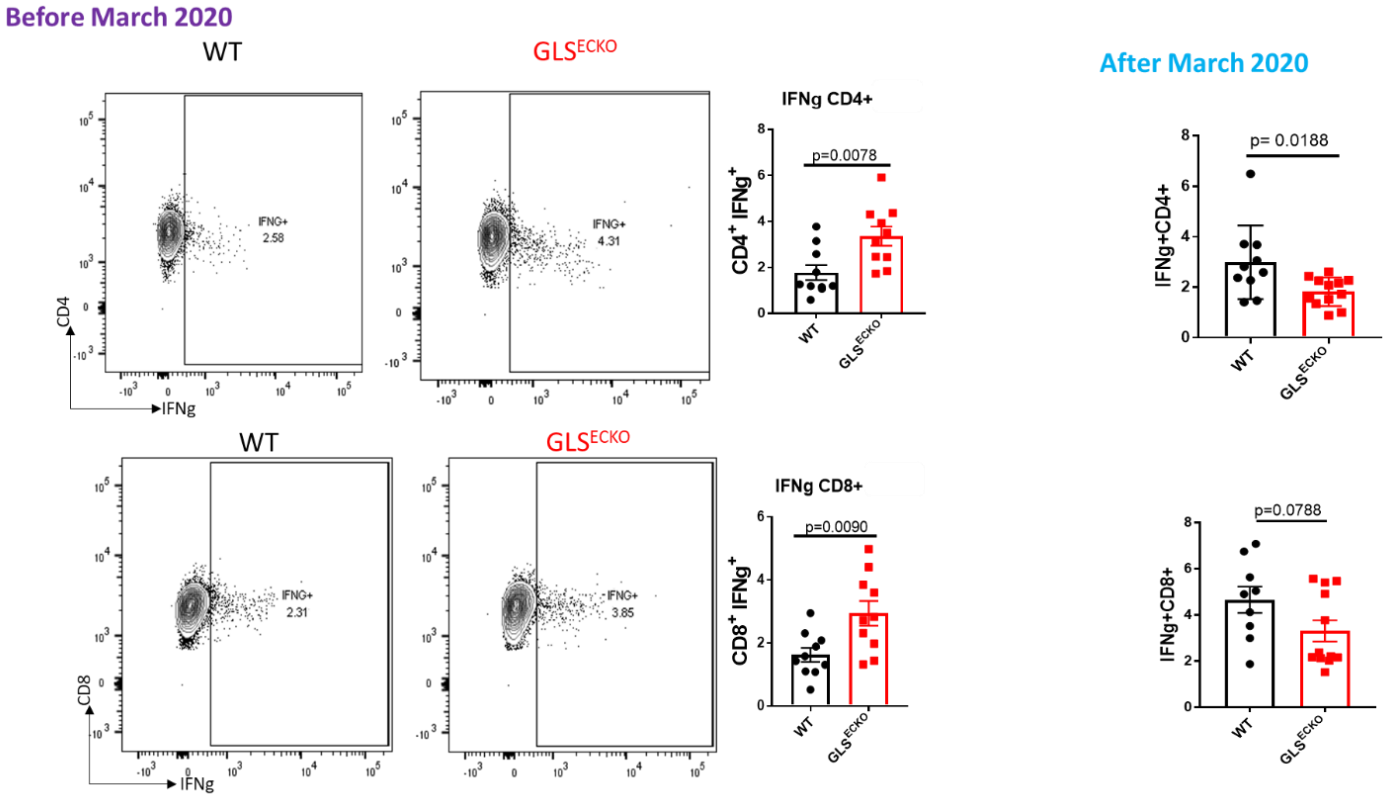

Figure 4.9: T cells activation markers in WT vs GLS^{ECKO}. Interferon-gamma increased in both CD4 and CD8 T cells before animal housing was changed, however, the effect was abrogated after change in housing.

2. Translational Potential of my Thesis Work

Many different cancers including triple negative breast cancers are addicted to glutamine consumption (26,174). As a monotherapy, the GLS inhibitor CB-839 has shown promising antitumor effects in pre-clinical models, but this drug has been largely ineffective in clinical trials as a monotherapy. Consequently, other avenues have been pursued for targeting the glutamine metabolism, including inhibiting glutamine transporters. As described in Chapter I, glutamine transporters can be targeted using the chemical compound V-9302, a

competitive small molecule antagonist of transmembrane glutamine transporters ASCT2, SNAT2, and LAT1 (247). It selectively and potently inhibits glutamine uptake in tumor cells but spares CD8+ T cells (26). Although the effect of V-9302 on glutamine uptake in endothelial cells is unknown, a previous report indicates that blocking uptake through glutamine deprivation in normal endothelial cells (NECs) decreased their proliferation (9). However, targeting GLS does not completely eliminate all glutaminolysis in ECs (Figure 3.8). Therefore, a combination of inhibitors targeting glutamine transporters and GLS could have more beneficial power in targeting the tumor vasculature. This combination may have an additional benefit in targeting glutamine-addicted tumor cells, as a recent study reported that the combination of V-9302 and CB-839 lead to a significant decrease in tumor growth in HCC (248).

In work presented in Chapter IV, RNA-seq analysis revealed transcriptional enrichment of oxidative phosphorylation in GLS knockout endothelial cells (Figure 4.4), suggesting that additional metabolic pathways may be compensating for loss of glutaminolysis. Deletion or pharmacological inhibition of PFKFB3, a key enzyme in the glycolysis pathway, similarly promoted vessel normalization to decrease tumor growth and reduce metastasis (13). Therefore, one could hypothesize that a combination approach to target both glycolysis and glutamine metabolism may have strong anti-angiogenic impacts. In addition to a potentially positive role on the tumor vasculature, this combination may also act to more effectively kill tumor cells. One study showed that using 2-DG, a glucose analog, in combination with V-9302 improved anti-tumor efficacy both *in vitro* and *in vivo* in a 4T1 breast cancer model (249).

In addition to combination therapies targeting metabolic pathways, inhibition of glutamine metabolism could increase tumor sensitivity to chemotherapies and targeted therapies. I

provided evidence in Chapter III that targeting GLS genetically or by using CB-839 in combination with the chemotherapeutic agent cisplatin yielded a potent antitumor effect (Fig. 4.10). In support to my studies, combination therapy of CB-839 with chemotherapies and other therapies in solid tumors are in several phase I clinical trials. For example, a Phase I clinical trial of the glutaminase inhibitor CB-839 plus capecitabine in patients with advanced solid tumors resulted in prolonged progression-free survival in patients who were previously resistant to fluoropyrimidine (ClinicalTrial.gov Identifier: NCT02861300) (250). In patients with clear cell and papillary metastatic renal cancer, a Phase I clinical trial of CB-839 plus cabozatinib was well tolerated (ClinicalTrial.gov Identifier: NCT02071862). A combination of CB-839 with cabozantinib or everolimus showed encouraging clinical activities and was well tolerated in deeply pretreated mRCC patients in a Phase I trial (251).

Glutamine, in addition to being an important nutrient for tumor cells, is also important for T-lymphocytes activation (252–254). Although it can be assumed that systemic treatment of a GLS inhibitor would also affect T cells thereby inhibiting the activities of tumor-infiltrating lymphocytes, Johnson et al. showed that acute GLS inhibition induced epigenetic changes that promoted the effector functions of Th1 and cytotoxic T cells (168). This implies that glutamine metabolism in the tumor microenvironment may differ depending on the cell type and/or context. In fact, a recent study from our lab showed that targeting glutamine transporters with V-9302 only reduced glutamine uptake in the tumor cells and promoted cytotoxic T cells function (26). Based on the above studies, it can be suggested that inhibition of glutamine metabolism may improve responses of immune checkpoint inhibitors to further eliminate solid tumors. Indeed, preclinical studies demonstrate that combination of CB-839 with anti-PD1 or anti-CTLA4 antibodies increased tumor infiltration of effector T cells in melanoma mouse models (255). Of note, a combination of CB-839 with anti-PD-1 (nivolumab) was recently performed in an open-label Phase 1/ 2 on clear cell renal cell

carcinoma, melanoma, and non-small cell lung cancer patients who had earlier progressed with prior PD-1 therapy (ClinicalTrials.gov ID: NCT02771626). The preliminary results showed that the combination was well tolerated and CB-839 could improve responses to ICIs in melanoma patients (256).

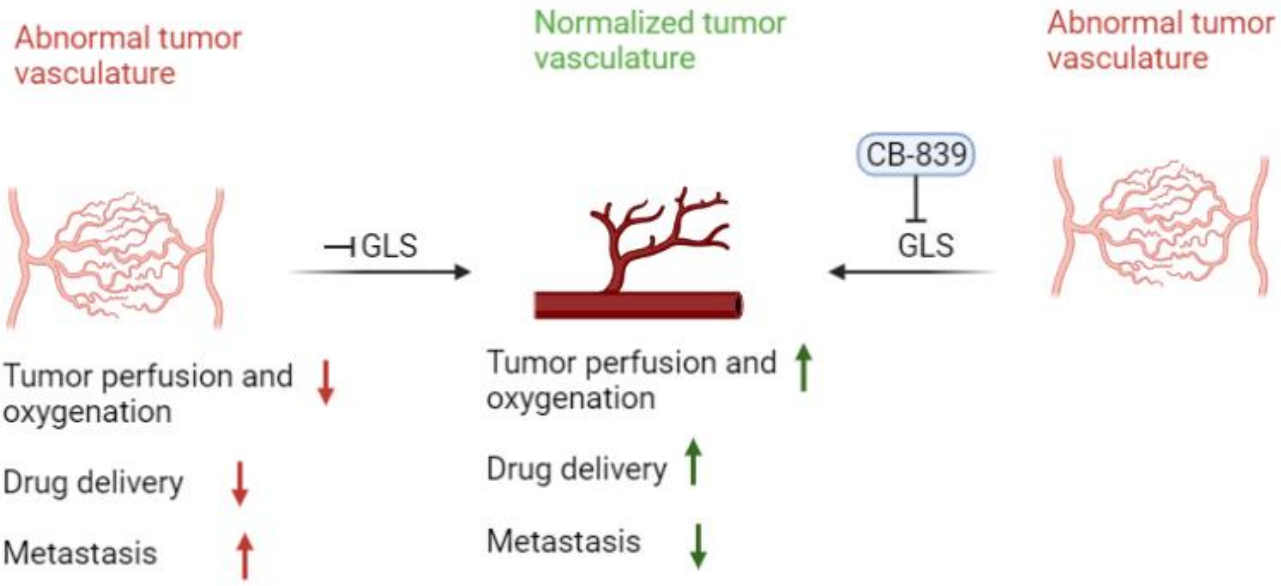

Figure 4.10: Proposed overall contribution of endothelial GLS deletion in breast tumor vasculature (Created in BioRender.com)

3. Study Limitations

One limitation of the work presented here is that the RNA-seq data was obtained from non-tumor endothelial cell mice. Isolation of tumor-associated endothelial cells (TECs) can be performed using CD31 beads, but this process is technically challenging from tumor tissue and results in low yields of TECs. TECs are inherently different from normal endothelial cells (NECs) with altered morphologic and genetic phenotypes, including increased mutational burden and unique chromosome structure (257–259). In contrast to NECs, TECs exhibit stem cell-like origin enabling them to orchestrate tumor neo-angiogenesis. TEC isolation and RNA-seq would likely provide a more accurate transcriptomic analysis of these cell populations in the described model systems, and potentially expose the mechanisms that are critical for the TECs but may not be involved in normal endothelial cell biology. With the challenges with traditional endothelial cell isolation from tumor tissue, other techniques could be implemented. For example, RNAScope is a fully automated RNA *in situ* hybridization (ISH) technique which allows detection of single RNA molecules from individual cells, which would allow evaluation of transcriptional changes in TECs as a whole as well as unique endothelial subpopulations, such as tip or stalk cells (260). In addition to direct changes occurring in endothelial cells upon GLS deletion, this might provide some evidences of how endothelial cells are responding to leptin and PEDF in the tumor microenvironment. These findings may also provide new targets that may normalize the tumor vasculature and could be exploited for future therapeutic development.

Secondly, since the tumor growth phenotype in this study was only seen when tumors were implanted in the mammary fat pad and not subcutaneously (Figure 4.3), it can be suggested that other cells in the microenvironment may be impacting the phenotype. Due to our limited knowledge regarding the role of cancer-associated adipocytes (CAAs) and cancer-associated fibroblast (CAFs) in this model, we cannot rule out their contributions. CAFs and CAAs are the most abundant cell populations in breast tumors, acting as key players in breast cancer

progression (261,262). Importantly, they reside adjacent to breast cancer cells allowing direct communication but also indirect, through release of a variety of factors (262). It has been suggested that cancer associate adipocytes (CAAs) reprogram their own glutamine metabolism to enhance expression of inflammatory cytokines and adipokines upregulation, leading to TNBC tumor growth (65). CAFs are also able to secret glutamine into the TME which becomes available to cancer cells and endothelial cells (263). It would be interesting to examine if changes in CAAs and CAFs are observed in GLS^{ECKO} tumors, particularly if endothelial GLS can regulate the numbers or functions of these cell populations in the tumor microenvironment.

Finally, these studies were performed using murine mammary cell lines (E0771 and MMTV-PyMT). It is necessary to investigate if the mechanism observed in this project is specific to these cell lines and mouse model or if it is applicable to other cancers. Because we focus on triple negative breast cancer, other murine TNBC cell lines such as 4T1, EMT6, and D2A1 or are worth investigating. It would also be interesting to examine the luminal or HER2-enriched cell lines. Furthermore, as shown in Figure 4.3, breast cancer cells were never implanted subcutaneously. It would be important to investigate if the phenotypes observed depend on the environment or cell specificity.

Concluding Remarks

Blood vessels have been recognized to play critical roles in tumor growth and metastasis, and the molecular basis of angiogenesis has been intensively investigated for over three decades. However, despite the fact that tumor endothelial cells are highly proliferative and carry intense metabolic demands, the investigation of endothelial metabolism in tumors is just beginning. Studies in the past few years revealed that many angiogenic factors rely on downstream

metabolic pathways to induce vessel sprouting, and perturbation of these pathways, i.e. glycolysis, can be potentially leveraged for cancer therapeutics. My thesis work assigned a unique role of endothelial glutaminase (GLS) in supporting tumor growth and metastasis in triple negative breast cancer. These studies open up new opportunities (Figure 4.1), for further investigation in the cross talk of metabolic pathways in non-tumor cells in the tumor microenvironment and how this knowledge can be exploited to clinical translation for future cancer therapy.

With the recent advances of technologies, it is possible to functionally screen for metabolic genes encoding enzymes and transporters that are critical for tumor growth and metastasis. It will be equally feasible to perform forward genetics using sgRNA library to identify metabolic pathways that regulate tumor sensitivity to therapeutic agents. Conversely, single cell RNA sequencing will allow us to study endothelial metabolism in tumor patient samples directly. The metabolic heterogeneity among different vascular beds, organ sites, and cell types within the tumor microenvironment can be dissected using this technology. As my work illustrated, not only targeting endothelial metabolic pathways as monotherapy should be considered, but also as combination therapy with chemotherapy, immunotherapy, and/or radiation therapy should be investigated with proper evaluation of potential toxicities. Addressing these questions will likely lead to new discovery for targeting the metabolic vulnerabilities in cancer.

REFERENCES

1. Hanahan D, Weinberg RA. Hallmarks of Cancer: The Next Generation. Cell [Internet]. 2011 Mar 4 [cited 2021 Oct 13];144(5):646–74. Available from: http://www.cell.com/article/S0092867411001279/fulltext
2. Hanahan D. Hallmarks of Cancer: New DimensionsHallmarks of Cancer: New Dimensions. Cancer Discov [Internet]. 2022 Jan 1 [cited 2022 Apr 12];12(1):31–46. Available from: https://aacrjournals.org/cancerdiscovery/article/12/1/31/675608/Hallmarks-of-Cancer-New-DimensionsHallmarks-of
3. Hanahan D, Weinberg RA. Hallmarks of cancer: The next generation [Internet]. Vol. 144, Cell. Cell; 2011 [cited 2021 Jun 22]. p. 646–74. Available from: https://pubmed.ncbi.nlm.nih.gov/21376230/
4. Altman BJ, Stine ZE, Dang C V. From Krebs to clinic: glutam therapy. Nat Rev Cancer. 2016 Oct;16(10):619–34.
5. Koundouros N, Poulogiannis G. Reprogramming of fatty acid metabolism in cancer. Br J Cancer 2019 1221 [Internet]. 2019 Dec 10 [cited 2022 Apr 12];122(1):4–22. Available from: https://www.nature.com/articles/s41416-019-0650-z
6. Folkman J. Tumor Angiogenesis: Therapeutic Implications. http://dx.doi.org/101056/NEJM197111182852108 [Internet]. 1971 Jan 14 [cited 2021 Aug 20];285(21):1182–6. Available from: https://www.nejm.org/doi/full/10.1056/NEJM197111182852108
7. Rohlenova K, Veys K, Miranda-Santos I, De Bock K, Carmeliet P. Endothelial Cell Metabolism in Health and Disease. Trends Cell Biol [Internet]. 2018 Mar 1 [cited 2022 Feb 16];28(3):224–36. Available from: http://www.cell.com/article/S0962892417302015/fulltext
8. Martin JD, Seano G, Jain RK. Normalizing Function of Tumor Vessels: Progress,

Opportunities, and Challenges [Internet]. Vol. 81, Annual Review of Physiology. Annual Reviews Inc.; 2019 [cited 2021 Jun 21]. p. 505–34. Available from: /pmc/articles/PMC6571025/

9. Kim B, Li J, Jang C, Arany Z. Glutamine fuels proliferation but not migration of endothelial cells. EMBO J. 2017 Aug;36(16):2321–33.
10. Huang H, Vandekeere S, Kalucka J, Bierhansl L, Zecchin A, Bruning U, et al. Role of glutamine and interlinked asparagine metabolism in vessel formation. EMBO J. 2017 Aug;36(16):2334–52.
11. Jain RK. Normalization of tumor vasculature: An emerging concept in antiangiogenic therapy [Internet]. Vol. 307, Science. Science; 2005 [cited 2020 Nov 3]. p. 58–62. Available from: https://pubmed.ncbi.nlm.nih.gov/15637262/
12. Jain RK. Normalizing tumor vasculature with anti-angiogenic therapy: a new paradigm for combination therapy. Nat Med. 2001 Sep;7(9):987–9.
13. Cantelmo AR, Conradi L-C, Brajic A, Goveia J, Kalucka J, Pircher A, et al. Inhibition of the Glycolytic Activator PFKFB3 in Endothelium Induces Tumor Vessel Normalization, Impairs Metastasis, and Improves Chemotherapy. Cancer Cell. 2016 Dec;30(6):968–85.
14. Hongling H, Saar V, Joanna K, Laura B, Annalisa Z, Ulrike B, et al. Role of glutamine and interlinked asparagine metabolism in vessel formation. EMBO J. 2017 Jun;36(16):2334–52.
15. Pelicano H, Zhang W, Liu J, Hammoudi N, Dai J, Xu RH, et al. Mitochondrial dysfunction in some triple-negative breast cancer cell lines: role of mTOR pathway and therapeutic potential. Breast Cancer Res [Internet]. 2014 Sep 11 [cited 2022 Apr 12];16(5). Available from: https://pubmed.ncbi.nlm.nih.gov/25209360/
16. Muz B, Puente P de la, Azab F, Azab AK. The role of hypoxia in cancer progression, angiogenesis, metastasis, and resistance to therapy. Hypoxia [Internet]. 2015 Dec [cited 2021 Oct 13];3:83. Available from: /pmc/articles/PMC5045092/

17. Shah M, Nunes MR, Stearns V. CDK4/6 Inhibitors: Game Changers in the Management of Hormone Receptor–Positive Advanced Breast Cancer? Oncology (Williston Park) [Internet]. 2018 [cited 2022 May 18];32(5):216. Available from: /pmc/articles/PMC6424488/

18. Royce ME, Osman D. Everolimus in the Treatment of Metastatic Breast Cancer. Breast Cancer (Auckl) [Internet]. 2015 Sep 6 [cited 2022 May 18];9:73. Available from: /pmc/articles/PMC4571987/

19. First PI3K Inhibitor for Breast Cancer. JAMA [Internet]. 2019 Jul 2;322(1):19. Available from: https://doi.org/10.1001/jama.2019.8916

20. Swain SM, Miles D, Kim SB, Im YH, Im SA, Semiglazov V, et al. Pertuzumab, trastuzumab, and docetaxel for HER2-positive metastatic breast cancer (CLEOPATRA): end-of-study results from a double-blind, randomised, placebo-controlled, phase 3 study. Lancet Oncol. 2020 Apr 1;21(4):519–30.

21. Wolff AC, Hammond MEH, Hicks DG, Dowsett M, McShane LM, Allison KH, et al. Recommendations for human epidermal growth factor receptor 2 testing in breast cancer: American Society of Clinical Oncology/College of American Pathologists clinical practice guideline update. Arch Pathol Lab Med [Internet]. 2014 Feb [cited 2022 May 19];138(2):241–56. Available from: https://pubmed.ncbi.nlm.nih.gov/24099077/

22. Hurvitz SA, Dalenc F, Campone M, O'Regan RM, Tjan-Heijnen VC, Gligorov J, et al. A phase 2 study of everolimus combined with trastuzumab and paclitaxel in patients with HER2-overexpressing advanced breast cancer that progressed during prior trastuzumab and taxane therapy. Breast Cancer Res Treat [Internet]. 2013 Oct [cited 2022 May 19];141(3):437–46. Available from: https://pubmed.ncbi.nlm.nih.gov/24101324/

23. Baselga J, Coleman RE, Cortés J, Janni W. Advances in the management of HER2-positive early breast cancer. Crit Rev Oncol Hematol. 2017 Nov 1;119:113–22.

24. Lampa M, Arlt H, He T, Ospina B, Reeves J, Zhang B, et al. Glutaminase is essential for

the growth of triple-negative breast cancer cells with a deregulated glutamine metabolism pathway and its suppression synergizes with mTOR inhibition. PLoS One. 2017 Sep;12(9):e0185092.

25. Van Geldermalsen M, Wang Q, Nagarajah R, Marshall AD, Thoeng A, Gao D, et al. ASCT2/SLC1A5 controls glutamine uptake and tumour growth in triple-negative basal-like breast cancer. Oncogene. 2016 Jun 16;35(24):3201–8.

26. Edwards DN, Ngwa VM, Raybuck AL, Wang S, Hwang Y, Kim LC, et al. Selective glutamine metabolism inhibition in tumor cells improves antitumor T lymphocyte activity in triple-negative breast cancer. J Clin Invest [Internet]. 2021 Feb 15 [cited 2021 Nov 14];131(4). Available from: https://pubmed.ncbi.nlm.nih.gov/33320840/

27. Emens LA. Immunotherapy in Triple-Negative Breast Cancer. Cancer J (United States) [Internet]. 2021 Jan 1 [cited 2022 Feb 8];27(1):59–66. Available from: https://journals.lww.com/journalppo/Fulltext/2021/01000/Immunotherapy_in_Triple_Negative_Breast_Cancer.9.aspx

28. Warburg O. On the origin of cancer cells. Science (80-) [Internet]. 1956 Feb 24 [cited 2022 May 18];123(3191):309–14. Available from: https://www.science.org/doi/abs/10.1126/science.123.3191.309

29. Warburg Berlin-Dahlem O. Association for Cancer Research. 2016;

30. Senyilmaz D, Teleman AA. Chicken or the egg: Warburg effect and mitochondrial dysfunction. F1000Prime Rep [Internet]. 2015 Apr 2 [cited 2022 May 18];7. Available from: /pmc/articles/PMC4447048/

31. Emmelot P, Bosch L. The metabolism of Neoplastic tissues: The relation of carbohydrate utilization to cholesterol and fatty acid synthesis in tumour tissue slices. Br J Cancer. 1955;9(2):339–43.

32. Pavlova N, metabolism CT-C, 2016 undefined. The emerging hallmarks of cancer metabolism. Elsevier [Internet]. [cited 2022 Apr 12]; Available from:

https://www.sciencedirect.com/science/article/pii/S155041311500621X

33. Wang Z, Jiang Q, Dong C. Metabolic reprogramming in triple-negative breast cancer. Cancer Biol Med. 2020 Feb 1;17(1):44–59.

34. Sun X, Wang M, Wang M, Yu X, Guo J, Sun T, et al. Metabolic Reprogramming in Triple-Negative Breast Cancer. Front Oncol. 2020 Mar 31;10:428.

35. Vander Heiden MG, Cantley LC, Thompson CB. Understanding the Warburg Effect: The Metabolic Requirements of Cell Proliferation. Science (80-) [Internet]. 2009 May 22;324(5930):1029 LP – 1033. Available from: http://science.sciencemag.org/content/324/5930/1029.abstract

36. Bergers G, Fendt SM. The metabolism of cancer cells during metastasis. Nat Rev Cancer [Internet]. 2021 Mar 1 [cited 2022 May 23];21(3):162–80. Available from: https://pubmed.ncbi.nlm.nih.gov/33462499/

37. DeBerardinis RJ, Lum JJ, Hatzivassiliou G, Thompson CB. The biology of cancer: metabolic reprogramming fuels cell growth and proliferation. Cell Metab. 2008 Jan;7(1):11–20.

38. Yang L, Venneti S, Nagrath D. Glutaminolysis: A Hallmark of Cancer Metabolism. Annu Rev Biomed Eng. 2017 Jun;19:163–94.

39. Wise DR, Ward PS, Shay JES, Cross JR, Gruber JJ, Sachdeva UM, et al. Hypoxia promotes isocitrate dehydrogenase-dependent carboxylation of α-ketoglutarate to citrate to support cell growth and viability. Proc Natl Acad Sci [Internet]. 2011 Dec 6 [cited 2018 Jul 15];108(49):19611–6. Available from: http://www.pnas.org/content/108/49/19611

40. Terunuma A, Putluri N, Mishra P, Mathe EA, Dorsey TH, Yi M, et al. MYC-driven accumulation of 2-hydroxyglutarate is associated with breast cancer prognosis. J Clin Invest. 2014 Jan;124(1):398–412.

41. Cao MD, Lamichhane S, Lundgren S, Bofin A, Fjosne H, Giskeodegard GF, et al. Metabolic characterization of triple negative breast cancer. BMC Cancer. 2014

Dec;14:941.

42. EAGLE H. Nutrition needs of mammalian cells in tissue culture. Science. 1955 Sep;122(3168):501–14.

43. Bhutia YD, Babu E, Ramachandran S, Ganapathy V. Amino Acid transporters in cancer and their relevance to “glutamine addiction”: novel targets for the design of a new class of anticancer drugs. Cancer Res. 2015 May;75(9):1782–8.

44. Kim S, Kim DH, Jung W-H, Koo JS. Metabolic phenotypes in triple-negative breast cancer. Tumour Biol. 2013 Jun;34(3):1699–712.

45. El Ansari R, Craze ML, Miligy I, Diez-Rodriguez M, Nolan CC, Ellis IO, et al. The amino acid transporter SLC7A5 confers a poor prognosis in the highly proliferative breast cancer subtypes and is a key therapeutic target in luminal B tumours. Breast Cancer Res. 2018;20(1):21.

46. Liang Z, Cho HT, Williams L, Zhu A, Liang K, Huang K, et al. Potential Biomarker of L-type Amino Acid Transporter 1 in Breast Cancer Progression. Nucl Med Mol Imaging (2010). 2011 Jun;45(2):93–102.

47. van Geldermalsen M, Wang Q, Nagarajah R, Marshall AD, Thoeng A, Gao D, et al. ASCT2/SLC1A5 controls glutamine uptake and tumour growth in triple-negative basal-like breast cancer. Oncogene. 2016 Jun;35(24):3201–8.

48. Sakata T, Ferdous G, Tsuruta T, Satoh T, Baba S, Muto T, et al. L-type amino-acid transporter 1 as a novel biomarker for high-grade malignancy in prostate cancer. Pathol Int. 2009 Jan;59(1):7–18.

49. Kaira K, Oriuchi N, Imai H, Shimizu K, Yanagitani N, Sunaga N, et al. Prognostic significance of L-type amino acid transporter 1 expression in resectable stage I-III nonsmall cell lung cancer. Br J Cancer. 2008 Feb;98(4):742–8.

50. Huang F, Zhao Y, Zhao J, Wu S, Jiang Y, Ma H, et al. Upregulated SLC1A5 promotes cell growth and survival in colorectal cancer. Int J Clin Exp Pathol. 2014 Aug;7(9):6006–

14.

51. Hassanein M, Hoeksema MD, Shiota M, Qian J, Harris BK, Chen H, et al. SLC1A5 mediates glutamine transport required for lung cancer cell growth and survival. Clin Cancer Res. 2013 Feb;19(3):560–70.

52. Cha YJ, Kim E-S, Koo JS. Amino Acid Transporters and Glutamine Metabolism in Breast Cancer. Int J Mol Sci. 2018 Mar;19(3):907.

53. Herranz D. Glutaminolysis gets the spotlight in cancer. Vol. 8, Oncotarget. United States; 2017. p. 10761–2.

54. Mates JM, Segura JA, Martin-Rufian M, Campos-Sandoval JA, Alonso FJ, Marquez J. Glutaminase isoenzymes as key regulators in metabolic and oxidative stress against cancer. Curr Mol Med. 2013 May;13(4):514–34.

55. de la Rosa V, Campos-Sandoval JA, Martín-Rufián M, Cardona C, Matés JM, Segura JA, et al. A novel glutaminase isoform in mammalian tissues. Neurochem Int [Internet]. 2009 Jan 1 [cited 2018 Jul 14];55(1–3):76–84. Available from: https://www.sciencedirect.com/science/article/pii/S019701860900093X?via%3Dihub#!

56. Li Y, Erickson JW, Stalnecker CA, Katt WP, Huang Q, Cerione RA, et al. Mechanistic Basis of Glutaminase Activation: A KEY ENZYME THAT PROMOTES GLUTAMINE METABOLISM IN CANCER CELLS. J Biol Chem. 2016 Sep;291(40):20900–10.

57. Katt WP, Ramachandran S, Erickson JW, Cerione RA. Dibenzophenanthridines as inhibitors of glutaminase C and cancer cell proliferation. Mol Cancer Ther. 2012 Jun;11(6):1269–78.

58. Kung H-N, Marks JR, Chi J-T. Glutamine Synthetase Is a Genetic Determinant of Cell Type–Specific Glutamine Independence in Breast Epithelia. PLOS Genet. 2011 Aug;7(8):e1002229.

59. Cassago A, Ferreira APS, Ferreira IM, Fornezari C, Gomes ERM, Greene KS, et al. Mitochondrial localization and structure-based phosphate activation mechanism of

Glutaminase C with implications for cancer metabolism. Proc Natl Acad Sci U S A. 2012 Jan;109(4):1092–7.

60. Dornier E, Rabas N, Mitchell L, Novo D, Dhayade S, Marco S, et al. Glutaminolysis drives membrane trafficking to promote invasiveness of breast cancer cells. Nat Commun. 2017;8(1):2255.

61. Budczies J, Denkert C. Tissue-Based Metabolomics to Analyze the Breast Cancer Metabolome. Recent results cancer Res Fortschritte der Krebsforsch Prog dans les Rech sur le cancer. 2016;207:157–75.

62. Liu J, Zhang C, Lin M, Zhu W, Liang Y, Hong X, et al. Glutaminase 2 negatively regulates the PI3K/AKT signaling and shows tumor suppression activity in human hepatocellular carcinoma. Oncotarget. 2014 May;5(9):2635–47.

63. Xiang L, Xie G, Liu C, Zhou J, Chen J, Yu S, et al. Knock-down of glutaminase 2 expression decreases glutathione, NADH, and sensitizes cervical cancer to ionizing radiation. Biochim Biophys Acta. 2013 Dec;1833(12):2996–3005.

64. Stine ZE, Schug ZT, Salvino JM, Dang C V. Targeting cancer metabolism in the era of precision oncology. Nat Rev Drug Discov 2021 212 [Internet]. 2021 Dec 3 [cited 2022 Apr 8];21(2):141–62. Available from: https://www.nature.com/articles/s41573-021-00339-6

65. Dong Y, Tu R, Liu H, Qing G. Regulation of cancer cell metabolism: oncogenic MYC in the driver's seat. Signal Transduct Target Ther 2020 51 [Internet]. 2020 Jul 10 [cited 2022 Apr 9];5(1):1–11. Available from: https://www.nature.com/articles/s41392-020-00235-2

66. Wise DR, DeBerardinis RJ, Mancuso A, Sayed N, Zhang X-Y, Pfeiffer HK, et al. Myc regulates a transcriptional program that stimulates mitochondrial glutaminolysis and leads to glutamine addiction. Proc Natl Acad Sci U S A. 2008 Dec;105(48):18782–7.

67. Wang Z, Liu F, Fan N, Zhou C, Li D, Macvicar T, et al. Targeting Glutaminolysis: New Perspectives to Understand Cancer Development and Novel Strategies for Potential Target Therapies. Front Oncol. 2020 Oct 26;10:2321.

68. Xiang L, Mou J, Shao B, Wei Y, Liang H, Takano N, et al. Glutaminase 1 expression in colorectal cancer cells is induced by hypoxia and required for tumor growth, invasion, and metastatic colonization. Cell Death Dis 2019 102 [Internet]. 2019 Jan 17 [cited 2021 Aug 5];10(2):1–15. Available from: https://www.nature.com/articles/s41419-018-1291-5

69. Youngblood VM, Kim LC, Edwards DN, Hwang Y, Santapuram PR, Stirdivant SM, et al. The Ephrin-A1/EPHA2 Signaling Axis Regulates Glutamine Metabolism in HER2-Positive Breast Cancer. Cancer Res. 2016 Apr;76(7):1825–36.

70. Edwards DN, Ngwa VM, Wang S, Shiuan E, Brantley-Sieders DM, Kim LC, et al. The receptor tyrosine kinase EphA2 promotes glutamine metabolism in tumors by activating the transcriptional coactivators YAP and TAZ. Sci Signal. 2017;10(508).

71. Hu W, Zhang C, Wu R, Sun Y, Levine A, Feng Z. Glutaminase 2, a novel p53 target gene regulating energy metabolism and antioxidant function. Proc Natl Acad Sci U S A [Internet]. 2010 Apr 20 [cited 2022 May 18];107(16):7455–60. Available from: www.pnas.org/cgi/doi/10.1073/pnas.1001006107

72. Suzuki S, Tanaka T, Poyurovsky M V., Nagano H, Mayama T, Ohkubo S, et al. Phosphate-activated glutaminase (GLS2), a p53-inducible regulator of glutamine metabolism and reactive oxygen species. Proc Natl Acad Sci U S A [Internet]. 2010 Apr 20 [cited 2022 May 18];107(16):7461–6. Available from: www.pnas.org/cgi/doi/10.1073/pnas.1002459107

73. Giacobbe A, Bongiorno-Borbone L, Bernassola F, Terrinoni A, Markert EK, Levine AJ, et al. p63 regulates glutaminase 2 expression. Cell Cycle [Internet]. 2013 May 1 [cited 2022 May 18];12(9):1395–405. Available from: https://pubmed.ncbi.nlm.nih.gov/23574722/

74. Velletri T, Romeo F, Tucci P, Peschiaroli A, Annicchiarico-Petruzzelli M, Niklison-Chirou MV, et al. GLS2 is transcriptionally regulated by p73 and contributes to neuronal differentiation. http://dx.doi.org/104161/cc26771 [Internet]. 2013 Nov 15 [cited 2022 May 18];12(22):3564–73. Available from:

https://www.tandfonline.com/doi/abs/10.4161/cc.26771

75. Tarantino P, Corti C, Schmid P, Cortes J, Mittendorf EA, Rugo H, et al. Immunotherapy for early triple negative breast cancer: research agenda for the next decade. npj Breast Cancer 2022 81 [Internet]. 2022 Feb 18 [cited 2022 May 26];8(1):1–7. Available from: https://www.nature.com/articles/s41523-022-00386-1

76. Corti A, Dominici S, Piaggi S, Belcastro E, Chiu M, Taurino G, et al. γ-Glutamyltransferase enzyme activity of cancer cells modulates L-γ-glutamyl-p-nitroanilide (GPNA) cytotoxicity. Sci Rep [Internet]. 2019 Dec 1 [cited 2022 May 18];9(1). Available from: /pmc/articles/PMC6351548/

77. Choi YK, Park KG. Targeting Glutamine Metabolism for Cancer Treatment. Biomol Ther (Seoul) [Internet]. 2018 Jan 1 [cited 2022 May 18];26(1):19. Available from: /pmc/articles/PMC5746034/

78. Schulte ML, Fu A, Zhao P, Li J, Geng L, Smith ST, et al. Pharmacological blockade of ASCT2-dependent glutamine transport leads to antitumor efficacy in preclinical models. Nat Med. 2018 Feb;24(2):194–202.

79. Griffiths M, Keast D, Patrick G, Crawford M, Palmer TN. The role of glutamine and glucose analogues in metabolic inhibition of human myeloid leukaemia in vitro. Int J Biochem. 1993 Dec;25(12):1749–55.

80. Lemberg KM, Vornov JJ, Rais R, Slusher BS. We're Not "DON" Yet: Optimal Dosing and Prodrug Delivery of 6-Diazo-5-oxo-L-norleucine. Mol Cancer Ther [Internet]. 2018 Sep 1 [cited 2022 May 18];17(9):1824–32. Available from: https://aacrjournals.org/mct/article/17/9/1824/92489/We-re-Not-DON-Yet-Optimal-Dosing-and-Prodrug

81. Jin L, Alesi GN, Kang S. Glutaminolysis as a target for cancer therapy. Oncogene. 2016 Jul;35(28):3619–25.

82. Ahluwalia GS, Grem JL, Hao Z, Cooney DA. Metabolism and action of amino acid analog

anti-cancer agents. Pharmacol Ther. 1990;46(2):243–71.

83. Rais R, Jančařík A, Tenora L, Nedelcovych M, Alt J, Englert J, et al. Discovery of 6-Diazo-5-oxo-l-norleucine (DON) Prodrugs with Enhanced CSF Delivery in Monkeys: A Potential Treatment for Glioblastoma. J Med Chem [Internet]. 2016 Sep 22 [cited 2022 May 18];59(18):8621–33. Available from: https://pubmed.ncbi.nlm.nih.gov/27560860/

84. Hanaford AR, Alt J, Rais R, Wang SZ, Kaur H, Thorek DLJ, et al. Orally bioavailable glutamine antagonist prodrug JHU-083 penetrates mouse brain and suppresses the growth of MYC-driven medulloblastoma. Transl Oncol. 2019 Oct 1;12(10):1314–22.

85. Stalnecker CA, Ulrich SM, Li Y, Ramachandran S, McBrayer MK, DeBerardinis RJ, et al. Mechanism by which a recently discovered allosteric inhibitor blocks glutamine metabolism in transformed cells. Proc Natl Acad Sci U S A. 2015 Jan;112(2):394–9.

86. Robinson MM, McBryant SJ, Tsukamoto T, Rojas C, Ferraris D V, Hamilton SK, et al. Novel mechanism of inhibition of rat kidney-type glutaminase by bis-2-(5-phenylacetamido-1,2,4-thiadiazol-2-yl)ethyl sulfide (BPTES). Biochem J. 2007 Sep;406(3):407–14.

87. Chen L, Cui H, Fang J, Deng H, Kuang P, Guo H, et al. Glutamine deprivation plus BPTES alters etoposide- and cisplatin-induced apoptosis in triple negative breast cancer cells. Oncotarget. 2016 Aug;7(34):54691–701.

88. Gross MI, Demo SD, Dennison JB, Chen L, Chernov-Rogan T, Goyal B, et al. Antitumor Activity of the Glutaminase Inhibitor CB-839 in Triple-Negative Breast Cancer. Mol Cancer Ther. 2014 Apr;13(4):890 LP – 901.

89. Huang Q, Stalnecker C, Zhang C, McDermott LA, Iyer P, O'Neill J, et al. Characterization of the interactions of potent allosteric inhibitors with glutaminase C, a key enzyme in cancer cell glutamine metabolism. J Biol Chem [Internet]. 2018 Mar 9 [cited 2018 Jul 18];293(10):3535–45. Available from: http://www.ncbi.nlm.nih.gov/pubmed/29317493

90. Parlati F, Gross M, Janes J, Lewis E, MacKinnon A, Rodriguez M, et al. Glutaminase

Inhibitor CB-839 Synergizes with Pomalidomide in Preclinical Multiple Myeloma Models. Blood. 2014 Dec;124(21):4720 LP – 4720.

91. Parlati F. Anti-Tumor Activity of Glutaminase Inhibitor CB-839 in Solid Tumor Malignancies. Calithera Biosci [Internet]. 2018; Available from: https://www.calithera.com/wp-content/uploads/2018/02/Keystone-Metabolism-2018-parlati-final.pdf

92. Xu X, Wang J, Wang M, Yuan X, Li L, Zhang C, et al. Structure-Enabled Discovery of Novel Macrocyclic Inhibitors Targeting Glutaminase 1 Allosteric Binding Site. Cite This J Med Chem [Internet]. 2021 [cited 2022 May 19];64:4611. Available from: https://doi.org/10.1021/acs.jmedchem.0c02044

93. Vailhé B, Vittet D, Feige JJ. In Vitro Models of Vasculogenesis and Angiogenesis. Lab Investig 2001 814 [Internet]. 2001 Apr 1 [cited 2022 Feb 10];81(4):439–52. Available from: https://www.nature.com/articles/3780252

94. Auerbach W, Auerbach R. Angiogenesis inhibition: A review. Pharmacol Ther. 1994;63(3):265–311.

95. Vailhé B, Vittet D, Feige J-J. In Vitro Models of Vasculogenesis and Angiogenesis. 2001;

96. Carmeliet P. Mechanisms of angiogenesis and arteriogenesis. Nat Med 2000 64 [Internet]. 2000 Apr [cited 2022 Apr 30];6(4):389–95. Available from: https://www.nature.com/articles/nm0400_389

97. Carmeliet P. VEGF as a key mediator of angiogenesis in cancer. Oncology [Internet]. 2005 Nov [cited 2022 Apr 30];69 Suppl 3(SUPPL. 3):4–10. Available from: https://pubmed.ncbi.nlm.nih.gov/16301830/

98. Lange C, Storkebaum E, De Almodóvar CR, Dewerchin M, Carmeliet P. Vascular endothelial growth factor: a neurovascular target in neurological diseases. Nat Rev Neurol 2016 128 [Internet]. 2016 Jul 1 [cited 2022 May 20];12(8):439–54. Available from: https://www.nature.com/articles/nrneurol.2016.88

99. Zecchin A, Kalucka J, Dubois C, Carmeliet P. How endothelial cells adapt their metabolism to form vessels in tumors. Front Immunol. 2017 Dec 11;8(DEC):1750.

100. Draoui N, De Zeeuw P, Carmeliet P. Angiogenesis revisited from a metabolic perspective: role and therapeutic implications of endothelial cell metabolism. Open Biol [Internet]. 2017 [cited 2021 Nov 16];7(12). Available from: /pmc/articles/PMC5746547/

101. Akil A, Gutiérrez-García AK, Guenter R, Rose JB, Beck AW, Chen H, et al. Notch Signaling in Vascular Endothelial Cells, Angiogenesis, and Tumor Progression: An Update and Prospective. Front Cell Dev Biol. 2021 Feb 16;9:177.

102. Bentley K, Gerhardt H, Bates PA. Agent-based simulation of notch-mediated tip cell selection in angiogenic sprout initialisation. J Theor Biol. 2008 Jan 7;250(1):25–36.

103. Blanco R, Gerhardt H. VEGF and Notch in Tip and Stalk Cell Selection. Cold Spring Harb Perspect Med [Internet]. 2013 Jan [cited 2022 May 26];3(1). Available from: /pmc/articles/PMC3530037/

104. Suchting S, Freitas C, Le Noble F, Benedito R, Bréant C, Duarte A, et al. The Notch ligand Delta-like 4 negatively regulates endothelial tip cell formation and vessel branching. Proc Natl Acad Sci U S A [Internet]. 2007 Feb 27 [cited 2022 May 19];104(9):3225–30. Available from: www.pnas.org/cgi/content/full/

105. Tammela T, Zarkada G, Nurmi H, Jakobsson L, Heinolainen K, Tvorogov D, et al. VEGFR-3 controls tip to stalk conversion at vessel fusion sites by reinforcing Notch signalling. Nat Cell Biol 2011 1310 [Internet]. 2011 Sep 11 [cited 2022 May 19];13(10):1202–13. Available from: https://www.nature.com/articles/ncb2331

106. Hellström M, Phng LK, Hofmann JJ, Wallgard E, Coultas L, Lindblom P, et al. Dll4 signalling through Notch1 regulates formation of tip cells during angiogenesis. Nat 2006 4457129 [Internet]. 2007 Jan 28 [cited 2022 May 19];445(7129):776–80. Available from: https://www.nature.com/articles/nature05571

107. Chatterjee S, Naik UP. Pericyte-endothelial cell interaction: A survival mechanism for the

tumor vasculature. Cell Adh Migr [Internet]. 2012 [cited 2022 Feb 12];6(3):157. Available from: /pmc/articles/PMC3427227/

108. Wakui S, Yokoo K, Muto T, Suzuki Y, Takahashi H, Furusato M, et al. Localization of Ang-1, -2, Tie-2, and VEGF expression at endothelial-pericyte interdigitation in rat angiogenesis. Lab Invest [Internet]. 2006 Oct 21 [cited 2022 Feb 12];86(11):1172–84. Available from: https://pubmed.ncbi.nlm.nih.gov/16969369/

109. Hirai H, Maru Y, Hagiwara K, Nishida J, Takaku F. A novel putative tyrosine kinase receptor encoded by the eph gene. Science [Internet]. 1987 [cited 2022 May 19];238(4834):1717–20. Available from: https://pubmed.ncbi.nlm.nih.gov/2825356/

110. Shiuan E, Chen J. Eph receptor tyrosine kinases in tumor immunity. Cancer Res [Internet]. 2016 Nov 11 [cited 2022 May 19];76(22):6452. Available from: /pmc/articles/PMC5290221/

111. Brantley DM, Cheng N, Thompson EJ, Lin Q, Brekken RA, Thorpe PE, et al. Soluble Eph A receptors inhibit tumor angiogenesis and progression in vivo. Oncogene 2002 2146 [Internet]. 2002 Oct 9 [cited 2022 May 19];21(46):7011–26. Available from: https://www.nature.com/articles/1205679

112. Brantley-Sieders DM, Caughron J, Hicks D, Pozzi A, Ruiz JC, Chen J. EphA2 receptor tyrosine kinase regulates endothelial cell migration and vascular assembly through phosphoinositide 3-kinase-mediated Rac1 GTPase activation. J Cell Sci [Internet]. 2004 Apr 15 [cited 2022 May 19];117(10):2037–49. Available from: https://journals.biologists.com/jcs/article/117/10/2037/27744/EphA2-receptor-tyrosine-kinase-regulates

113. Kullander K, Klein R. Mechanisms and functions of eph and ephrin signalling. Nat Rev Mol Cell Biol 2002 37 [Internet]. 2002 [cited 2022 May 19];3(7):475–86. Available from: https://www.nature.com/articles/nrm856

114. Kuijper S, Turner CJ, Adams RH. Regulation of Angiogenesis by Eph–Ephrin

Interactions. Trends Cardiovasc Med. 2007 Jul 1;17(5):145–51.

115. Loizzi V, del Vecchio V, Gargano G, de Liso M, Kardashi A, Naglieri E, et al. Biological Pathways Involved in Tumor Angiogenesis and Bevacizumab Based Anti-Angiogenic Therapy with Special References to Ovarian Cancer. Int J Mol Sci 2017, Vol 18, Page 1967 [Internet]. 2017 Sep 14 [cited 2022 Feb 12];18(9):1967. Available from: https://www.mdpi.com/1422-0067/18/9/1967/htm

116. Cantelmo AR, Pircher A, Kalucka J, Carmeliet P. Vessel pruning or healing: endothelial metabolism as a novel target? Expert Opin Ther Targets [Internet]. 2017 Mar 4 [cited 2021 Nov 14];21(3):239. Available from: /pmc/articles/PMC5526136/

117. Ebos JML, Lee CR, Cruz-Munoz W, Bjarnason GA, Christensen JG, Kerbel RS. Accelerated metastasis after short-term treatment with a potent inhibitor of tumor angiogenesis. Cancer Cell. 2009 Mar;15(3):232–9.

118. Pàez-Ribes M, Allen E, Hudock J, Takeda T, Okuyama H, Viñals F, et al. Antiangiogenic Therapy Elicits Malignant Progression of Tumors to Increased Local Invasion and Distant Metastasis. Cancer Cell. 2009 Mar 3;15(3):220–31.

119. Yonenaga Y, Mori A, Onodera H, Yasuda S, Oe H, Fujimoto A, et al. Absence of smooth muscle actin-positive pericyte coverage of tumor vessels correlates with hematogenous metastasis and prognosis of colorectal cancer patients. Oncology [Internet]. 2005 Sep [cited 2022 Apr 30];69(2):159–66. Available from: https://pubmed.ncbi.nlm.nih.gov/16127287/

120. Gilreath C, Boerma M, Qin Z, Hudson MK, Wang S. The Hypoxic Microenvironment of Breast Cancer Cells Promotes Resistance in Radiation Therapy. Front Oncol [Internet]. 2020 Feb 18 [cited 2022 Feb 15];10. Available from: /pmc/articles/PMC7930560/

121. Jain RK. Normalization of tumor vasculature: an emerging concept in antiangiogenic therapy. Science. 2005 Jan;307(5706):58–62.

122. Tong RT, Boucher Y, Kozin S V., Winkler F, Hicklin DJ, Jain RK. Vascular Normalization

by Vascular Endothelial Growth Factor Receptor 2 Blockade Induces a Pressure Gradient Across the Vasculature and Improves Drug Penetration in Tumors. Cancer Res. 2004 Jun 1;64(11):3731–6.

123. Chauhan VP, Stylianopoulos T, Martin JD, PopoviÄ Z, Chen O, Kamoun WS, et al. Normalization of tumour blood vessels improves the delivery of nanomedicines in a size-dependent manner. Nat Nanotechnol [Internet]. 2012 [cited 2022 Feb 15];7(6):383–8. Available from: https://pubmed.ncbi.nlm.nih.gov/22484912/

124. Dickson P V., Hamner JB, Sims TL, Fraga CH, Ng CYC, Rajasekeran S, et al. Bevacizumab-induced transient remodeling of the vasculature in neuroblastoma xenografts results in improved delivery and efficacy of systemically administered chemotherapy. Clin Cancer Res [Internet]. 2007 Jul 1 [cited 2022 Apr 30];13(13):3942–50. Available from: https://pubmed.ncbi.nlm.nih.gov/17606728/

125. Huang Y, Kim BYS, Chan CK, Hahn SM, Weissman IL, Jiang W. Improving immune-vascular crosstalk for cancer immunotherapy. Nat Rev Immunol. 2018 Mar;18(3):195–203.

126. Hamzah J, Jugold M, Kiessling F, Rigby P, Manzur M, Marti HH, et al. Vascular normalization in Rgs5-deficient tumours promotes immune destruction. Nature. 2008 May 15;453(7193):410–4.

127. Mazzone M, Dettori D, de Oliveira RL, Loges S, Schmidt T, Jonckx B, et al. Heterozygous deficiency of PHD2 restores tumor oxygenation and inhibits metastasis via endothelial normalization. Cell. 2009 Mar;136(5):839–51.

128. Tian L, Goldstein A, Wang H, Lo HC, Kim IS, Welte T, et al. Mutual regulation of tumour vessel normalization and immunostimulatory reprogramming. Nature. 2017 Apr 13;544(7649):250–4.

129. Algars A, Karikoski M, Yegutkin GG, Stoitzner P, Niemela J, Salmi M, et al. Different role of CD73 in leukocyte trafficking via blood and lymph vessels. Blood. 2011

Apr;117(16):4387–93.

130. Huang Y, Kim BYS, Chan CK, Hahn SM, Weissman IL, Jiang W. Improving immune-vascular crosstalk for cancer immunotherapy. Vol. 18, Nature Reviews Immunology. Nature Publishing Group; 2018. p. 195–203.

131. Rolny C, Mazzone M, Tugues S, Laoui D, Johansson I, Coulon C, et al. HRG inhibits tumor growth and metastasis by inducing macrophage polarization and vessel normalization through downregulation of PlGF. Cancer Cell. 2011 Jan;19(1):31–44.

132. Schmittnaegel M, Rigamonti N, Kadioglu E, Cassara A, Wyser Rmili C, Kiialainen A, et al. Dual angiopoietin-2 and VEGFA inhibition elicits antitumor immunity that is enhanced by PD-1 checkpoint blockade. Sci Transl Med. 2017 Apr;9(385).

133. He B, Jabouille A, Steri V, Johansson-Percival A, Michael IP, Kotamraju VR, et al. Vascular targeting of LIGHT normalizes blood vessels in primary brain cancer and induces intratumoural high endothelial venules. J Pathol [Internet]. 2018 Mar 30;245(2):209–21. Available from: https://doi.org/10.1002/path.5080

134. Carter T, Shaw H, Cohn-Brown D, Chester K, Mulholland P. Ipilimumab and Bevacizumab in Glioblastoma. Clin Oncol (R Coll Radiol). 2016 Oct;28(10):622–6.

135. McGranahan T, Li G, Nagpal S. History and current state of immunotherapy in glioma and brain metastasis. Ther Adv Med Oncol. 2017 May;9(5):347–68.

136. Treps L. EnLIGHTenment of tumor vessel normalization and immunotherapy in glioblastoma. J Pathol. 2018 Sep;246(1):3–6.

137. Shrimali RK, Yu Z, Theoret MR, Chinnasamy D, Restifo NP, Rosenberg SA. Antiangiogenic agents can increase lymphocyte infiltration into tumor and enhance the effectiveness of adoptive immunotherapy of cancer. Cancer Res. 2010 Aug;70(15):6171–80.

138. Carretero R, Sektioglu IM, Garbi N, Salgado OC, Beckhove P, Hammerling GJ. Eosinophils orchestrate cancer rejection by normalizing tumor vessels and enhancing

infiltration of CD8(+) T cells. Nat Immunol. 2015 Jun;16(6):609–17.

139. De Bock K, Georgiadou M, Carmeliet P. Role of endothelial cell metabolism in vessel sprouting. Cell Metab. 2013 Nov;18(5):634–47.

140. Theodorou K, Boon RA. Endothelial cell metabolism in atherosclerosis. Front Cell Dev Biol. 2018 Aug 7;6(AUG):82.

141. Zecchin A, Kalucka J, Dubois C, Carmeliet P. How Endothelial Cells Adapt Their Metabolism to Form Vessels in Tumors. Front Immunol [Internet]. 2017 Dec 11;8:1750. Available from: https://www.ncbi.nlm.nih.gov/pubmed/29321777

142. De Bock K, Georgiadou M, Schoors S, Kuchnio A, Wong BW, Cantelmo AR, et al. Role of PFKFB3-driven glycolysis in vessel sprouting. Cell. 2013 Aug;154(3):651–63.

143. Schoors S, De Bock K, Cantelmo AR, Georgiadou M, Ghesquiere B, Cauwenberghs S, et al. Partial and transient reduction of glycolysis by PFKFB3 blockade reduces pathological angiogenesis. Cell Metab. 2014 Jan;19(1):37–48.

144. Yeh WL, Lin CJ, Fu WM. Enhancement of glucose transporter expression of brain endothelial cells by vascular endothelial growth factor derived from glioma exposed to hypoxia. Mol Pharmacol [Internet]. 2008 Jan [cited 2022 Apr 30];73(1):170–7. Available from: https://pubmed.ncbi.nlm.nih.gov/17942749/

145. Schoors S, Bruning U, Missiaen R, Queiroz KCS, Borgers G, Elia I, et al. Fatty acid carbon is essential for dNTP synthesis in endothelial cells. Nat 2015 5207546 [Internet]. 2015 Apr 1 [cited 2022 Apr 30];520(7546):192–7. Available from: https://www.nature.com/articles/nature14362

146. Rohlenova K, Veys K, Miranda-Santos I, De Bock K, Carmeliet P. Endothelial Cell Metabolism in Health and Disease. Trends Cell Biol [Internet]. 2018 Mar 1 [cited 2022 Feb 18];28(3):224–36. Available from: http://www.cell.com/article/S0962892417302015/fulltext

147. Bruning U, Morales-Rodriguez F, Kalucka J, Goveia J, Taverna F, Queiroz KCS, et al.

Impairment of Angiogenesis by Fatty Acid Synthase Inhibition Involves mTOR Malonylation. Cell Metab. 2018 Dec 4;28(6):866-880.e15.

148. Bastos DC, Paupert J, Maillard C, Seguin F, Carvalho MA, Agostini M, et al. Effects of fatty acid synthase inhibitors on lymphatic vessels: an in vitro and in vivo study in a melanoma model. Lab Investig 2017 972 [Internet]. 2016 Dec 5 [cited 2022 Feb 16];97(2):194–206. Available from: https://www-nature-com.proxy.library.vanderbilt.edu/articles/labinvest2016125

149. Guo Y, Deng Y, Li X, Ning Y, Lin X, Guo S, et al. Glutaminolysis Was Induced by TGF-β1 through PP2Ac Regulated Raf-MEK-ERK Signaling in Endothelial Cells. PLoS One [Internet]. 2016 Sep 1 [cited 2022 Feb 16];11(9):e0162658. Available from: https://journals-plos-org.proxy.library.vanderbilt.edu/plosone/article?id=10.1371/journal.pone.0162658

150. Sanchez EL, Carroll PA, Thalhofer AB, Lagunoff M. Latent KSHV Infected Endothelial Cells Are Glutamine Addicted and Require Glutaminolysis for Survival. PLOS Pathog [Internet]. 2015 Jul 1 [cited 2022 Feb 16];11(7):e1005052. Available from: https://journals-plos-org.proxy.library.vanderbilt.edu/plospathogens/article?id=10.1371/journal.ppat.1005052

151. Hurwitz H, Fehrenbacher L, Novotny W, Cartwright T, Hainsworth J, Heim W, et al. Bevacizumab plus irinotecan, fluorouracil, and leucovorin for metastatic colorectal cancer. N Engl J Med [Internet]. 2004 Jun 3 [cited 2022 Apr 30];350(23):2335–42. Available from: https://pubmed.ncbi.nlm.nih.gov/15175435/

152. Giantonio BJ, Catalano PJ, Meropol NJ, O'Dwyer PJ, Mitchell EP, Alberts SR, et al. Bevacizumab in combination with oxaliplatin, fluorouracil, and leucovorin (FOLFOX4) for previously treated metastatic colorectal cancer: results from the Eastern Cooperative Oncology Group Study E3200. J Clin Oncol [Internet]. 2007 Apr 20 [cited 2022 Apr 30];25(12):1539–44. Available from: https://pubmed.ncbi.nlm.nih.gov/17442997/

153. Ferrara N, Kerbel RS. Angiogenesis as a therapeutic target. Nature [Internet]. 2005 Dec 15 [cited 2022 Jan 21];438(7070):967–74. Available from: https://pubmed.ncbi.nlm.nih.gov/16355214/

154. Comunanza V, Bussolino F. Therapy for cancer: Strategy of combining anti-angiogenic and target therapies. Front Cell Dev Biol. 2017 Dec 7;5(DEC):101.

155. Van Cutsem E, Tabernero J, Lakomy R, Prenen H, Prausová J, Macarulla T, et al. Addition of aflibercept to fluorouracil, leucovorin, and irinotecan improves survival in a phase III randomized trial in patients with metastatic colorectal cancer previously treated with an oxaliplatin-based regimen. J Clin Oncol [Internet]. 2012 Oct 1 [cited 2022 Feb 17];30(28):3499–506. Available from: https://pubmed.ncbi.nlm.nih.gov/22949147/

156. Clarke JM, Hurwitz HI, Rangwala F. Understanding the mechanisms of action of antiangiogenic agents in metastatic colorectal cancer: A clinician's perspective. Cancer Treat Rev [Internet]. 2014 Oct 1 [cited 2022 Feb 18];40(9):1065–72. Available from: http://www.cancertreatmentreviews.com/article/S0305737214001236/fulltext

157. Wilke H, Muro K, Van Cutsem E, Oh SC, Bodoky G, Shimada Y, et al. Ramucirumab plus paclitaxel versus placebo plus paclitaxel in patients with previously treated advanced gastric or gastro-oesophageal junction adenocarcinoma (RAINBOW): a double-blind, randomised phase 3 trial. Lancet Oncol [Internet]. 2014 Oct 1 [cited 2022 Apr 30];15(11):1224–35. Available from: https://pubmed.ncbi.nlm.nih.gov/25240821/

158. Nakagawa K, Garon EB, Seto T, Nishio M, Ponce Aix S, Paz-Ares L, et al. Ramucirumab plus erlotinib in patients with untreated, EGFR-mutated, advanced non-small-cell lung cancer (RELAY): a randomised, double-blind, placebo-controlled, phase 3 trial. Lancet Oncol [Internet]. 2019 Dec 1 [cited 2022 May 26];20(12):1655–69. Available from: https://pubmed.ncbi.nlm.nih.gov/31591063/

159. Gotink KJ, Verheul HMW. Anti-angiogenic tyrosine kinase inhibitors: what is their mechanism of action? Angiogenesis [Internet]. 2010 Mar [cited 2022 May 26];13(1):1.

Available from: /pmc/articles/PMC2845892/

160. Wilhelm SM, Dumas J, Adnane L, Lynch M, Carter CA, Schütz G, et al. Regorafenib (BAY 73-4506): A new oral multikinase inhibitor of angiogenic, stromal and oncogenic receptor tyrosine kinases with potent preclinical antitumor activity. Int J Cancer [Internet]. 2011 Jul 1 [cited 2022 Apr 30];129(1):245–55. Available from: https://onlinelibrary.wiley.com/doi/full/10.1002/ijc.25864

161. Casanovas O, Hicklin DJ, Bergers G, Hanahan D. Drug resistance by evasion of antiangiogenic targeting of VEGF signaling in late-stage pancreatic islet tumors. Cancer Cell [Internet]. 2005 [cited 2022 Feb 18];8(4):299–309. Available from: https://pubmed.ncbi.nlm.nih.gov/16226705/

162. Montemagno C, Pagès G. Resistance to Anti-angiogenic Therapies: A Mechanism Depending on the Time of Exposure to the Drugs. Front Cell Dev Biol. 2020 Jul 7;8:584.

163. Sood AK, Seftor EA, Fletcher MS, Gardner LMG, Heidger PM, Buller RE, et al. Molecular determinants of ovarian cancer plasticity. Am J Pathol [Internet]. 2001 [cited 2022 Apr 30];158(4):1279–88. Available from: https://pubmed.ncbi.nlm.nih.gov/11290546/

164. Van Der Schaft DWJ, Hillen F, Pauwels P, Kirschmann DA, Castermans K, Oude Egbrink MGA, et al. Tumor cell plasticity in Ewing sarcoma, an alternative circulatory system stimulated by hypoxia. Cancer Res [Internet]. 2005 Dec 15 [cited 2022 Apr 30];65(24):11520–8. Available from: https://pubmed.ncbi.nlm.nih.gov/16357161/

165. Lupo G, Caporarello N, Olivieri M, Cristaldi M, Motta C, Bramanti V, et al. Anti-angiogenic therapy in cancer: Downsides and new pivots for precision medicine. Front Pharmacol. 2017 Jan 6;7(JAN):519.

166. Chen HX, Cleck JN. Adverse effects of anticancer agents that target the VEGF pathway. Nat Rev Clin Oncol [Internet]. 2009 Aug [cited 2022 Jan 21];6(8):465–77. Available from: https://pubmed.ncbi.nlm.nih.gov/19581909/

167. Miller K, Wang M, Gralow J, Dickler M, Cobleigh M, Perez EA, et al. Paclitaxel plus

Bevacizumab versus Paclitaxel Alone for Metastatic Breast Cancer. N Engl J Med [Internet]. 2007 Dec 27 [cited 2022 Feb 18];357(26):2666–76. Available from: https://www.nejm.org/doi/full/10.1056/nejmoa072113

168. Johnson MO, Wolf MM, Madden MZ, Andrejeva G, Sugiura A, Contreras DC, et al. Distinct Regulation of Th17 and Th1 Cell Differentiation by Glutaminase-Dependent Metabolism. Cell. 2018 Dec;175(7):1780-1795.e19.

169. Balko JM, Miller TW, Morrison MM, Hutchinson K, Young C, Rinehart C, et al. The receptor tyrosine kinase ErbB3 maintains the balance between luminal and basal breast epithelium. Proc Natl Acad Sci U S A. 2012 Jan 3;109(1):221–6.

170. Johnstone CN, Smith YE, Cao Y, Burrows AD, Cross RSN, Ling X, et al. Functional and molecular characterisation of EO771.LMB tumours, a new C57BL/6-mouse-derived model of spontaneously metastatic mammary cancer. DMM Dis Model Mech [Internet]. 2015 Mar 1 [cited 2022 Apr 29];8(3):237–51. Available from: /pmc/articles/PMC4348562/

171. Zimmerman M, Hu X, Liu K. Experimental Metastasis and CTL Adoptive Transfer Immunotherapy Mouse Model. J Vis Exp [Internet]. 2010 [cited 2021 Nov 16];(45):45. Available from: /pmc/articles/PMC3159593/

172. Wang S, Raybuck A, Shiuan E, Cho SH, Wang Q, Brantley-Sieders DM, et al. Selective inhibition of mTORC1 in tumor vessels increases antitumor immunity. JCI Insight [Internet]. 2020 Aug 6 [cited 2021 Jun 22];5(15). Available from: https://doi.org/10.1172/jci.insight.139237

173. F A Schmid, F M Sirotnak, G M Otter, J I DeGraw. Combination chemotherapy with a new folate analog: activity of 10-ethyl-10-deaza-aminopterin compared to methotrexate with 5-fluorouracil and alkylating agents against advanced metastatic disease in murine tumor models - PubMed [Internet]. Cancer Treatment Reports. 1987 [cited 2021 Sep 30]. p. 727–32. Available from: https://pubmed.ncbi.nlm.nih.gov/3607784/

174. Edwards DN, Ngwa VM, Wang S, Shiuan E, Brantley-Sieders DM, Kim LC, et al. The

receptor tyrosine kinase EphA2 promotes glutamine metabolism in tumors by activating the transcriptional coactivators YAP and TAZ. Sci Signal [Internet]. 2017 Dec 5 [cited 2022 Mar 15];10(508). Available from: https://www.science.org/doi/abs/10.1126/scisignal.aan4667

175. Jain RK. ANTIANGIOGENESIS STRATEGIES REVISITED: FROM STARVING TUMORS TO ALLEVIATING HYPOXIA. Cancer Cell [Internet]. 2014 Nov 10;26(5):605–22. Available from: http://www.ncbi.nlm.nih.gov/pmc/articles/PMC4269830/

176. De Bock K, Mazzone M, Carmeliet P. Antiangiogenic therapy, hypoxia, and metastasis: risky liaisons, or not? Nat Rev Clin Oncol. 2011 May;8(7):393–404.

177. Cantelmo AR, Pircher A, Kalucka J, Carmeliet P. Vessel pruning or healing: endothelial metabolism as a novel target? Expert Opin Ther Targets [Internet]. 2017/01/27. 2017 Mar 4;21(3):239–47. Available from: https://www.ncbi.nlm.nih.gov/pubmed/28081641

178. Kim JY, Heo S-H, Choi SK, Song IH, Park IA, Kim Y-A, et al. Glutaminase expression is a poor prognostic factor in node-positive triple-negative breast cancer patients with a high level of tumor-infiltrating lymphocytes. Virchows Arch. 2017 Apr;470(4):381–9.

179. Monvoisin A, Alva JA, Hofmann JJ, Zovein AC, Lane TF, Iruela-Arispe ML. VE-cadherin-CreERT2 transgenic mouse: A model for inducible recombination in the endothelium. Dev Dyn [Internet]. 2006 Dec 1 [cited 2022 Jun 27];235(12):3413–22. Available from: https://onlinelibrary.wiley.com/doi/full/10.1002/dvdy.20982

180. Franco M, Man S, Chen L, Emmenegger U, Shaked Y, Cheung AM, et al. Targeted Anti–Vascular Endothelial Growth Factor Receptor-2 Therapy Leads to Short-term and Long-term Impairment of Vascular Function and Increase in Tumor Hypoxia. Cancer Res [Internet]. 2006 Apr 1 [cited 2021 Oct 12];66(7):3639–48. Available from: https://cancerres.aacrjournals.org/content/66/7/3639

181. Tian L, Goldstein A, Wang H, Ching Lo H, Sun Kim I, Welte T, et al. Mutual regulation of tumour vessel normalization and immunostimulatory reprogramming. Nature [Internet].

2017 Apr 3;544:250. Available from: https://doi.org/10.1038/nature21724

182. Fu R, Li Y, Jiang N, Ren BX, Zang CZ, Liu LJ, et al. Inactivation of endothelial ZEB1 impedes tumor progression and sensitizes tumors to conventional therapies. J Clin Invest [Internet]. 2020 Mar 2 [cited 2021 Jun 22];130(3):1252–70. Available from: https://doi.org/10.1172/JCI131507DS1

183. Obradovic M, Sudar-Milovanovic E, Soskic S, Essack M, Arya S, Stewart AJ, et al. Leptin and Obesity: Role and Clinical Implication. Front Endocrinol (Lausanne). 2021 May 18;12:563.

184. Klok MD, Jakobsdottir S, Drent ML. The role of leptin and ghrelin in the regulation of food intake and body weight in humans: a review. Obes Rev [Internet]. 2007 Jan [cited 2021 Nov 16];8(1):21–34. Available from: https://pubmed.ncbi.nlm.nih.gov/17212793/

185. de Candia P, Prattichizzo F, Garavelli S, Alviggi C, Cava A La, Matarese G. The pleiotropic roles of leptin in metabolism, immunity, and cancer. J Exp Med [Internet]. 2021 Apr 15 [cited 2022 Apr 8];218(5). Available from: https://doi.org/10.1084/jem.20191593

186. Münzberg H, Heymsfield SB. New Insights into the Regulation of Leptin Gene Expression. Cell Metab [Internet]. 2019 May 7 [cited 2022 Apr 19];29(5):1013. Available from: /pmc/articles/PMC7346278/

187. Gonzalez RR, Cherfils S, Escobar M, Yoo JH, Carino C, Styer AK, et al. Leptin signaling promotes the growth of mammary tumors and increases the expression of vascular endothelial growth factor (VEGF) and its receptor type two (VEGF-R2). J Biol Chem [Internet]. 2006 Sep 8 [cited 2021 Feb 2];281(36):26320–8. Available from: http://www.jbc.org/article/S0021925819351622/fulltext

188. Fan Y, Gan Y, Shen Y, Cai X, Song Y, Zhao F, et al. Leptin signaling enhances cell invasion and promotes the metastasis of human pancreatic cancer via increasing MMP-13 production. Oncotarget [Internet]. 2015 [cited 2021 Nov 16];6(18):16120–34. Available from: https://pubmed.ncbi.nlm.nih.gov/25948792/

189. Dieudonne MN, Machinal-Quelin F, Serazin-Leroy V, Leneveu MC, Pecquery R, Giudicelli Y. Leptin mediates a proliferative response in human MCF7 breast cancer cells. Biochem Biophys Res Commun. 2002;293(1):622–8.

190. Cao H, Huang Y, Wang L, Wang H, Pang X, Li K, et al. Leptin promotes migration and invasion of breast cancer cells by stimulating IL-8 production in M2 macrophages. Oncotarget [Internet]. 2016 [cited 2021 Nov 16];7(40):65441. Available from: /pmc/articles/PMC5323167/

191. Laud K, Gourdou I, Pessemesse L, Peyrat JP, Djiane J. Identification of leptin receptors in human breast cancer: Functional activity in the T47-D breast cancer cell line. Mol Cell Endocrinol. 2002 Feb 25;188(1–2):219–26.

192. Martin M, Ramos-Medina R, Bernat R, García-Saenz JA, del Monte-Millan M, Alvarez E, et al. Activity of docetaxel, carboplatin, and doxorubicin in patient-derived triple-negative breast cancer xenografts. Sci Reports 2021 111 [Internet]. 2021 Mar 29 [cited 2021 Oct 12];11(1):1–12. Available from: https://www.nature.com/articles/s41598-021-85962-4

193. A E, L L, E B, J A, R W, BB H, et al. Doxorubicin plus interleukin-2 chemoimmunotherapy against breast cancer in mice. Cancer Res [Internet]. 2006 May 15 [cited 2021 Oct 12];66(10):5419–26. Available from: https://pubmed.ncbi.nlm.nih.gov/16707470/

194. Rohlenova K, Veys K, Miranda-Santos I, De Bock K, Carmeliet P. Endothelial Cell Metabolism in Health and Disease. Vol. 28, Trends in Cell Biology. Elsevier Ltd; 2018. p. 224–36.

195. Fitzgerald G, Soro-Arnaiz I, De Bock K. The Warburg Effect in Endothelial Cells and its Potential as an Anti-angiogenic Target in Cancer. Front Cell Dev Biol [Internet]. 2018 Sep 11 [cited 2021 Nov 16];6(SEP). Available from: /pmc/articles/PMC6141712/

196. Park J, Kusminski CM, Chua SC, Scherer PE. Leptin receptor signaling supports cancer cell metabolism through suppression of mitochondrial respiration in vivo. Am J Pathol [Internet]. 2010 [cited 2021 Feb 2];177(6):3133–44. Available from:

/pmc/articles/PMC2993284/?report=abstract

197. Ishikawa M, Kitayama J, Nagawa H. Enhanced expression of leptin and leptin receptor (OB-R) in human breast cancer. Clin Cancer Res [Internet]. 2004 Jul 1 [cited 2021 Feb 2];10(13):4325–31. Available from: https://clincancerres.aacrjournals.org/content/10/13/4325

198. Cleary MP, Juneja SC, Phillips FC, Hu X, Grande JP, Maihle NJ. Leptin Receptor-Deficient MMTV-TGF-{alpha}/LeprdbLeprdb Female Mice Do Not Develop Oncogene-Induced Mammary Tumors. Exp Biol Med. 2004;229(2):182–93.

199. Herold J, Kalucka J. Angiogenesis in Adipose Tissue: The Interplay Between Adipose and Endothelial Cells. Front Physiol. 2021 Feb 9;11:1861.

200. Harris RBS. Direct and indirect effects of leptin on adipocyte metabolism. Biochim Biophys Acta - Mol Basis Dis. 2014 Mar 1;1842(3):414–23.

201. Anderson NM, Simon MC. The tumor microenvironment. Curr Biol [Internet]. 2020 Aug 17 [cited 2021 Nov 16];30(16):R921–5. Available from: https://pubmed.ncbi.nlm.nih.gov/32810447/

202. Huang Y, Yuan J, Righi E, Kamoun WS, Ancukiewicz M, Nezivar J, et al. Vascular normalizing doses of antiangiogenic treatment reprogram the immunosuppressive tumor microenvironment and enhance immunotherapy. Proc Natl Acad Sci U S A [Internet]. 2012 Oct 23 [cited 2018 Oct 14];109(43):17561–6. Available from: http://www.ncbi.nlm.nih.gov/pubmed/23045683

203. Andò S, Catalano S. The multifactorial role of leptin in driving the breast cancer microenvironment. Nat Rev Endocrinol 2011 85 [Internet]. 2011 Nov 15 [cited 2021 Sep 17];8(5):263–75. Available from: https://www.nature.com/articles/nrendo.2011.184

204. Andò S, Barone I, Giordano C, Bonofiglio D, Catalano S. The multifaceted mechanism of Leptin signaling within tumor microenvironment in driving breast cancer growth and progression. Front Oncol. 2014;4(NOV):340.

205. Newman G, Gonzalez-Perez RR. Leptin-cytokine crosstalk in breast cancer. Mol Cell Endocrinol [Internet]. 2014 Jan 25 [cited 2022 May 9];382(1):570–82. Available from: https://pubmed.ncbi.nlm.nih.gov/23562747/

206. Ishikawa M, Kitayama J, Nagawa H. Enhanced Expression of Leptin and Leptin Receptor (OB-R) in Human Breast Cancer. Clin Cancer Res. 2004 Jul 1;10(13):4325–31.

207. Miyoshi Y, Funahashi T, Tanaka S, Taguchi T, Tamaki Y, Shimomura I, et al. High expression of leptin receptor mRNA in breast cancer tissue predicts poor prognosis for patients with high, but not low, serum leptin levels. Int J cancer [Internet]. 2006 Mar 15 [cited 2022 May 26];118(6):1414–9. Available from: https://pubmed.ncbi.nlm.nih.gov/16206269/

208. Cascio S, Bartella V, Auriemma A, Johannes GJ, Russo A, Giordano A, et al. Mechanism of leptin expression in breast cancer cells: role of hypoxia-inducible factor-1α. Oncogene 2008 274 [Internet]. 2007 Jul 23 [cited 2022 Apr 23];27(4):540–7. Available from: https://www.nature.com/articles/1210660

209. Wang B, Wood IS, Trayhurn P. Hypoxia induces leptin gene expression and secretion in human preadipocytes: differential effects of hypoxia on adipokine expression by preadipocytes. J Endocrinol [Internet]. 2008 Jul 1 [cited 2022 May 9];198(1):127–34. Available from: https://joe.bioscientifica.com/view/journals/joe/198/1/127.xml

210. He X, Cheng R, Benyajati S, Ma JX. PEDF and its roles in physiological and pathological conditions: implication in diabetic and hypoxia-induced angiogenic diseases. Clin Sci (Lond) [Internet]. 2015 [cited 2022 Apr 15];128(Pt 11):805. Available from: /pmc/articles/PMC4557399/

211. Famulla S, Lamers D, Hartwig S, Passlack W, Horrighs A, Cramer A, et al. Pigment epithelium-derived factor (PEDF) is one of the most abundant proteins secreted by human adipocytes and induces insulin resistance and inflammatory signaling in muscle and fat cells. Int J Obes (Lond) [Internet]. 2011 Jun [cited 2021 Dec 21];35(6):762–72.

Available from: https://pubmed.ncbi.nlm.nih.gov/20938440/

212. Filleur S, Nelius T, De Riese W, Kennedy RC. Characterization of PEDF: A multi-functional serpin family protein. J Cell Biochem [Internet]. 2009 Apr 1 [cited 2022 May 9];106(5):769–75. Available from: https://onlinelibrary.wiley.com/doi/full/10.1002/jcb.22072

213. Becerra SP, Sagasti A, Spinella P, Notario V. Pigment epithelium-derived factor behaves like a noninhibitory serpin. Neurotrophic activity does not require the serpin reactive loop. J Biol Chem. 1995;270(43):25992–9.

214. Ansari D, Althini C, Ohlsson H, Bauden M, Andersson R. The Role of PEDF in Pancreatic Cancer. Anticancer Res [Internet]. 2019 Jul 1 [cited 2022 May 28];39(7):3311–5. Available from: https://ar.iiarjournals.org/content/39/7/3311

215. Cai J, Parr C, Watkins G, Jiang WG, Boulton M. Decreased Pigment Epithelium–Derived Factor Expression in Human Breast Cancer Progression. Clin Cancer Res [Internet]. 2006 Jun 1 [cited 2022 May 9];12(11):3510–7. Available from: https://aacrjournals.org/clincancerres/article/12/11/3510/285006/Decreased-Pigment-Epithelium-Derived-Factor

216. Fernández-Barral A, Orgaz JL, Gomez V, del Peso L, Calzada MJ, Jiménez B. Hypoxia negatively regulates antimetastatic PEDF in melanoma cells by a hypoxia inducible factor-independent, autophagy dependent mechanism. PLoS One [Internet]. 2012 Mar 23 [cited 2022 May 9];7(3). Available from: https://pubmed.ncbi.nlm.nih.gov/22457728/

217. Ablonczy Z, Prakasam A, Fant J, Fauq A, Crosson C, Sambamurti K. Pigment Epithelium-derived Factor Maintains Retinal Pigment Epithelium Function by Inhibiting Vascular Endothelial Growth Factor-R2 Signaling through γ-Secretase *. J Biol Chem [Internet]. 2009 Oct 30 [cited 2022 May 28];284(44):30177–86. Available from: http://www.jbc.org/article/S002192582038073X/fulltext

218. Cai J, Jiang WG, Grant MB, Boulton M. Pigment Epithelium-derived Factor Inhibits

Angiogenesis via Regulated Intracellular Proteolysis of Vascular Endothelial Growth Factor Receptor 1 *. J Biol Chem [Internet]. 2006 Feb 10 [cited 2022 May 28];281(6):3604–13. Available from: http://www.jbc.org/article/S0021925820817542/fulltext

219. Xu Z, Dong Y, Peng F, Yu Z, Zuo Y, Dai Z, et al. Pigment epithelium-derived factor enhances tumor response to radiation through vasculature normalization in allografted lung cancer in mice. Cancer Gene Ther [Internet]. 2015 Mar 25 [cited 2022 Jun 13];22(4):181–7. Available from: https://pubmed.ncbi.nlm.nih.gov/25591809/

220. Yamagishi SI, Amano S, Inagaki Y, Okamoto T, Takeuchi M, Inoue H. Pigment epithelium-derived factor inhibits leptin-induced angiogenesis by suppressing vascular endothelial growth factor gene expression through anti-oxidative properties. Microvasc Res. 2003 May 1;65(3):186–90.

221. Lim SC, Tajika M, Shimura M, Carey KT, Stroud DA, Murayama K, et al. Loss of the Mitochondrial Fatty Acid β-Oxidation Protein Medium-Chain Acyl-Coenzyme A Dehydrogenase Disrupts Oxidative Phosphorylation Protein Complex Stability and Function. Sci Reports 2017 81 [Internet]. 2018 Jan 9 [cited 2022 May 17];8(1):1–17. Available from: https://www.nature.com/articles/s41598-017-18530-4

222. Jones PM, Bennett MJ. Disorders of mitochondrial fatty acid β-oxidation. Biomarkers Inborn Errors Metab. 2017 Jan 1;87–101.

223. Sancak Y, Peterson TR, Shaul YD, Lindquist RA, Thoreen CC, Bar-Peled L, et al. The Rag GTPases bind raptor and mediate amino acid signaling to mTORC1. Science [Internet]. 2008 Jun 13 [cited 2022 May 17];320(5882):1496–501. Available from: https://pubmed.ncbi.nlm.nih.gov/18497260/

224. Meng D, Yang Q, Wang H, Melick CH, Navlani R, Frank AR, et al. Glutamine and asparagine activate mTORC1 independently of Rag GTPases. J Biol Chem [Internet]. 2020 Mar 6 [cited 2022 May 17];295(10):2890–9. Available from:

http://www.jbc.org/article/S0021925817494968/fulltext

225. Zheng X, Liang Y, He Q, Yao R, Bao W, Bao L, et al. Current Models of Mammalian Target of Rapamycin Complex 1 (mTORC1) Activation by Growth Factors and Amino Acids. Int J Mol Sci 2014, Vol 15, Pages 20753-20769 [Internet]. 2014 Nov 13 [cited 2022 May 21];15(11):20753–69. Available from: https://www.mdpi.com/1422-0067/15/11/20753/htm

226. Lysosomes - The Cell - NCBI Bookshelf [Internet]. [cited 2022 Jun 3]. Available from: https://www.ncbi.nlm.nih.gov/books/NBK9953/

227. Duran R V, Oppliger W, Robitaille AM, Heiserich L, Skendaj R, Gottlieb E, et al. Glutaminolysis activates Rag-mTORC1 signaling. Mol Cell. 2012 Aug;47(3):349–58.

228. Harjunpää H, Asens ML, Guenther C, Fagerholm SC. Cell adhesion molecules and their roles and regulation in the immune and tumor microenvironment. Front Immunol. 2019;10(MAY):1078.

229. Jain RK. Antiangiogenesis Strategies Revisited: From Starving Tumors to Alleviating Hypoxia. Cancer Cell [Internet]. 2014 Nov 10 [cited 2021 Oct 13];26(5):605–22. Available from: http://www.cell.com/article/S1535610814004103/fulltext

230. Pelaia C, Paoletti G, Puggioni F, Racca F, Pelaia G, Canonica GW, et al. Interleukin-5 in the Pathophysiology of Severe Asthma. Front Physiol. 2019 Dec 17;10:1514.

231. White JR, Imburgia C, Dul E, Appelbaum E, O'Donnell K, O'Shannessy DJ, et al. Cloning and functional characterization of a novel human CC chemokine that binds to the CCR3 receptor and activates human eosinophils. J Leukoc Biol [Internet]. 1997 Nov 1 [cited 2022 May 30];62(5):667–75. Available from: https://onlinelibrary.wiley.com/doi/full/10.1002/jlb.62.5.667

232. Cho H, Lim SJ, Won KY, Bae GE, Kim GY, Min JW, et al. Eosinophils in Colorectal Neoplasms Associated with Expression of CCL11 and CCL24. J Pathol Transl Med [Internet]. 2016 [cited 2022 May 12];50(1):45. Available from: /pmc/articles/PMC4734969/

233. Ikutani M, Yanagibashi T, Ogasawara M, Tsuneyama K, Yamamoto S, Hattori Y, et al. Identification of innate IL-5-producing cells and their role in lung eosinophil regulation and antitumor immunity. J Immunol [Internet]. 2012 Jan 15 [cited 2022 May 12];188(2):703–13. Available from: https://pubmed.ncbi.nlm.nih.gov/22174445/

234. Grisaru-Tal S, Itan M, Klion AD, Munitz A. A new dawn for eosinophils in the tumour microenvironment. Nat Rev Cancer 2020 2010 [Internet]. 2020 Jul 16 [cited 2022 May 30];20(10):594–607. Available from: https://www.nature.com/articles/s41568-020-0283-9

235. Mazmanian SK, Cui HL, Tzianabos AO, Kasper DL. An Immunomodulatory Molecule of Symbiotic Bacteria Directs Maturation of the Host Immune System. Cell. 2005 Jul 15;122(1):107–18.

236. Tlaskalová-Hogenová H, Tpánková R, Kozáková H, Hudcovic T, Vannucci L, Tuková L, et al. The role of gut microbiota (commensal bacteria) and the mucosal barrier in the pathogenesis of inflammatory and autoimmune diseases and cancer: contribution of germ-free and gnotobiotic animal models of human diseases. Cell Mol Immunol 2011 82 [Internet]. 2011 Jan 31 [cited 2022 May 20];8(2):110–20. Available from: https://www.nature.com/articles/cmi201067

237. Wu HJ, Wu E. The role of gut microbiota in immune homeostasis and autoimmunity. Gut Microbes [Internet]. 2012 Jan 1 [cited 2022 May 20];3(1):4. Available from: /pmc/articles/PMC3337124/

238. Jain T, Sharma P, Are AC, Vickers SM, Dudeja V. New Insights Into the Cancer–Microbiome–Immune Axis: Decrypting a Decade of Discoveries. Front Immunol. 2021 Feb 23;12:102.

239. Dapito DH, Mencin A, Gwak GY, Pradere JP, Jang MK, Mederacke I, et al. Promotion of Hepatocellular Carcinoma by the Intestinal Microbiota and TLR4. Cancer Cell. 2012 Apr 17;21(4):504–16.

240. Yu LX, Yan HX, Liu Q, Yang W, Wu HP, Dong W, et al. Endotoxin accumulation prevents

carcinogen-induced apoptosis and promotes liver tumorigenesis in rodents. Hepatology [Internet]. 2010 Oct 1 [cited 2022 May 31];52(4):1322–33. Available from: https://onlinelibrary.wiley.com/doi/full/10.1002/hep.23845

241. Baker JM, Al-Nakkash L, Herbst-Kralovetz MM. Estrogen–gut microbiome axis: Physiological and clinical implications. Maturitas. 2017 Sep 1;103:45–53.

242. Yoshimoto S, Loo TM, Atarashi K, Kanda H, Sato S, Oyadomari S, et al. Obesity-induced gut microbial metabolite promotes liver cancer through senescence secretome. Nat 2013 4997456 [Internet]. 2013 Jun 26 [cited 2022 May 31];499(7456):97–101. Available from: https://www.nature.com/articles/nature12347

243. Costarelli V, Sanders TAB. Plasma deoxycholic acid concentration is elevated in postmenopausal women with newly diagnosed breast cancer. Eur J Clin Nutr [Internet]. 2002 Sep [cited 2022 May 31];56(9):925–7. Available from: https://pubmed.ncbi.nlm.nih.gov/12209383/

244. Sethi V, Kurtom S, Tarique M, Lavania S, Malchiodi Z, Hellmund L, et al. Gut Microbiota Promotes Tumor Growth in Mice by Modulating Immune Response. Gastroenterology [Internet]. 2018 Jul 1 [cited 2022 May 31];155(1):33-37.e6. Available from: https://pubmed.ncbi.nlm.nih.gov/29630898/

245. Ma C, Han M, Heinrich B, Fu Q, Zhang Q, Sandhu M, et al. Gut microbiome-mediated bile acid metabolism regulates liver cancer via NKT cells. Science [Internet]. 2018 May 25 [cited 2022 Jun 1];360(6391). Available from: https://pubmed.ncbi.nlm.nih.gov/29798856/

246. Huggins MA, Jameson SC, Hamilton SE. Embracing microbial exposure in mouse research. J Leukoc Biol [Internet]. 2019 Jan 1 [cited 2022 Jun 3];105(1):73. Available from: /pmc/articles/PMC6318123/

247. Bröer A, Fairweather S, Bröer S. Disruption of amino acid homeostasis by novel ASCT2 inhibitors involves multiple targets. Front Pharmacol. 2018 Jul 19;9(JUL).

248. Jin H, Wang S, Zaal EA, Wang C, Wu H, Bosma A, et al. A powerful drug combination

strategy targeting glutamine addiction for the treatment of human liver cancer. Elife. 2020 Oct 1;9:1–20.

249. Luo Z, Xu J, Sun J, Huang H, Zhang Z, Ma W, et al. Co-delivery of 2-Deoxyglucose and a Glutamine Metabolism Inhibitor V9302 via a Prodrug Micellar Formulation for Synergistic Targeting of Metabolism in Cancer. Acta Biomater [Internet]. 2020 Mar 3 [cited 2022 May 31];105:239. Available from: /pmc/articles/PMC7105957/

250. Zhao Y, Feng X, Chen Y, Eva Selfridge J, Gorityala S, Du Z, et al. 5-fluorouracil enhances the anti-tumor activity of the glutaminase inhibitor CB-839 against PIK3CA-mutant colorectal cancers. Cancer Res [Internet]. 2020 Nov 11 [cited 2022 May 24];80(21):4815. Available from: /pmc/articles/PMC7642187/

251. Meric-Bernstam F, Tannir NM, Iliopoulos O, Lee RJ, Telli ML, Fan AC, et al. Telaglenastat Plus Cabozantinib or Everolimus for Advanced or Metastatic Renal Cell Carcinoma: An Open-Label Phase I Trial. Clin Cancer Res [Internet]. 2022 Apr 14 [cited 2022 May 31];28(8):1540–8. Available from: https://pubmed.ncbi.nlm.nih.gov/35140121/

252. Carr EL, Kelman A, Wu GS, Gopaul R, Senkevitch E, Aghvanyan A, et al. Glutamine uptake and metabolism are coordinately regulated by ERK/MAPK during T lymphocyte activation. J Immunol. 2010 Jul;185(2):1037–44.

253. Wang R, Green DR. Metabolic reprogramming and metabolic dependency in T cells. Immunol Rev [Internet]. 2012 Sep [cited 2022 May 24];249(1):14. Available from: /pmc/articles/PMC3422760/

254. Ngwa VM, Edwards DN, Philip M, Chen J. Microenvironmental metabolism regulates antitumor immunity. Cancer Res [Internet]. 2019 Aug 15 [cited 2022 May 24];79(16):4003–8. Available from: https://aacrjournals.org/cancerres/article/79/16/4003/638289/Microenvironmental-Metabolism-Regulates-Antitumor

255. Varghese S, Pramanik S, Williams LJ, Hodges HR, Hudgens CW, Fischer GM, et al. The

glutaminase inhibitor CB-839 (Telaglenastat) enhances the antimelanoma activity of T-cell-mediated immunotherapies. Mol Cancer Ther [Internet]. 2021 Mar 1 [cited 2022 May 24];20(3):500–11. Available from: https://aacrjournals.org/mct/article/20/3/500/93232/The-Glutaminase-Inhibitor-CB-839-Telaglenastat

256. Meric-Bernstam F;, Gordon M;, Tykodi. CX-839-004: A phase 1/2 study of CB-839, a first-in-class glutaminase inhibitor, combined with nivolumab in patients with advanced Melanoma (MEL), Renal Cell Carcinoma (RCC), or Non-Small Cell Lung Cancer (NSCLC).

257. St. Croix B, Rago C, Velculescu V, Traverso G, Romans KE, Montegomery E, et al. Genes expressed in human tumor endothelium. Science (80-) [Internet]. 2000 Aug 18 [cited 2022 May 13];289(5482):1197–202. Available from: https://www.science.org/doi/full/10.1126/science.289.5482.1197

258. Nagl L, Horvath L, Pircher A, Wolf D. Tumor Endothelial Cells (TECs) as Potential Immune Directors of the Tumor Microenvironment – New Findings and Future Perspectives [Internet]. Vol. 8, Frontiers in Cell and Developmental Biology. Frontiers Media S.A.; 2020 [cited 2021 Jun 8]. p. 766. Available from: www.frontiersin.org

259. Maishi N, Annan DA, Kikuchi H, Hida Y, Hida K. Tumor Endothelial Heterogeneity in Cancer Progression. Cancers (Basel) [Internet]. 2019 Oct 1 [cited 2022 May 13];11(10). Available from: https://pubmed.ncbi.nlm.nih.gov/31600937/

260. Duncan DJ, Scott M, Scorer P, Barker C. Assessment of PD-L1 mRNA and protein expression in non-small cell lung cancer, head and neck squamous cell carcinoma and urothelial carcinoma tissue specimens using RNAScope and immunohistochemistry. PLoS One [Internet]. 2019 Apr 1 [cited 2022 May 21];14(4). Available from: https://pubmed.ncbi.nlm.nih.gov/30986253/

261. Lappano R, Rigiracciolo DC, Belfiore A, Maggiolini M, De Francesco EM. Cancer associated fibroblasts: role in breast cancer and potential as therapeutic targets. Expert

Opin Ther Targets [Internet]. 2020 Jun 2 [cited 2022 May 31];24(6):559–72. Available from: https://pubmed.ncbi.nlm.nih.gov/32249708/

262. Wu Q, Li B, Li Z, Li J, Sun S, Sun S. Cancer-associated adipocytes: key players in breast cancer progression. J Hematol Oncol 2019 121 [Internet]. 2019 Sep 10 [cited 2022 May 24];12(1):1–15. Available from: https://jhoonline.biomedcentral.com/articles/10.1186/s13045-019-0778-6

263. Li X, Zhu H, Sun W, Yang X, Nie Q, Fang X. Role of glutamine and its metabolite ammonia in crosstalk of cancer-associated fibroblasts and cancer cells. Cancer Cell Int [Internet]. 2021 Dec 1 [cited 2022 May 31];21(1). Available from: /pmc/articles/PMC8427881/